

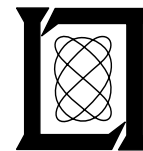
**Project Report
ATC-218**

Summer 1992 Terminal Area-Local Analysis and Prediction System (T-LAPS) Evaluation

**S. R. Finch
R. E. Cole
R. G. Rasmussen
F. W. Wilson
S. Kim**

7 October 1994

Lincoln Laboratory
MASSACHUSETTS INSTITUTE OF TECHNOLOGY
LEXINGTON, MASSACHUSETTS



Prepared for the Federal Aviation Administration,
Washington, D.C. 20591

This document is available to the public through
the National Technical Information Service,
Springfield, VA 22161

This document is disseminated under the sponsorship of the Department of Transportation in the interest of information exchange. The United States Government assumes no liability for its contents or use thereof.

1. Report No. ATC-218		2. Government Accession No. DOT/FAA/RD-94/13		3. Recipient's Catalog No.	
4. Title and Subtitle Summer 1992 Terminal area—Local Analysis and Prediction System (T-LAPS) Evaluation				5. Report Date 7 October 1994	
				6. Performing Organization Code	
7. Author(s) Steven R. Finch, Rodney E. Cole, R. Gary Rasmussen, F. Wesley Wilson, Stephen Kim				8. Performing Organization Report No. ATC-218	
9. Performing Organization Name and Address Lincoln Laboratory, MIT P.O. Box 73 Lexington, MA 02173-9108				10. Work Unit No. (TRAIS)	
				11. Contract or Grant No. DTFA01-91-Z-02036	
12. Sponsoring Agency Name and Address Department of Transportation Federal Aviation Administration Washington, DC 20591				13. Type of Report and Period Covered Project Report	
				14. Sponsoring Agency Code	
15. Supplementary Notes This report is based on studies performed at Lincoln Laboratory, a center for research operated by Massachusetts Institute of Technology. The work was sponsored by the Air Force under Contract F19628-95-C-0002.					
16. Abstract The Integrated Terminal Weather System (ITWS) is a development program initiated by the Federal Aviation Administration (FAA) to produce a fully automated, integrated terminal weather information system to improve the safety, efficiency and capacity of terminal area aviation operations. The ITWS will acquire data from FAA and National Weather Service sensors as well as from aircraft in flight in the terminal area. The ITWS will provide Air Traffic personnel with products that are immediately usable without further meteorological interpretation. Among the products are the current terminal area weather, short-term (0-30 minute) predictions of significant weather phenomena, and the terminal winds product. The terminal winds product is the component of ITWS which produces estimates of the horizontal winds on a three-dimensional grid of points encompassing an airport terminal region. It uses information from a variety of sensors, including Doppler weather radars. In 1992, an operational test of an initial prototype Terminal Winds system was conducted at the MIT Lincoln Laboratory testbed in Orlando, FL. This report describes our evaluation of the initial Terminal Winds prototype.					
17. Key Words ITWS Doppler Radar T-LAPS Terminal Winds NEXRAD TDWR LAPS			18. Distribution Statement This document is available to the public through the National Technical Information Service, Springfield, VA 22161.		
19. Security Classif. (of this report) Unclassified		20. Security Classif. (of this page) Unclassified		21. No. of Pages 141	22. Price

ABSTRACT

The Integrated Terminal Weather System (ITWS) is a development program initiated by the Federal Administration (FAA) to produce a fully automated, integrated terminal weather information system to improve the safety, efficiency and capacity of terminal area aviation operations. The ITWS will acquire data from FAA and National Weather Service sensors as well as from aircraft in flight in the terminal area. The ITWS will provide Air Traffic personnel with products that are immediately usable without further meteorological interpretation. Among the products are current terminal area weather, short-term (0–30 minute) predictions of significant weather phenomena, and the Terminal Winds product.

The terminal winds product is the component of the ITWS which produces estimates of the horizontal winds on a three dimensional grid of points encompassing an airport terminal region. It uses information from a variety of sensors, including Doppler weather radars. In 1992, an operational test of an initial prototype Terminal Winds system was conducted at the MIT Lincoln Laboratory testbed in Orlando, FL. This report describes our evaluation of the initial Terminal Winds prototype.

ACKNOWLEDGMENTS

Shian-Shi Yao, Cynthia McLain, William Comery, and James Capucci also contributed to the evaluation effort.

TABLE OF CONTENTS

Abstract	iii
Acknowledgments	v
List of Illustrations	ix
List of Tables	xi
1 INTRODUCTION	1
1.1. Overview	1
1.2. Issues	2
1.3. Organization	2
2 DATA	3
2.1. Nine-Day Data Set	3
2.2. Types of Gridded Winds Analyses	4
2.3. Types of Observational Data	5
3 COMPARATIVE EVALUATION	9
4 CONTINUITY EVALUATION	15
5 SOME EXAMPLES	17
5.1. An Example of the Benefit of a Fine Scale Analysis	17
5.2. An Example of Spatial Discontinuity	17
5.3. An Example of Temporal Discontinuity	18
6 SUMMARY	41
GLOSSARY	43
REFERENCES	45
APPENDIX A: T-LAPS ANALYSIS	47
A.1 Introduction	47
A.2 LAPS Winds Analysis Overview	47
A.2.1 LAPS Barnes Interpolation	47
A.2.2 LAPS Single-Doppler Analysis	49
A.3 Multiple Single-Doppler Analysis	50
A.3.1 BI-2	50
A.3.2 BI-3	51
A.4 Consequences of the T-LAPS Analysis	52
A.5 Cascade of Scales	53

TABLE OF CONTENTS (Continued)

APPENDIX B: RADAR DATA ANALYSIS	57
B.1 Introduction	57
B.2 Radar Data Quality	57
B.3 Radar Data Resampler	57
B.4 Dual-Doppler Analysis	58
APPENDIX C: DETAILED EVALUATION STATISTICS	61

LIST OF ILLUSTRATIONS

Figure No.		Page
1	Horizontal distribution of ACARS observations.	7
2	Vertical distribution of ACARS observations.	7
3	Horizontal distribution of dual-Doppler observations.	8
4	Key for distribution line plots.	10
5	Norm of wind vector difference distributions.	10
6	Wind speed difference distributions.	11
7	Wind direction difference distributions.	11
8	Norm of wind vector difference distributions stratified by day.	12
9	MAPS wind field at 2310 UTC, August 20, 1992, 3200 feet MSL.	19
10	T-LAPS10 BI-3 wind field at 2310 UTC, August 20, 1992, 3200 feet MSL.	21
11	T-LAPS10 BI-2 wind field at 2310 UTC, August 20, 1992, 3200 feet MSL.	23
12	T-LAPS10 BI-2 wind field and TDWR reflectivity at 2310 UTC, August 20, 1992, 3200 feet MSL.	25
13	T-LAPS BI3 wind field at 1540 UTC, September 22, 1992, 8100 feet MSL.	27
14	T-LAPS BI3 wind field at 1555 UTC, September 22, 1992, 8100 feet MSL.	29
15	T-LAPS BI2 wind field at 2110 UTC, August 20, 1992, 3200 feet MSL.	31
16	T-LAPS BI2 wind field at 2115 UTC, August 20, 1992, 3200 feet MSL.	33
17	T-LAPS BI3 wind field at 2110 UTC, August 20, 1992, 3200 feet MSL.	35
18	T-LAPS BI3 wind field at 2115 UTC, August 20, 1992, 3200 feet MSL.	37
A-1	Data flow for the LAPS single-Doppler analysis.	49
A-2	Data flow for the two-pass Barnes MSDA.	51
A-3	Data flow for the three-pass Barnes MSDA.	52
A-4	Weights vs. distance to analysis location.	53
A-5	Data flow for T-LAPS cascade of scales.	54
A-6	T-LAPS domain and sensor locations.	55
B-1	T-LAPS dual-Doppler analysis region.	59

LIST OF TABLES

Table No.		Page
1	T-LAPS10 Data Characteristics	4
2	T-LAPS2 Data Characteristics	5
3	Height Distribution for the Three Observational Data Sets	8
4	T-LAPS2 Spatial Continuity – Adjacent Grid Points, Same Level	15
5	T-LAPS2 Temporal Continuity – Five Minutes Separation, Same Grid Point	15
6	Median and RMS (in parentheses) Vector Differences (m/s)	41
A-1	Values of K1 in Equation 2	49

1. INTRODUCTION

1.1. Overview

The Terminal Winds product is an important component of the Integrated Terminal Weather System (ITWS). This product provides estimates of the horizontal winds in a three-dimensional terminal region for use by the Terminal Air Traffic Control Automation (TATCA) program, as well as ITWS Ceiling and Visibility and Runway Winds products, and Wake Vortex Advisory Systems (WVAS) (Cole, *et al.*, 1993). A primary task in 1992 was to assess the ability of current technology and FAA sensors to provide the high resolution and rapid update rate desired for this product. The Terminal area-Local Analysis and Prediction System (T-LAPS) was developed for this assessment. T-LAPS is a direct descendent of the wind analysis component of the Local Analysis and Prediction System (LAPS) developed at the National Oceanic and Atmospheric Administration (NOAA) Forecast Systems Laboratory (FSL).

Prior to 1992, LAPS did not operate at the spatial and temporal resolutions desired for the Terminal Winds product, nor was it able to accept data from more than one Doppler radar. Two important modifications were made to LAPS in the development of T-LAPS. The first is a Cascade of Scales Analysis to produce the desired resolution, and the second is the development of a Multiple Single-Doppler Analysis (MSDA) technique for the incorporation of data from several Doppler radars. These modifications were designed jointly by FSL and the MIT Lincoln Laboratory Weather Sensing Group. Details of the T-LAPS analysis are given in Appendix A.

The centerpiece of the overall 1992 T-LAPS effort was a demonstration of the system at the Lincoln Laboratory prototype Terminal Doppler Weather Radar (TDWR) field site (FL-2C) in Kissimmee, FL during August and early September. The primary area of coverage was a 120 km by 120 km region centered on the Orlando International Airport in Orlando, FL. The T-LAPS system utilized radar information from both the prototype TDWR radar on site and the NEXRAD/WSR-88D radar located in Melbourne, FL. T-LAPS also used aircraft reports, surface sensor observations and the Mesoscale Analysis and Prediction System (MAPS) national forecast fields as background. This report presents an evaluation of T-LAPS performance by Lincoln Laboratory on a nine-day subset of the summer 1992 demonstration data archive.

The questions addressed in this report are:

- How well do T-LAPS analyses compare against various types of observational data?
- What are the characteristics of T-LAPS analyses in and by themselves?
- What are the benefits of fine-scale analysis?
- What are the benefits of proposed modifications?
- What are the T-LAPS failure modes?

Three approaches are used in evaluating T-LAPS:

- Compute analysis vs. observation comparative statistics,
- Compute wind analysis self-consistency statistics—Temporal continuity, Spatial continuity, and
- Examine individual cases which contain discontinuous behavior.

1.2. Issues

There are relevant issues which are beyond the scope of this report. For the sake of completeness, we mention these issues briefly.

The characterization of a “perfect” local winds analysis has not been made yet. In particular, the desired degree of smoothing of the wind field has not been specified. At any given instant, a wind field is a superposition of wind structures with a wide spectrum of spatial and temporal scales. For a given application, some of these structures will be at scales that are unimportant, and others too small or short lived to be captured on the analysis grid or with the analysis update rate. However, these subscale features may be captured by an observation. When these observations are compared with the analysis, the differences reflect a combination of errors in the analysis, errors in the observations, and the sub-scale features captured in the observations. Given the limited set of observations used in the evaluation, we have not attempted to separate out the effects of the different sources of error.

We expect performance results to depend on the weather and to differ in convective and non-convective situations. It would be interesting to quantify these differences, but the present convective weather data set is small (see Section 2.1). We have consequently deferred such study until a later time.

1.3. Organization

This report is organized as follows. Section 2 discusses the nine days used in the evaluation, the analyses being evaluated, and the observational data sets to which analyses are compared. Section 3 presents the comparison of wind analyses and observed winds. Section 4 is devoted to the temporal and spatial continuity evaluation. Section 5 presents three examples which illustrate the benefit of the fine scale analysis in convective weather, and T-LAPS failure modes. A summary of the report is provided in Section 6.

Appendix A describes the summer 1992 T-LAPS system in detail and elaborates on the distinction between two versions of T-LAPS analyses (based on two-pass or three-pass Barnes interpolation). Appendix B explains the procedure used to derive dual-Doppler wind fields for comparison against T-LAPS. Appendix C provides detailed statistical and graphical results.

2. DATA

This section discusses the data connected with the T-LAPS evaluation. Section 2.1 presents the nine days which make up the evaluation data set. Section 2.2 describes the gridded winds analyses being evaluated:

- T-LAPS2 (T-LAPS on the 2 km resolution grid, 5 minute update)
- T-LAPS10 (T-LAPS on the 10 km resolution grid, 30 minute update)
- BI2 (T-LAPS with two-pass Barnes Interpolation routine,¹ 2 or 10 km)
- BI3 (T-LAPS with three-pass Barnes Interpolation routine,¹ 2 or 10 km)
- MAPS (Mesoscale Analysis and Prediction System: 60 km, three-hour update)

Section 2.3 discusses the three observational data sets used in the analysis-vs-observation comparative evaluation:

- ACARS (commercial aircraft weather observations)
- CLASS (balloon sounding observations)
- dual Doppler (based on prototype TDWR and Melbourne NEXRAD radars)

Although each of these three data sets is treated as a standard against which the quality of T-LAPS is ascertained, it is important to keep in mind that observations are not perfect. We refer to the performance of T-LAPS “relative to the Aircraft Communications Addressing and Reporting System (ACARS),” for example, keeping explicit that any conclusions we draw are subject to the error characteristics of the observational data as well as the error characteristics of the analysis.

2.1. Nine-Day Data Set

The summer 1992 T-LAPS demonstration ran from August 17 until September 25. T-LAPS operated on certain days without MAPS forecast fields because they were unavailable. It was felt that such days do not represent T-LAPS performance adequately. On other days, few or no ACARS were available. No Cross-Loran Atmospheric Sounding System (CLASS) soundings were taken after August 29. We decided to concentrate only on days with suitable data. Nine days containing 70 hours of data were regarded as appropriate for evaluation:

- August 20 (with strongly convective activity at end of day)
- August 21 (quiet weather conditions throughout)
- August 25 (quiet weather conditions throughout)
- August 27 (quiet weather conditions throughout)
- August 28 (with strongly convective activity for the first half of day)
- August 29 (moderately convective activity throughout)
- September 19 (moderately convective activity throughout)
- September 21 (quiet weather conditions throughout)
- September 22 (quiet weather conditions throughout)

1. Details are in Appendix A.

Only six hours of the 70-hour data set are classified as strongly convective, so a stratification of the evaluation according to weather category is deemed infeasible. The statistics presented in Section 3 characterize the full nine-day data set, with calm weather and active weather alike included in the sample distributions.

2.2. Types of Gridded Winds Analyses

This brief survey is intended to familiarize the reader with the winds analyses studied in the evaluation. A more detailed description of the inner workings of T-LAPS is found in Appendix A. In this section, we start first with the coarsest analysis (MAPS) and move toward finer analyses.

The Mesoscale Analysis and Prediction System (Benjamin, *et al.*, 1991) is a national forecast product. The MAPS grid resolution is 60 km by 60 km by 25 (θ/σ hybrid) levels with a three-hour update. This resolution is too coarse to model most convective weather. Both the three-hour and six-hour MAPS forecast fields are used in the T-LAPS system.

The 1992 Orlando T-LAPS10 analysis grid spatially extends over a region 180 km by 180 km by 53000 feet centered at the Orlando airport. The grid resolution is 10 km by 10 km by 50 mb (21 pressure levels) with a 30-minute update rate. There are three-hour and six-hour MAPS forecasts which are valid, respectively, before and after each T-LAPS10 analysis time. These forecasts are interpolated (linearly in all four dimensions) to the 10 km grid to provide the large-scale structure supporting the T-LAPS10 wind field. T-LAPS10 uses recent observations to refine the MAPS winds. The characteristics of these data are summarized in Table 1.

Table 1.
T-LAPS10 Data Characteristics

SOURCE NAME	SENSOR TYPE	WIND INFORMATION	DATA AGE AT ANALYSIS TIME
TDWR	Doppler radar	radial component	0 – 10 min
NEXRAD	Doppler radar	radial component	0 – 10 min
ACARS	aircraft	horizontal vector	15 – 90 min
SAO/ASOS/AWOS	surface anemometer	horizontal vector	10 – 60 min
LLWAS	surface anemometer	horizontal vector	0 – 5 min

The 1992 Orlando T-LAPS2 analysis grid has 2 km by 2 km by 50 mb (13 pressure level) resolution with a five-minute update. This grid extends spatially over a region 120 km by 120 km by 18000 feet centered at the Orlando airport, nested within the T-LAPS10 grid. T-LAPS10, interpolated to the 2 km grid, serves as the background wind field for T-LAPS2. The characteristics of the data used by T-LAPS2 are summarized in Table 2.

**Table 2.
T-LAPS2 Data Characteristics**

source name	sensor type	wind information	data age at analysis time
TDWR	Doppler radar	radial component	0 – 10 min
NEXRAD	Doppler radar	radial component	0 – 10 min
LLWAS	surface anemometer	horizontal vector	0 – 5 min

These are the only sensor systems with sufficiently rapid data update rates to support the update cycle of T-LAPS2. When available, the Doppler radar data dominate the T-LAPS2 winds analysis in the lowest levels and contribute small-scale inputs to the wind field. There are several factors which contribute to the availability of quality radar data (Appendix B). At altitudes above radar returns (e.g., above 16,000 feet above ground level (AGL)), T-LAPS2 is T-LAPS10 interpolated to the 2 km grid. Other data sources are not included in T-LAPS2 due to data latency. For example, a gap of 20 to 30 minutes typically exists between an ACARS measurement and the receipt of that measurement in real time by the T-LAPS system.

T-LAPS uses one of two Barnes interpolation schemes to fuse background wind analyses and data observations. The Barnes scheme needs vector inputs, but Doppler data contains only radial components. T-LAPS BI2 and BI3 differ in how wind vector inputs are built from Doppler data. BI2 is the version of T-LAPS which was executed during the summer 1992 demonstration. T-LAPS BI3 is an upgrade which reflects FSL's latest thinking on building Doppler vectors (Appendix A).

2.3. Types of Observational Data

There are three types of observational data used in the evaluation to assess the performance of T-LAPS. Two of these, ACARS wind observations and CLASS soundings, are independent of the associated T-LAPS analysis field in the sense that random observation/analysis errors are statistically uncorrelated. The independence of ACARS is explained later in this section. The third, dual-Doppler winds based on TDWR and NEXRAD, is highly dependent on associated T-LAPS winds since both T-LAPS analysis winds and dual-Doppler winds are derived from the same Doppler data and use the same data quality control.

Aeronautical Radio, Inc. (ARINC) has developed MDCRS (Meteorological Data Collection and Reporting System) to collect vector winds and other atmospheric information aloft automatically from planes equipped with ACARS. ACARS in the summer 1992 data set are quite sparse in space and time (approximately five per hour). An advantage to using ACARS in the evaluation is that the measurements are taken at locations where aircraft operate and thus are relevant to air traffic concerns.

As mentioned in Section 2.2., ACARS observations are used as inputs to T-LAPS10 but are always at least 15 minutes old by the time they are assimilated. We use this latency feature of ACARS to the advantage of the evaluation in the following manner. ACARS observed winds are compared with corresponding analysis winds at the analysis update time closest to the ACARS measurement

time, which precedes the ACARS assimilation time. Despite the fact that ACARS are T-LAPS inputs for a subsequent analyses, each is independent of the concurrent T-LAPS analysis.

The University of Massachusetts—Lowell CLASS rawinsondes were launched several times per day from the University of North Dakota radar site located slightly east of the airport. Launches occurred during August only. Several of the soundings were omitted because of poor data quality or balloon position alignment errors. Seven CLASS soundings, representing seven vertical profiles, were judged acceptable, with a total effective sample size of roughly 100 data points (Appendix C). The CLASS sounding data set is very sparse in both space and time. The accuracy of rawinsonde wind speed observations, measured by root mean square (RMS) error, is typically 3 m/s. For wind direction, the accuracy is typically 14 degrees when the true wind speed exceeds 5 m/s (Cairns, *et al.*, 1993). This represents an RMS vector difference of 3.2 m/s.

The dual-Doppler data set was computed based on the fact that the wind velocity component measured by a Doppler radar is the projection of the actual wind vector in the radar beam direction. When there exist two Doppler measurements at a given location, the original wind vector can be reliably recovered from the two measured components, assuming certain geometrical constraints are satisfied. The dual-Doppler computations were performed in regions where the angle between the TDWR and NEXRAD radar beams is greater than 30 degrees and less than 150 degrees to avoid the numerical instability which occurs when the two radials are nearly parallel. High reflectivity regions were eliminated since wind velocity variations in convective weather make it difficult to characterize a 2 km cell by a single representative value. Further discussion of the dual-Doppler data set is found in Appendix B.

Dual-Doppler analysis produces the best-estimate of the wind field, based on the highly accurate Doppler radar measurements. It is generally viewed as one of the best wind observation systems, but it is difficult to quantify the magnitude of its error, since no other system is believed to be as accurate. It is generally believed that the RMS errors in dual-Doppler analysis are on the order of 1 m/s. In any event, most meteorologists would view favorably an analysis which shows good agreement with dual-Doppler analysis.

Figure 1 illustrates the distribution of the 368 available ACARS observations (\approx five per hour) according to horizontal location. The origin ($x=0$, $y=0$) is positioned at the Orlando airport and the indicated region (160 km by 120 km) encompasses the T-LAPS2 grid. The CLASS sounding launch site is indicated by the asterisk. Figure 2 illustrates the distribution of ACARS according to height (pressure level) and horizontal separation from the airport. All ten T-LAPS2 pressure levels above 400 feet are indicated. The nominal altitude for each pressure level is given in Table 3. The median ACARS height is 750 mb (roughly 8100 feet). Table 3 presents height distribution information for ACARS, CLASS soundings and dual Doppler together.

Dual-Doppler data were available for eight of the nine days (September 19 had no NEXRAD data throughout), giving rise to a sample size of over 70,000 data points. The distribution of these data points according to horizontal location is given by Figure 3. Approximately 80 percent of the dual-Doppler values were concentrated in the lowest 4 analysis levels (See table 3).

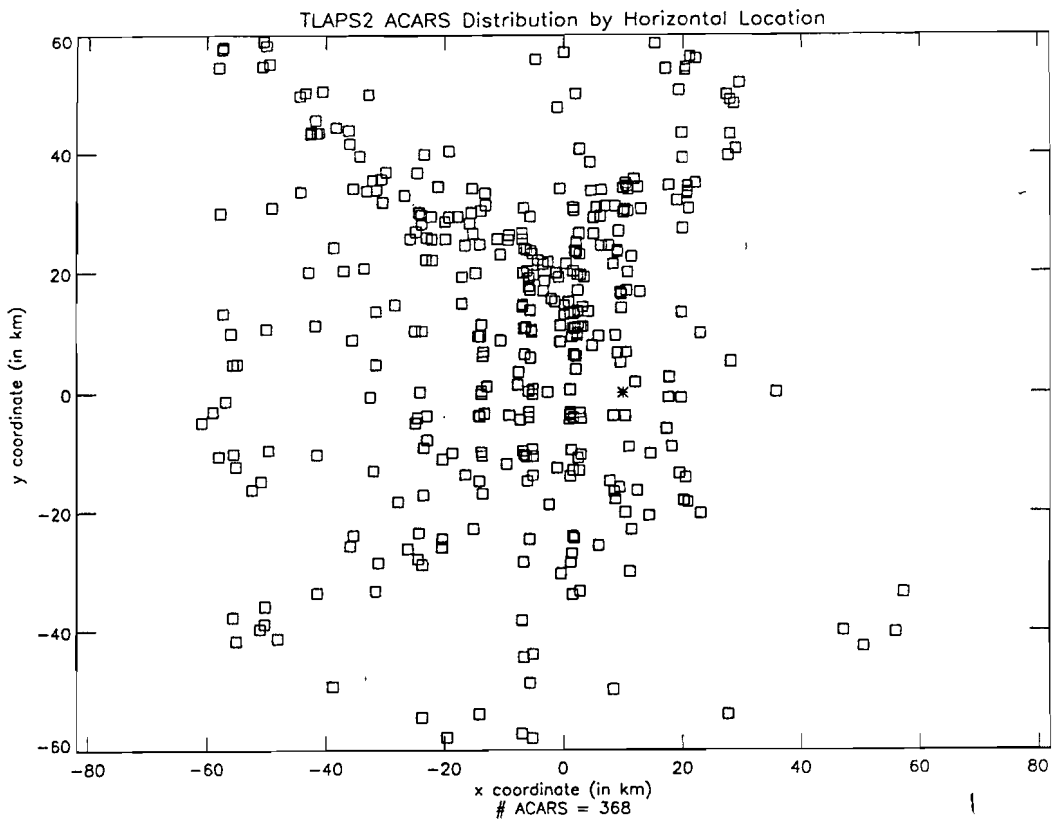


Figure 1. Horizontal distribution of ACARS observations.

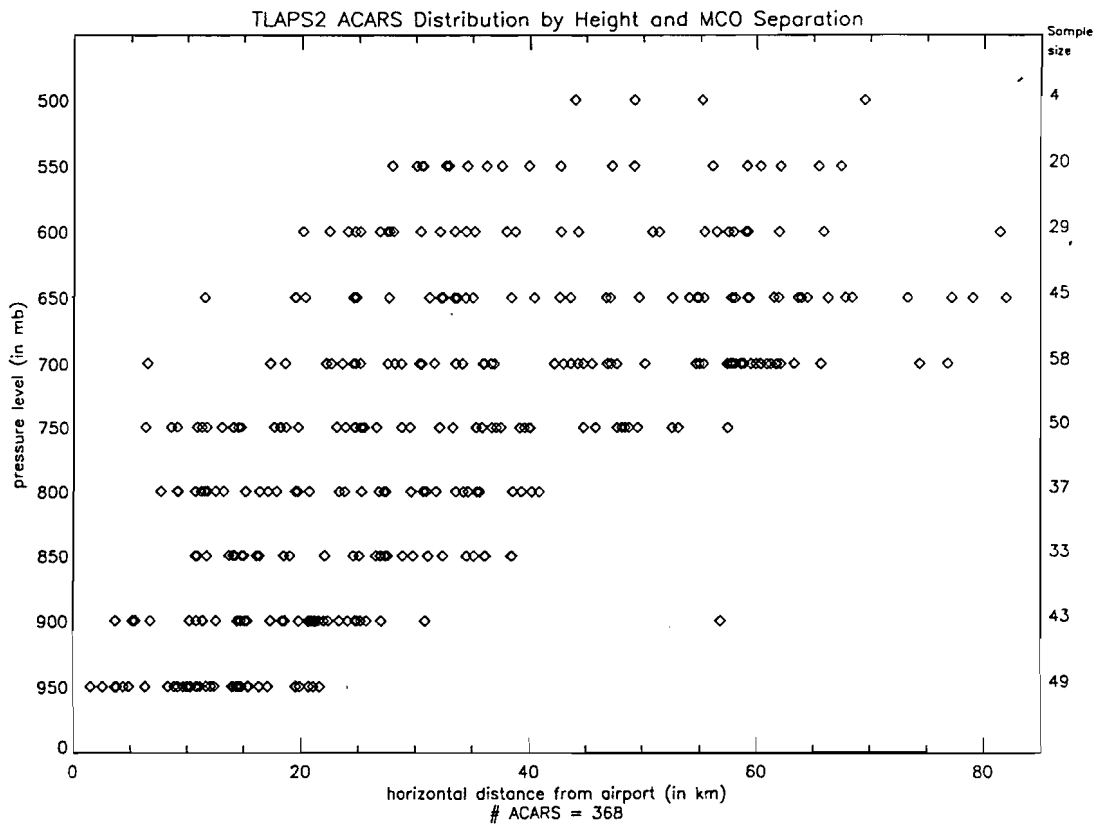


Figure 2. Vertical distribution of ACARS observations.

Table 3.
Height Distribution for the Three Observational Data Sets

Sample Size per Level	Level (in mb) Nominal	Altitude MSL (in feet)	Observational Data set Type		
			ACARS	CLASS	Dual Doppler
	500	18290	4	9	0
	550	15960	20	7	2.9K
	600	13800	29	10	1.8K
	650	11780	45	9	1.3K
	700	9880	58	10	2.1K
	750	8090	50	12	2.3K
	800	6390	37	12	2.7K
	850	4780	33	10	1.6K
	900	3240	43	10	6.2K
	950	1770	49	11	47.8K
	1000	360	0	4	1.4K
	Totals		368	104	70.1K

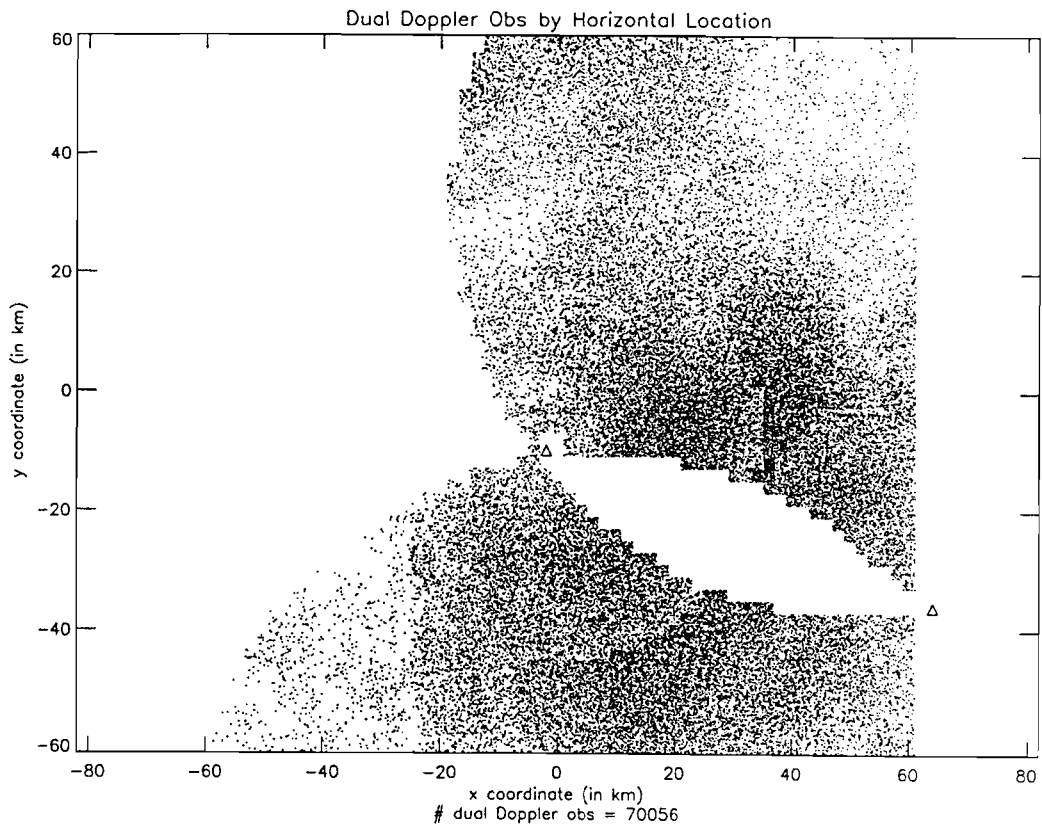


Figure 3. Horizontal distribution of dual-Doppler observations.

3. COMPARATIVE EVALUATION

A focal point of the T-LAPS evaluation is the comparison of gridded analysis winds with observed winds. We emphasize that observations are not perfect. Errors in the observations can be due to the sensor, or to the representativeness of an observation. By the latter we refer to the fact that instantaneous point measurements contain high-frequency components which are noise relative to the 2 km or 10 km scales of analysis. We cannot expect the agreement between independent observations and analyses, on average, to be less than the average magnitude of the error in the observations. This limits the ability of the comparison to discern product accuracy to the accuracy of the comparison observations.

Five types of wind analyses are evaluated:

- T-LAPS2 BI2 (2 km grid, five-minute update with two-pass Barnes routine)
- T-LAPS2 BI3 (2 km grid, five-minute update with three-pass Barnes routine)
- T-LAPS10 BI2 (10 km grid, 30-minute update with two-pass Barnes routine)
- T-LAPS10 BI3 (10 km grid, 30-minute update with three-pass Barnes routine)
- MAPS (forecast interpolated to 10 km grid, 30-minute update)

and three verification data sets are available:

- ACARS observations
- CLASS sounding observations
- Dual-Doppler data

Comparisons between gridded winds and observed winds were constrained to the T-LAPS2 domain to ensure consistent evaluation data sets and because product accuracy is paramount in this region. We also decided, for evaluation purposes only, to interpolate T-LAPS10 and MAPS to the same 2 km grid as T-LAPS2. This was done so that the error associated with positioning an observation at the nearest analysis grid point would be equal in all cases. We refer to this finely-interpolated T-LAPS10 as the “10 km analysis.”

Figure 4 provides an explanation of the symbols used in Figures 5, 6, 7, and 8. The extreme tail percentiles should be interpreted with caution for the CLASS sounding comparison, in particular, since the CLASS effective sample size was quite small (Appendix C). The RMS differences, unlike the central percentiles, are sensitive to outliers in the relevant data sets. For this reason, the 50th percentile (as a measure of centrality) and the difference of the 75th percentile and the 25th percentile (as a measure of variability) are more appropriate than RMS differences.

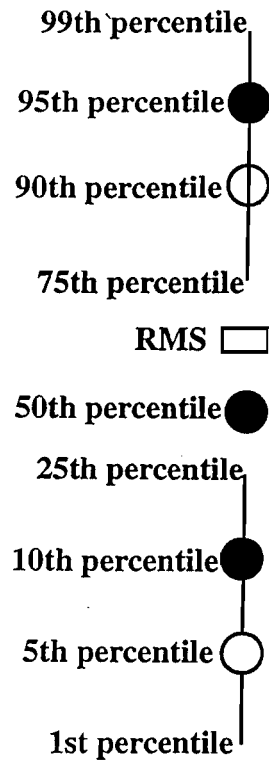


Figure 4. Key for distribution line plots.

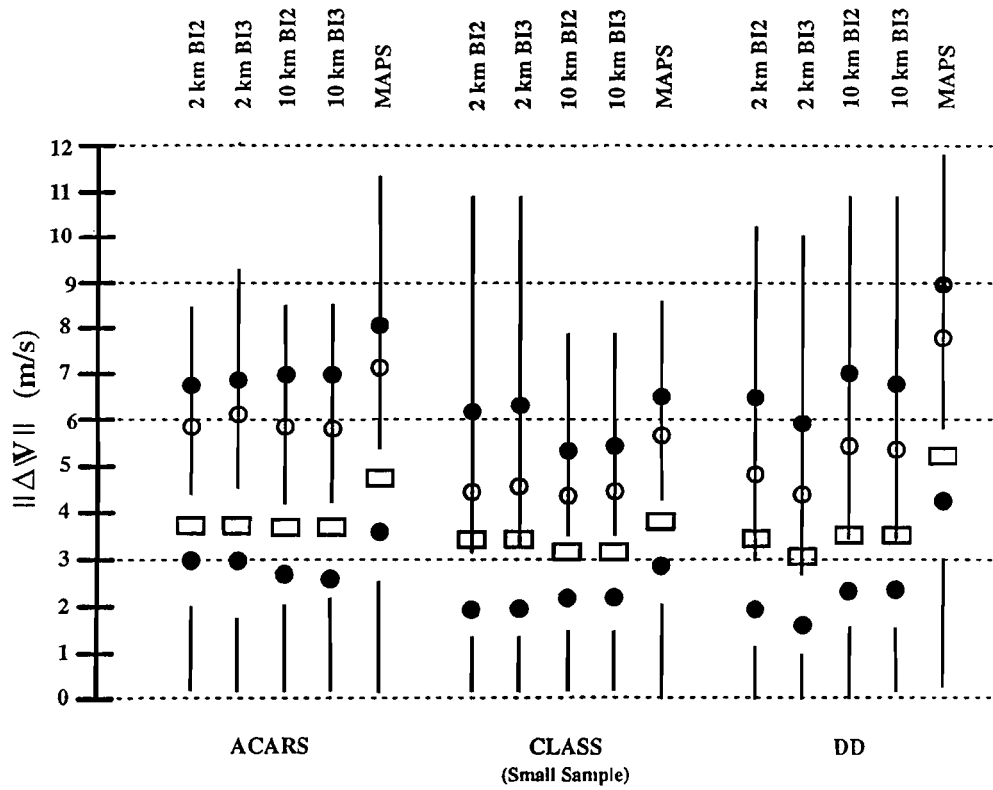


Figure 5. Norm of wind vector difference distributions.

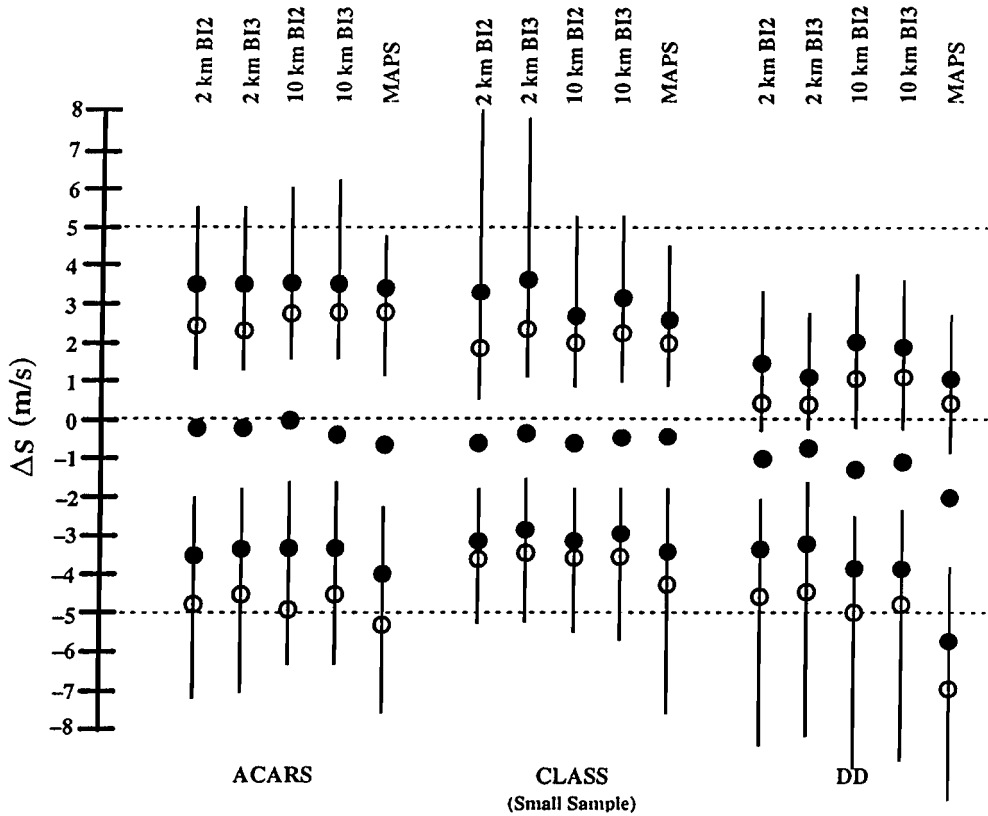


Figure 6. Wind speed difference distributions.

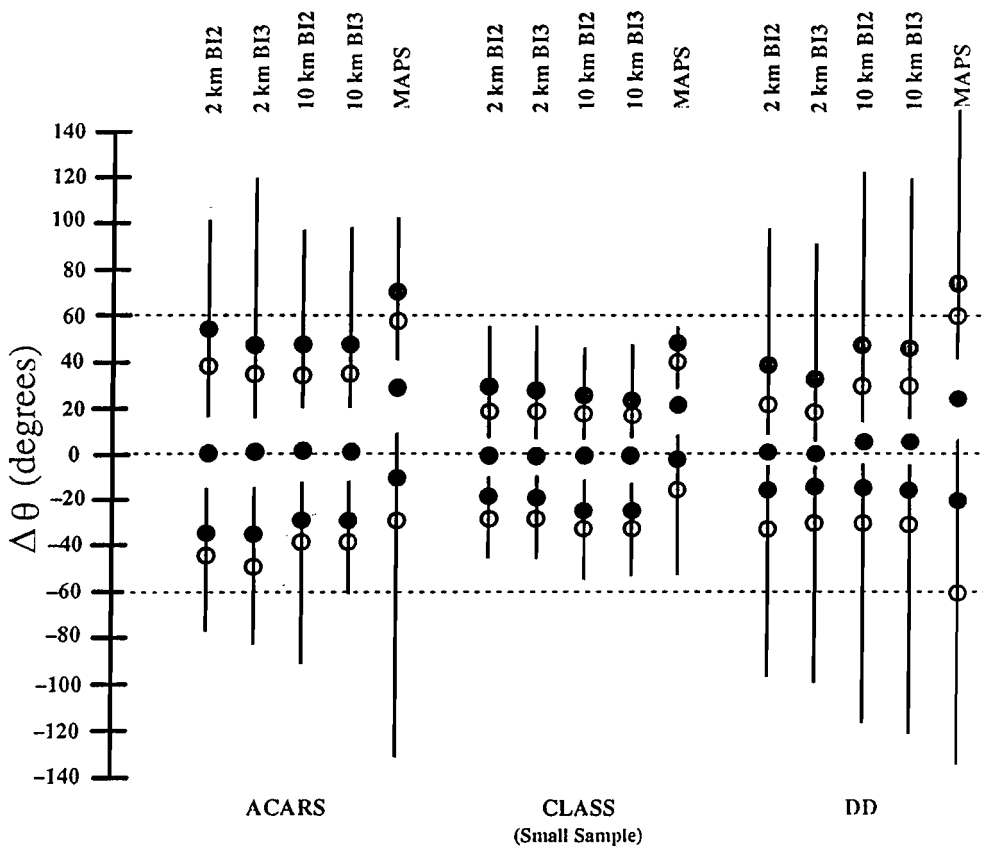


Figure 7. Wind direction difference distributions.

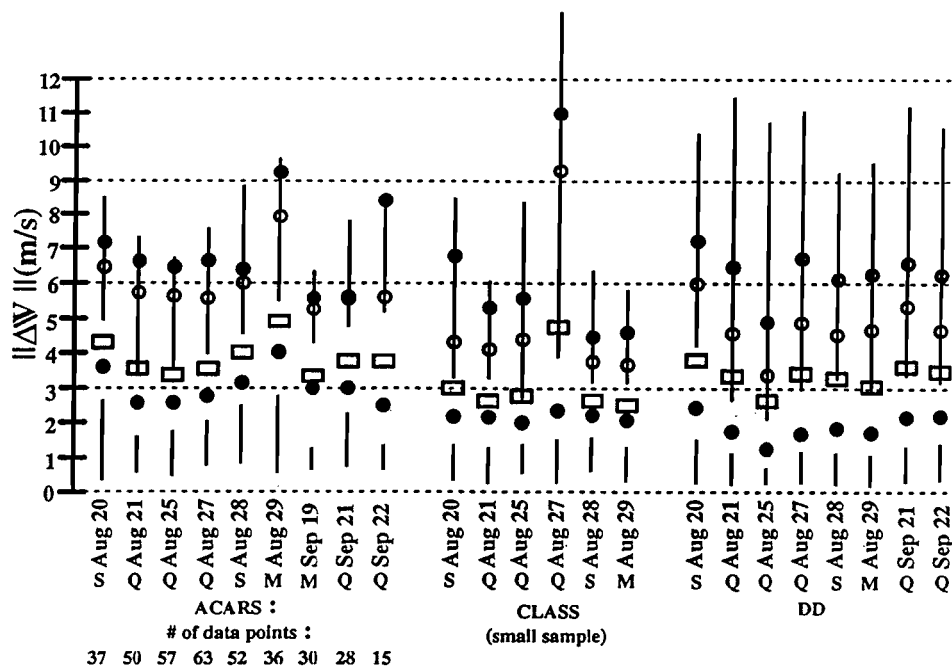


Figure 8. Norm of wind vector difference distributions stratified by day.

Fifteen distributions, one for each pair of wind analysis and observational data set, were studied. Figures 5, 6, and 7 exhibit fifteen distributions apiece and provide statistical information regarding:

- Norm of wind vector differences (Figure 5)
- s (wind speed) differences (Figure 6)
- θ (wind direction) differences (Figure 7)

By “norm of wind vector difference” we mean the square root of the sum of the u wind difference, squared, and the v wind difference, squared. The norm of wind vector difference is a non-negative random variable and is non-Gaussian. This contrasts with the other random variables under consideration, which each appear to be nearly Gaussian (Appendix C).

One important issue these results address is the winds analysis performance as a function of grid resolution and update rate. For simplicity of discussion, let us restrict attention to Figure 5. T-LAPS clearly outperforms MAPS relative to each of the three observational data sets. It is surprising, nevertheless, how well MAPS performs. The blended three-hour and six-hour MAPS forecasts have a root mean square vector difference (RMSVD) of 4.7 m/s relative to ACARS. One might have expected a larger RMSVD. Cairns, *et al.*, 1993 reports an RMSVD of 5.6 m/s for the MAPS three-hour forecast and an RMSVD of 5.8 m/s for the MAPS six-hour forecast. The latter two RMSVDs represent national averages. Since Orlando has lower than average wind speeds, the Orlando MAPS RMSVD is not unexpectedly smaller.

The performance of T-LAPS2 versus T-LAPS10 is more ambiguous. Against ACARS, T-LAPS2 BI3 has an RMSVD of 3.8 m/s whereas T-LAPS10 BI3 has an RMSVD of 3.7 m/s, and T-LAPS2 BI3 has a median vector difference (MVD) of 3.0 m/s whereas T-LAPS10 BI3 has an MVD of 2.8 m/s. The distinction between these values is insignificant, given the ACARS sample size of 368. There is no statistical evidence that T-LAPS2 compares better against ACARS than T-LAPS10. Against CLASS soundings, the RMSVD favors T-LAPS10 whereas the MVD favors T-LAPS2, but again the distinction is insignificant. The similarity in performance of T-LAPS2 and T-LAPS10 may reflect that we have reached the limit of these data sets to discern algorithm performance. Against the CLASS sounding data, the two analyses have nearly a 3 m/s RMSVD, which is the reported accuracy of the CLASS system.

Against the dual-Doppler observations T-LAPS2 compares significantly better than T-LAPS10. However, since the data used by the dual-Doppler analysis is also used by the T-LAPS2 analyses, it is theoretically possible for them to be in complete agreement. The fact that their differences are large compared to the expected errors in the dual-Doppler analysis reflect the fact T-LAPS uses a Doppler data assimilation that is mathematically inferior to dual-Doppler analysis and that T-LAPS imposes substantial area averaging.

Figure 6 indicates that T-LAPS has a low speed bias relative to observed winds. When the observed wind speeds exceeds 5 m/s, T-LAPS2 underestimates the wind speed on average by 12 percent relative to ACARS, 14 percent relative to CLASS, and 16 percent relative to dual-Doppler analysis. Figure 7 indicates that T-LAPS wind direction estimates are unbiased.

Figure 8 illustrates the day-to-day variability of the norm of the vector difference statistics for T-LAPS BI2. Quiet weather days are denoted by "Q," moderately convective days by "M" and strongly convective days by "S." Nine days of ACARS (with daily sample sizes indicated), eight days of dual-Doppler analyses, and six days of CLASS soundings are available. Caution must be applied, again, when examining extreme percentiles for ACARS or CLASS differences since sample sizes are small. There is a considerable amount of variability in day-to-day performance. It appears that with ACARS, but not dual-Doppler, convective days (M and S) have larger 50th percentile differences than quiet days (Q).

The statistics portrayed in Figures 5, 6, and 7 reflect the full nine-day evaluation data set, with quiet and active weather considered together. One might expect T-LAPS2 to be more accurate than T-LAPS10 in strongly convective situations when the radars provide dense coverage and the wind patterns are elaborate. The six-hour strongly convective weather data set is insufficient to assess the performance difference between the fine and coarse analyses, relative to ACARS and CLASS. Comparisons against dual Doppler in this six-hour period indicate a slight benefit in using the 2 km analysis over the 10 km analysis. The improvement is similar to that observed in Figure 5 for the entire nine-day period.

Another issue these results address is the performance of T-LAPS BI3 versus T-LAPS BI2. Against the ACARS and CLASS data sets, the two techniques appear to be indistinguishable. That the T-LAPS BI3 analysis is better tuned to radar data than T-LAPS BI2 is shown by the comparison to dual-Doppler analysis.

4. CONTINUITY EVALUATION

The T-LAPS analysis self-consistency checks, mentioned in Section 1.1., are based on the principle that winds usually vary continuously over space and time. Exceptions to this principle include meteorological events such as gust fronts, sea breezes, and microbursts. We have computed the empirical distributions of differences of T-LAPS winds at all levels from:

- Adjacent grid points (points immediately to the north, south, east and west) on the same level and at the same time
- The same grid points with five minutes separation.

These two types of computations are called, respectively, spatial continuity evaluation and temporal continuity evaluation. Relevant statistical parameters include MVD, RMSVD, and various percentiles. Tables 4 and 5 present the results of the continuity evaluation. The parameter estimates are largely consistent with the principle that winds usually vary continuously.

Table 4.
T-LAPS2 Spatial Continuity – Adjacent Grid Points, Same Level

Parameter Estimates (In m/s)		BI2	BI3
	RMSVD		0.1
99 th percentile		0.5	0.6
95 th percentile		0.3	0.3
90 th percentile		0.2	0.2
75 th percentile		0.1	0.1
MVD		0.1	0.1

Table 5.
T-LAPS2 Temporal Continuity – Five Minutes Separation, Same Grid Point

Parameter Estimates (In m/s)		BI2	BI3
	RMSVD		1.4
99 th percentile		5.6	5.8
95 th percentile		3.0	3.3
90 th percentile		2.0	2.3
75 th percentile		1.0	1.2
MVD		0.4	0.5

The temporal continuity for BI3 shows 95th and 99th percentiles, 3.0 m/s and 5.6 m/s, respectively, that are not consistent with the hypotheses that the wind fields usually vary continuously. The large temporal discontinuities usually occur at horizontal levels without Doppler data and are primarily the result of the method used to assimilate ACARS observations. ACARS observations are often sparse, and when only one ACARS observation is available for a few

horizontal levels it is given full weight at each analysis point on the level at which the observation was taken, and the two adjacent levels. When this single observation disagrees with the MAPS background field, the T-LAPS10 wind field for the three levels affected abruptly shifts to match the observation. This shift occurs when the ACARS observation is first brought into the analysis. The analysis abruptly shifts back when the observation is dropped from the analysis 90 minutes after the observation time. Since this occurs above levels with Doppler data, the temporal discontinuity is passed on to T-LAPS2. In T-LAPS2 this causes a discontinuity at each point on three of the eleven horizontal levels. Very few occurrences of this behavior give the large 99th percentile value. A similar effect is seen when a small number of ACARS are available, but usually over only portions of horizontal levels. Examples 5.2. and 5.3. illustrate similar phenomena when Doppler data are scarce.

5. SOME EXAMPLES

This section presents three examples which provide insight into the success and failure modes of T-LAPS. The first example demonstrates that T-LAPS2 provides benefit over T-LAPS10 during strongly convective weather. An examination of the LAPS Barnes Interpolation led us to anticipate that the T-LAPS analysis is vulnerable to undesirable behavior at times of sparse input data (Appendix A). The last two examples in this section demonstrate extreme cases of this behavior. Analysis discontinuities like these, on the order of 15 to 20 m/s, are very rare as indicated by Tables 4 and 5.

In figures depicting wind fields, T-LAPS2 wind vectors are depicted by white arrows and T-LAPS10 wind vectors are depicted by red arrows. The 2 km resolution wind fields are displayed at a 4 km resolution to reduce visual clutter. Wind vectors are scaled to wind speed, with a 5 m/s arrow shown for scale in the upper right corner of the display. The airport runways are shown in the center, the four outlines are lakes, and the ocean coast appears along the northeast. The TDWR radar site is slightly south of the airport and the NEXRAD radar site is near the southeastern corner of the display. Radial velocities are shown by color: warm colors for wind directed away from the radar and cool colors for wind directed towards the radar.

5.1. An Example of the Benefit of a Fine Scale Analysis

While bulk statistics do not indicate that the 2 km analysis provides much value beyond the 10 km analysis, the following example shows that the 2 km analysis contains much more detailed information.

A line of intense thunderstorms passed through the Orlando area in the evening of August 20. The MAPS forecast winds for 2310 Greenwich Mean Time (GMT) at 3200 feet mean sea level (MSL), Figure 9, shows weak uniform southwest winds. The corresponding T-LAPS10 BI3 wind field, Figure 10, exhibits somewhat greater wind variability than MAPS but does not indicate the level of storm-induced wind.

In contrast, the T-LAPS2 BI3 wind field, Figure 11, is far from uniform, with the wind field containing circulations resulting from the outflows of several storm cells. Surface level TDWR reflectivity data, shown as the colored background in Figure 12, indicate storms with reflectivities up to 55 dbZ, confirming the strength of the storm.

5.2. An Example of Spatial Discontinuity

In this example we examine the effect of sparse data in the T-LAPS Barnes analysis. When there are two widely spaced observations on the same analysis level, T-LAPS produces a wind field whose wind vectors agree closely with the nearest observation (See Appendix A). If the two observations are significantly different, the resulting wind field splits abruptly along the line of points at an equal distance from the two observations. On each side of this line the winds agree closely with the observation lying on that side. In this example the two observations are from the NEXRAD radar, but this will occur with any two observations. We show BI3 wind fields, but this occurs in BI2 as well.

Figure 13 depicts the T-LAPS BI3 wind field on September 22, at 1540 UTC, and 8100 feet MSL. At this time and level, no radar data were available from either TDWR or NEXRAD. This light, uniform wind flow persisted in the analysis for ten minutes and then was interrupted at 1555 UTC (Figure 14). The only change at 1555 was the introduction of two widely separated NEXRAD data points to the T-LAPS2 analysis. The TDWR radar was not operating at the time. Radial velocity estimates, indicated by small color squares in the display, are 9 m/s toward NEXRAD in the northeast quadrant and 0 m/s in the southeast quadrant. The wind field is divided into two regions, each containing wind vectors in close agreement with the observation located within it.

5.3. An Example of Temporal Discontinuity

In this example we examine the sensitivity of the BI3 analysis when the overlap in the regions of Doppler radar return from two radars contains very few analysis points. This sensitivity is not seen in the BI2 analysis. We examine the wind fields from BI2 and BI3 for two consecutive analysis times. There is a strong correlation between the consecutive wind fields produced by the BI2 analysis. The consecutive wind fields produced by the BI3 analysis are very dissimilar. The difference in the wind fields produced by BI2 and BI3 arises from their different use of the Doppler data for the points that have Doppler data from both radars. In the BI3 analysis, these data are treated as a special class of observations. When there are very few observations of this type the analysis is very sensitive to them (See Appendix A). A similar discontinuity arises in both BI2 and BI3 when a single ACARS observation or data point is brought into the analysis that does not agree with the background wind field.

Each wind field in this example is from August 20, at 3200 feet MSL. Figure 15 depicts the T-LAPS BI2 wind field at 2110 UTC and NEXRAD radial velocities. Figure 16 depicts the corresponding T-LAPS BI2 wind field and NEXRAD data five minutes later. These two wind fields are very similar, as are the corresponding NEXRAD data.

Figure 17 depicts the T-LAPS BI3 wind field at 2110 UTC and TDWR radial velocities. This wind field is very similar to the corresponding BI-2 wind field. Figure 18 depicts the T-LAPS BI3 wind field and TDWR data five minutes later. The BI3 wind field at 2115 is very dissimilar to both 2110 UTC analyses and the BI2 2115 UTC analysis.

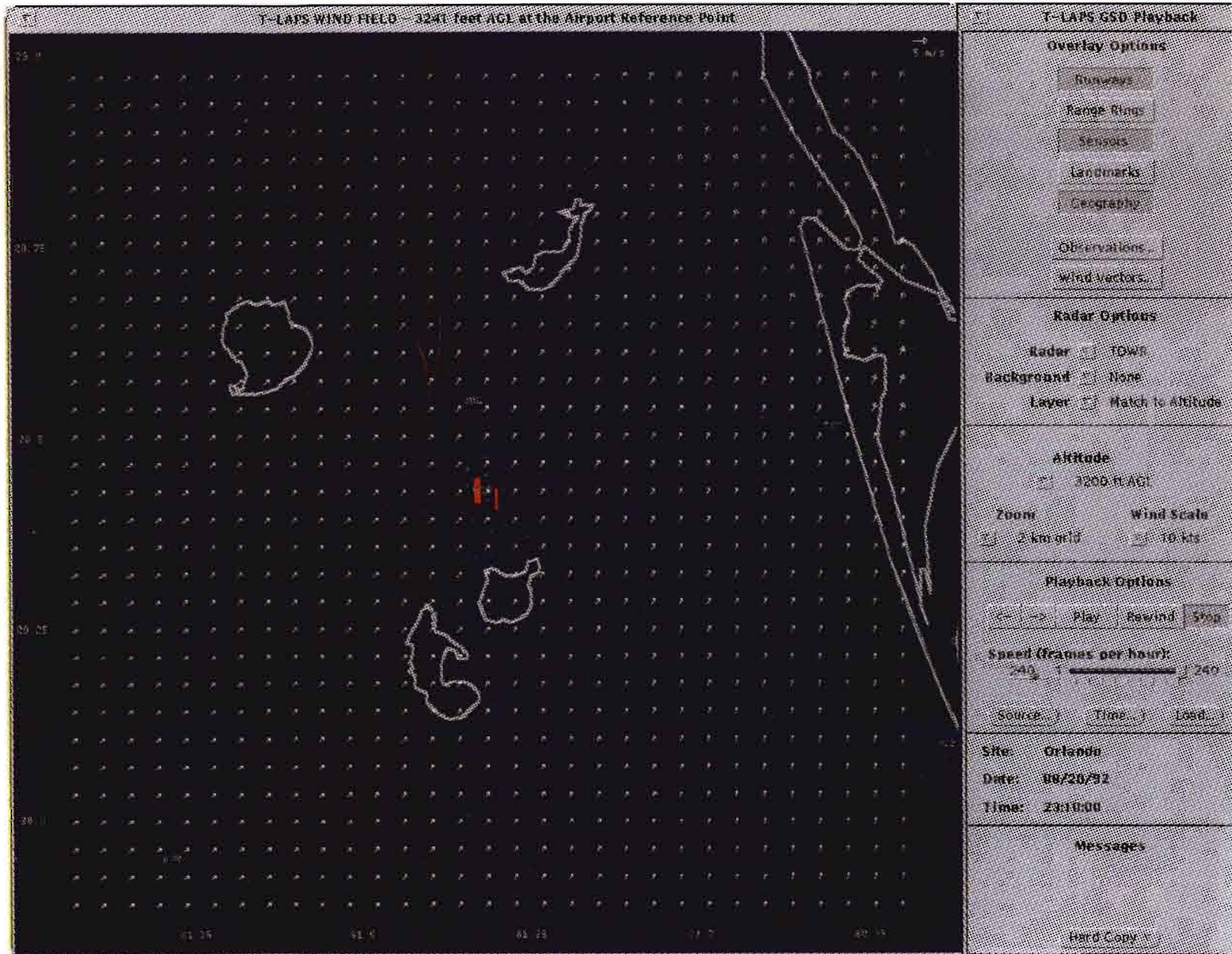


Figure 9. MAPS wind field at 2310 UTC, August 20, 1992, 3200 feet mean sea level (MSL).

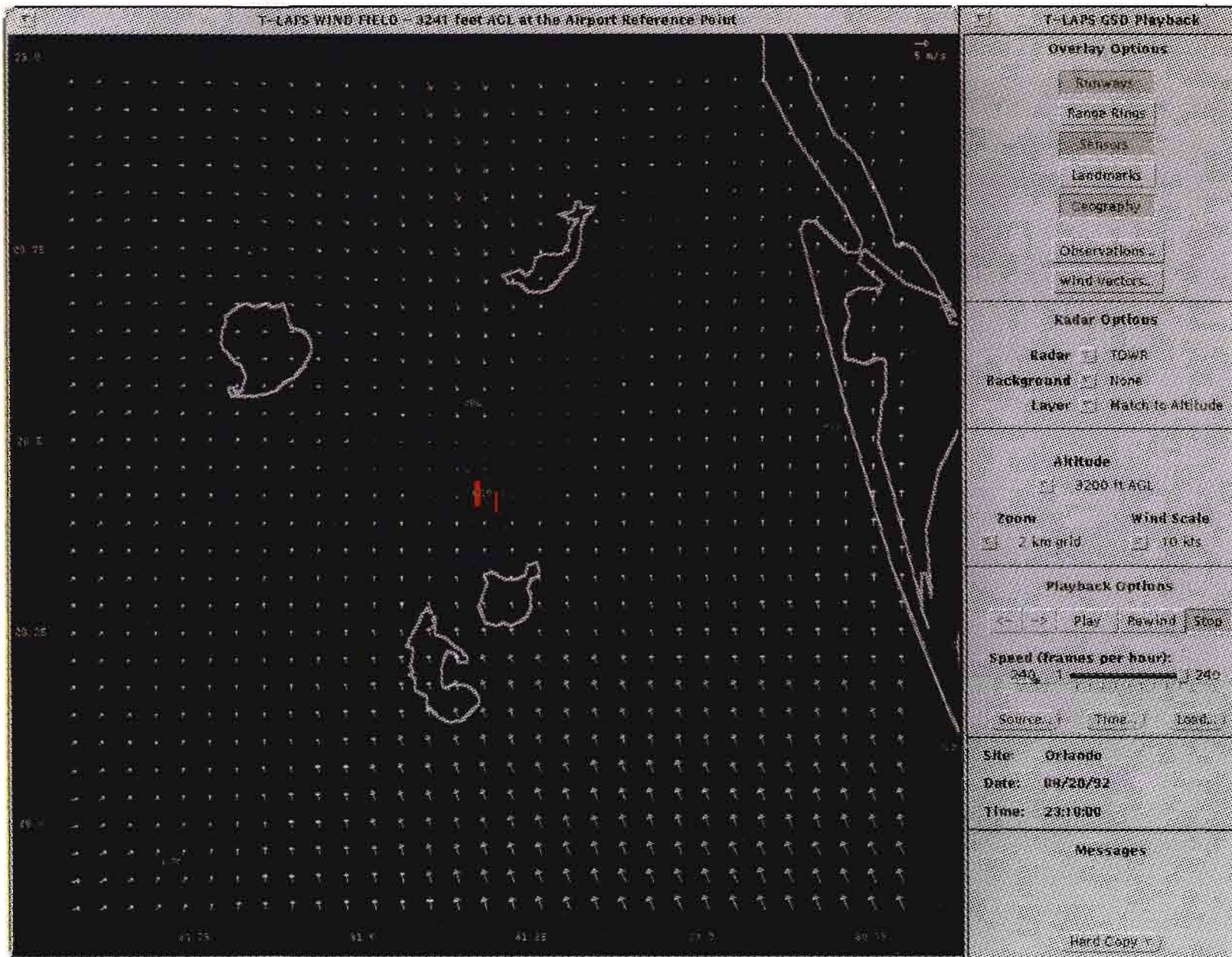


Figure 10. T-LAPS10 BI-3 wind field at 2310 UTC, August 20, 1992, 3200 feet MSL.



Figure 11. T-LAPS10 BI-2 wind field at 2310 UTC, August 20, 1992, 3200 feet MSL.

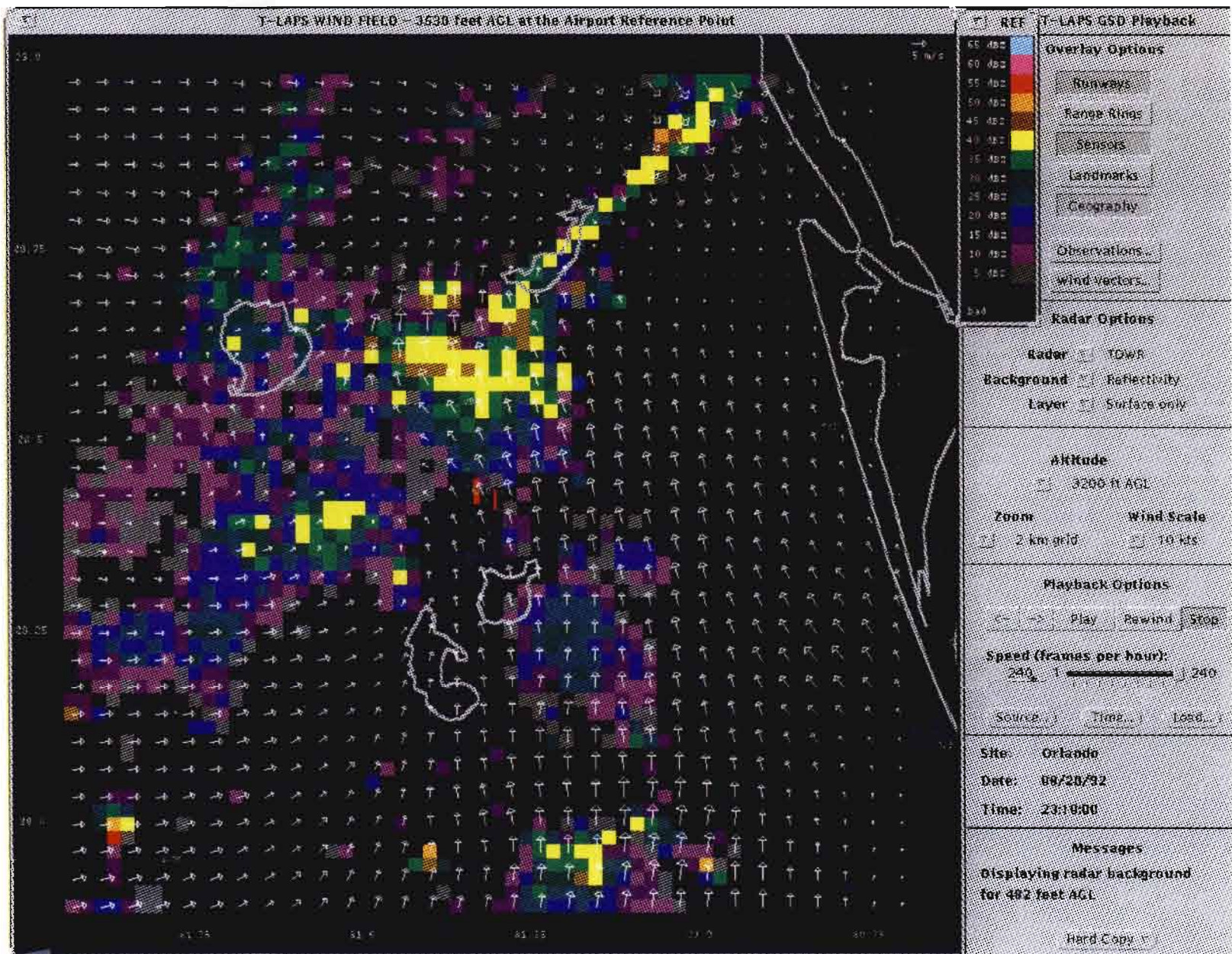


Figure 12. T-LAPS10 BI-2 wind field and TDWR reflectivity at 2310 UTC, August 20, 1992, 3200 feet MSL.

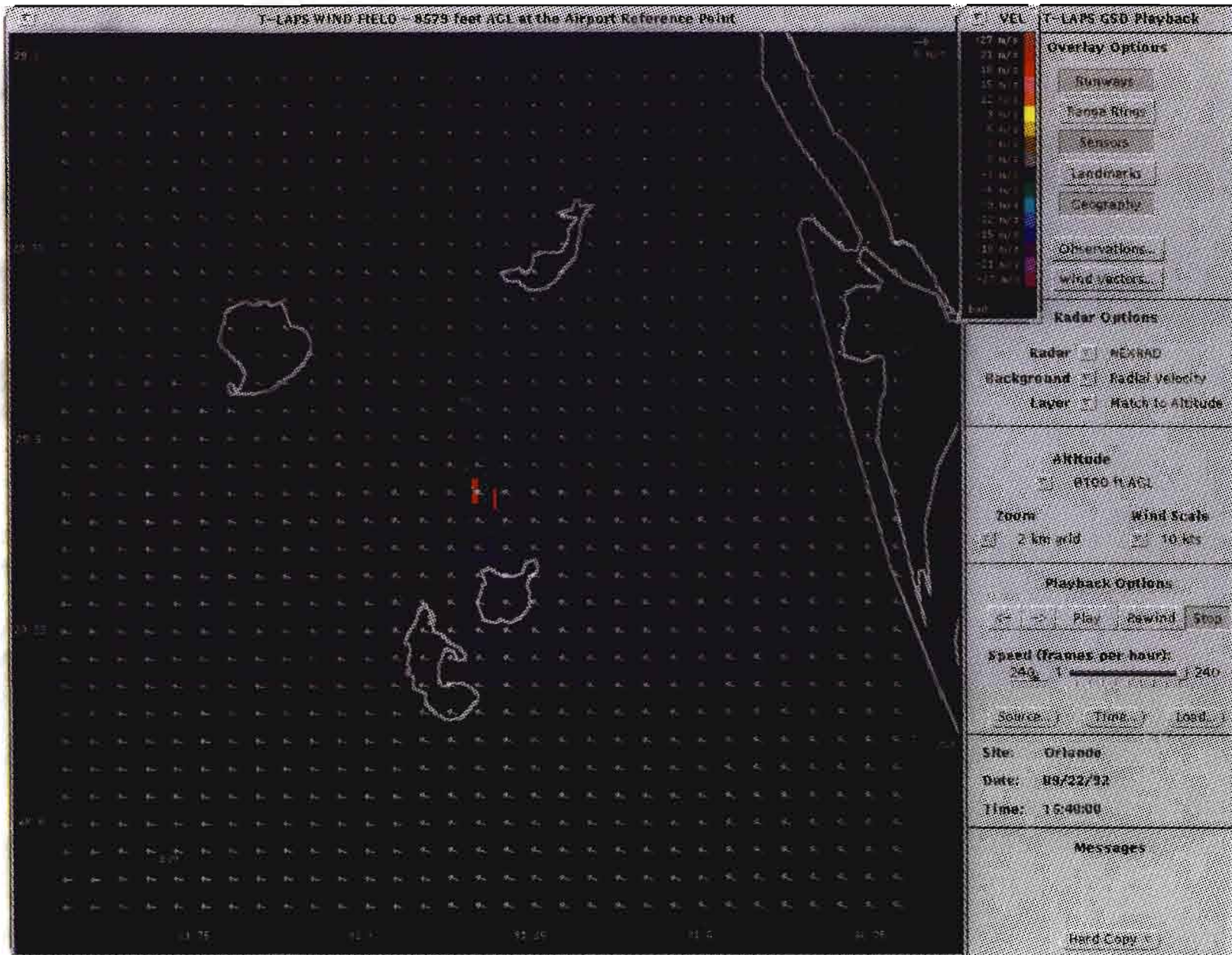


Figure 13. T-LAPS BI3 wind field at 1540 UTC, September 22, 1992, 8100 feet MSL.

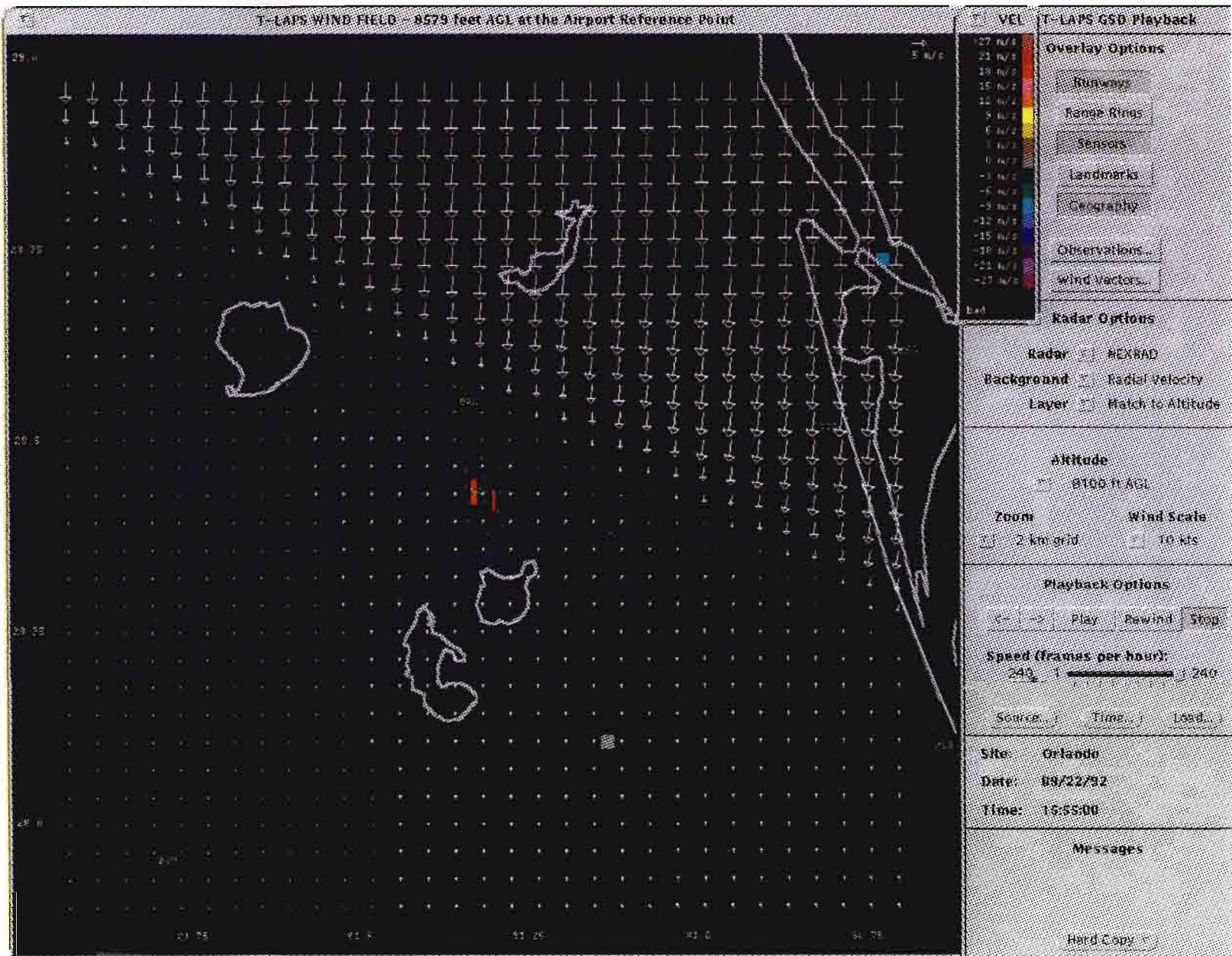


Figure 14. T-LAPS B13 wind field at 1555 UTC, September 22, 1992, 8100 feet MSL.

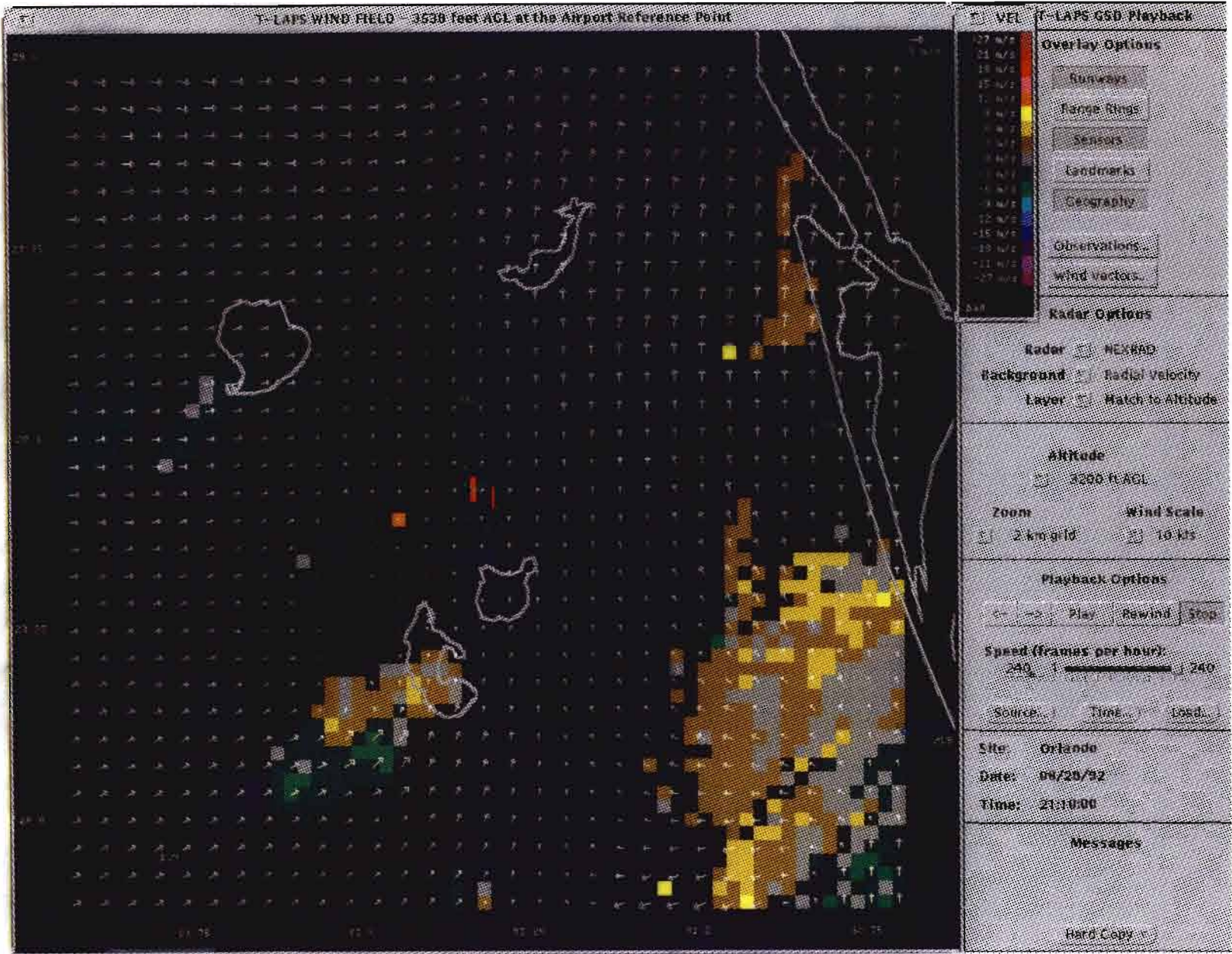


Figure 15. T-LAPS BI2 wind field at 2110 UTC, August 20, 1992, 3200 feet MSL.

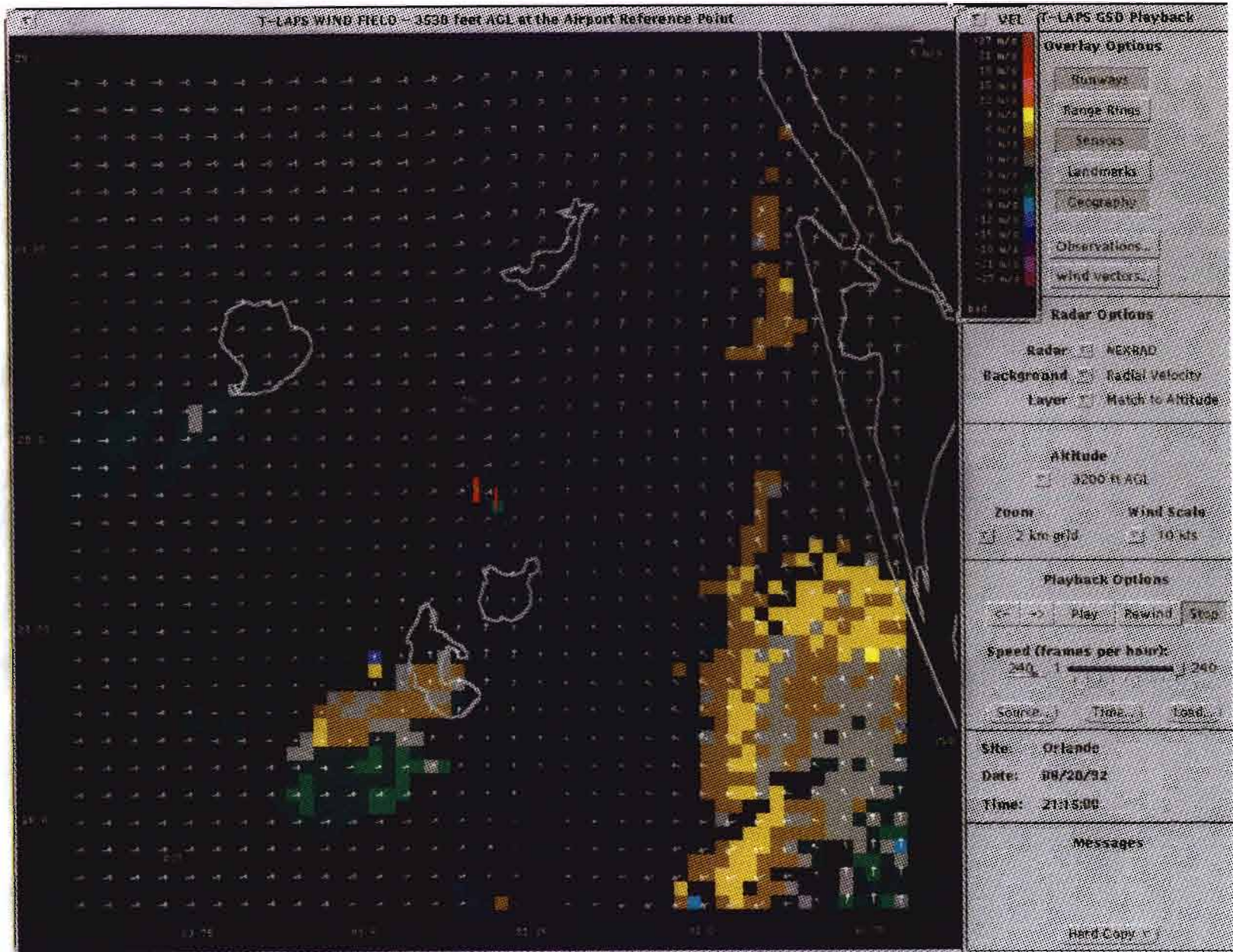


Figure 16. T-LAPS B12 wind field at 2115 UTC, August 20, 1992, 3200 feet MSL.

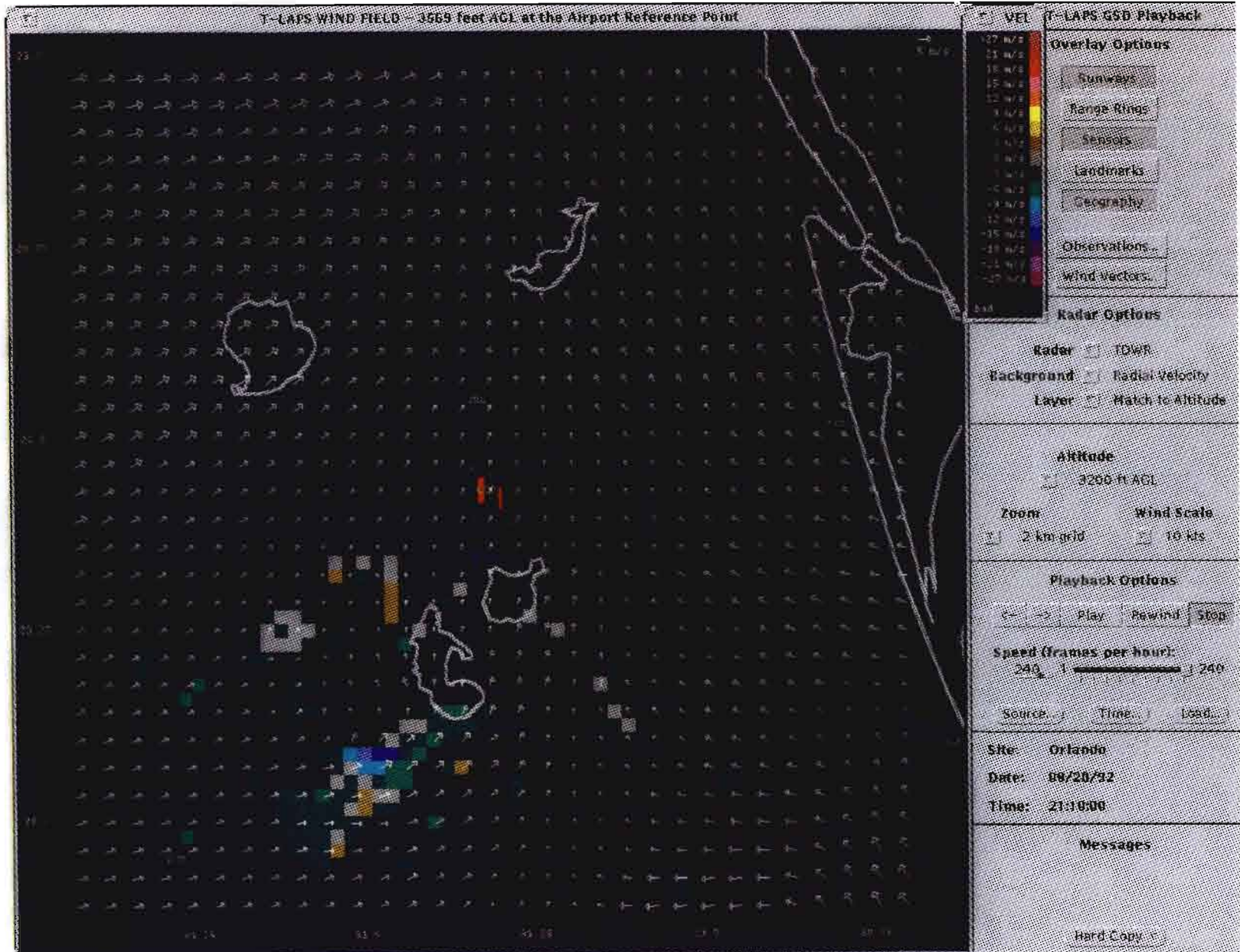


Figure 17. T-LAPS B13 wind field at 2110 UTC, August 20, 1992, 3200 feet MSL.



Figure 18. T-LAPS B13 wind field at 2115 UTC, August 20, 1992, 3200 feet MSL.

At 2115 UTC, the TDWR region of Doppler return dwindles to a single point (Figure 18). NEXRAD also has a Doppler return at this point. This pair of Doppler returns is used by BI3 to produce a wind vector that is treated as a special type of observation. BI3 assigns effectively infinite influence to this single observation. Since this observation does not agree with the other wind fields, it causes the dissimilarities.

6. SUMMARY

T-LAPS, a gridded three-dimensional winds analysis for the airport terminal area, is based on LAPS, which was developed at NOAA's FSL. LAPS was jointly modified by FSL and Lincoln Laboratory to function on a fine spatial scale with rapid temporal update and to incorporate multiple-Doppler radar data inputs. This modification was done for the purpose of assessing the capability of current technology.

This report describes the evaluation of the summer 1992 Orlando demonstration of T-LAPS. Three approaches were used:

- Compute analysis-vs-observation comparative statistics
- Assess analysis continuity in space and time
- Examine cases of discontinuous behavior

The report focuses on the results of the first approach in this report. The observational data sets used in the comparison were ACARS observations, CLASS soundings, and dual-Doppler analysis. Nine days containing 70 hours of data from the demonstration period were selected for evaluation.

The comparison of the T-LAPS analysis wind fields with observations shows that T-LAPS provides a significant improvement over MAPS. The median and RMS vector differences for T-LAPS and MAPS against the three comparison data sets are given in Table 6. The bulk statistics show only a slight benefit from the 2 km resolution T-LAPS analysis beyond the 10 km resolution analysis. A significant benefit of the 2 km resolution analysis was found during some convective weather situations.

Table 6.
Median and RMS (in parentheses) Vector Differences (m/s)

	T-LAPS2 BI3	T-LAPS10 BI3	MAPS
ACARS	3.0 (3.8)	2.8 (3.7)	3.6 (4.7)
CLASS	2.1 (3.2)	2.3 (3.0)	3.0 (3.7)
dual Doppler	1.6 (3.1)	2.3 (3.6)	4.1 (5.3)

The magnitude of the disagreement between the T-LAPS 2 km analysis and the dual-Doppler analysis is quite large. The 1.6 m/s MVD and 3.1 m/s RMSVD are large compared with the expected RMSVD of 1 m/s for the dual-Doppler analysis. The disagreement is especially large given the data dependence between the two analyses. Consequently, one suspects that the 2 km resolution analysis is not making the best possible use of the Doppler data.

T-LAPS has a low wind speed bias, compared with observations. When the observed wind speed exceeds 5 m/s, T-LAPS underestimates the wind speed on average by 12 percent against ACARS, 14 percent against CLASS soundings, and 16 percent against dual-Doppler analysis. T-LAPS wind direction estimates were unbiased.

Case studies show improved detail for T-LAPS2 in convective weather. The nine-day evaluation data set consists of 70 hours of data collected during quiet and active weather. Only six hours of the data were collected during strongly convective weather. Since we expect the benefits of fine-scale T-LAPS to show most of all within convective and rapidly evolving situations, there is a compelling need for further data collection and evaluation.

GLOSSARY

ACARS	Aircraft Communications Addressing and Reporting System
AGL	Above Ground Level
ARINC	Aeronautical Radio, Inc.
CLASS	Cross Loran Atmospheric Sounding System
DDA	Dual-Doppler Analysis
ERL	Environmental Research Laboratory
FSL	Forecast Systems Laboratory
UTC	Universal Coordinated Time
ITWS	Integrated Terminal Weather System
LAPS	Local Analysis and Prediction System
LLWAS	Low Level Wind Shear Alert System
MAPS	Mesoscale Analysis and Prediction System
MCO	Orlando International Airport
MDCRS	Meteorological Data Collection and Reporting System
MIT	Massachusetts Institute of Technology
MSDA	Multiple Single-Doppler Analysis
MSL	Mean Sea Level
MVD	Mean Vector Difference
NEXRAD	Next Generation Weather Radar (WSR-88D)
NOAA	National Oceanic and Atmospheric Administration
RMS	Root Mean Square
RMSVD	Root Mean Square Vector Difference
T-LAPS	Terminal area-Local Analysis and Prediction System
TATCA	Terminal Air Traffic Control Automation
TDWR	Terminal Doppler Weather Radar
WVAS	Wake Vortex Advisory System

REFERENCES

- Albers, S. C., "The LAPS Wind Analysis," *Fourth Workshop on Operational Meteorology*, Whistler, B.C., Canada, 1992.
- Armijo, L., "A Theory for the Determination of Wind and Precipitation Velocities with Doppler Radars," *Journal of Atmospheric Sciences*, 26, 570–573, 1969.
- Barnes, S., "A Technique for Maximizing Details in Numerical Weather Map Analysis," *Journal Applied Meteorology*, 3, No 4, 1964.
- Benjamin, S., K. Brewster, R. Brummer, B. Jewett, T. Schlatter, T. Smith and P. Stamus, "An Isentropic Three-Hourly Data Assimilation System Using ACARS Aircraft Observations," *Monthly Weather Review*, Vol. 119, No 4, 888–906, 1991.
- Cairns, M., *et al.*, "A Preliminary Evaluation of Aviation-Impact Variables Derived From Numerical Models," NOAA Technical Memo., ERL FSL-5, 1993.
- Cole, R., F. W. Wilson, J. McGinley and S. Albers, "ITWS Gridded Analysis," Preprints, American Meteorological Society, *Fifth International Conference on the Aviation Weather System*, Vienna, VA, 2–6 August 1993.
- McGinley, J., S. Albers and P. Stamus, "Validation of a Composite Convective Index as Defined by a Real-Time Local Analysis System," *Weather and Forecasting*, 6, 337–356, 1991.
- Papoulis, A., "Probability, Random Variables, and Stochastic Processes," McGraw Hill, Inc., 1965.
- Thiebaux, H. and F. Zwiers, "The Interpretation and Estimation of Effective Sample Size," *Journal of Climate and Applied Meteorology*, 23, 800–811, 1984.
- Wilson, F.W. and R.H. Gramzow, "The Redesigned Low Level Wind Shear Alert System," *Fourth International Conference on the Aviation Weather Systems*, Paris, France, 24–26 June 1991.
- Zar, J., "Biostatistical Analysis," Prentice-Hall, Inc., 1974.

APPENDIX A. T-LAPS ANALYSIS

Rodney E. Cole

A.1 Introduction

The initial prototype ITWS Terminal Winds product is an extension of the winds analysis portion of the Local Analysis and Prediction System (LAPS) (McGinley *et al.*, 1991), developed by NOAA/ERL/FSL. This prototype is called the Terminal area-LAPS (T-LAPS). The LAPS analysis combines data from the Mesoscale Analysis and Prediction System (MAPS) (Benjamin, *et al.*, 1991) with observations from a variety of sensors, such as wind profilers, ground stations, and aircraft. Several enhancements have been added to LAPS, creating an analysis system that is appropriate for terminal-area sensors and the temporal and spatial scales required for terminal operations.

There are two primary enhancements to LAPS to produce T-LAPS. The first is the development of Multiple Single-Doppler Analysis (MSDA) procedures for the assimilation of Doppler data from multiple radars. The MSDA procedures are extensions of the LAPS single-Doppler analysis. The second is the development of a "cascade of scales" to allow the analysis to step from MAPS, with a grid resolution of 60 km and an update rate of three hours, to an analysis with a grid resolution of 2 km and an update rate of five minutes. Both LAPS and T-LAPS have incorporated these enhancements.

A.2 LAPS Winds Analysis Overview

A.2.1 LAPS Barnes Interpolation

The LAPS horizontal winds analysis (Albers, 1992) uses a single iteration Barnes (1964) objective analysis scheme. The analysis acquires a background wind field and recent wind observations in the analysis region, and produces an analyzed wind field on a 3D grid. LAPS uses a 600 km x 600 km horizontal domain and a vertical extent from the surface to 100 mb, with a horizontal resolution of 10 km and a vertical resolution of 50 mb. LAPS is designed to be compatible with a background wind field provided by a previous analysis or numerical forecast model. The standard practice is to use the MAPS forecasts as the background field. The Barnes analysis used in LAPS requires that all observations be vector quantities decomposed into u and v components (north and east components). Each observation location is assigned to the grid point nearest the true observation location. This allows all distance computations to be done in integer arithmetic for efficiency. Doppler weather radars measure only a single component of the wind. These single component measurements are transformed into vector quantities during the LAPS analysis by a process discussed in Section A.2.2. For the moment, we discuss the basic LAPS Barnes analysis with the assumption that all observations are vector quantities which have been decomposed into u and v components.

The steps in the analysis process are as follows:

- Compute vector differences between observations and background (Δobs)
- Analyze Δobs to each grid point by Barnes interpolation
- Add analyzed Δobs to the background

For each observation the vector difference between the observed horizontal wind (u and v) and the background wind at the corresponding grid point is computed. These differences are corrections to the background at the observation locations.

Next, the corrections at the observation locations are analyzed to each grid point by a single iteration Barnes analysis. This gives correction terms which are estimates of the vector difference between the actual wind and the background wind at each grid point. The weights used in the Barnes analysis depend on the horizontal and vertical distances from the observation location to the analysis point, a weighting factor that varies depending on the local data density and sensor type. The correction terms are then added to the background wind to form the analyzed wind field.

In particular, at each grid point the weighted mean of the Δobs is computed using Equation A-1. The sum is over all observations, vector and Doppler, on the horizontal level of the analysis point as well as the vector observations on adjacent levels above and below. Radar data are spread vertically in the resampling prior to the analysis so only Doppler observations on the analysis level are used. The weights w_i are computed using Equation A-2. The value of d is the horizontal distance from the analysis location to the observation location measured in number of grid points. The value of $K_{1,i}$ depends on whether the i th observation is a true vector observation or derived from a Doppler observation and whether the i th observation is on the analysis level or one of the adjacent levels, as shown in table A-1. The value of K_2 varies inversely with the density of data in the vicinity of the analysis point, from $K_2 = 3$ if there is full data near the analysis point to $K_2 = 144$ if there is no data near the analysis point.

$$\overline{\Delta ob} = \frac{\sum w_i \Delta ob_i}{\sum w_i} \quad (\text{A-1})$$

$$w_i = K_{1,i} \exp(-d^2/K_2) \quad (\text{A-2})$$

Table A-1.
Values of K_1 in Equation A-2.

$K_{1,i} = 1.0$	if the i th observation is a vector observation located on the same horizontal level as the analysis location
$K_{1,i} = 0.14$	if the i th observation is a vector observation located on a horizontal level adjacent to the analysis level
$K_{1,i} = 0.05$	if the i th observation is a “radar vector observation”

A.2.2 LAPS Single-Doppler Analysis

We first review the process by which Doppler radar radial velocity observations are brought into the original LAPS analysis. The idea is to transform the radial velocity observations from a Doppler radar into vector quantities called “radar vector observations” and then to use these vectors as additional observations. The “radar vector observations” are built by estimating the missing component in the Doppler observations from the background field and the vector observations. The process utilizes the Barnes analysis step twice, and hence is called the two-pass Barnes Interpolation (BI-2) method. The fusion of the background field and vector observations for the estimation of the missing components is the purpose of the first Barnes pass. The second Barnes pass analyzes the background field, the true vector observations, and the “radar vector observations” to form the final analysis. A data flow diagram for the LAPS single-Doppler analysis is shown in Figure A-1.

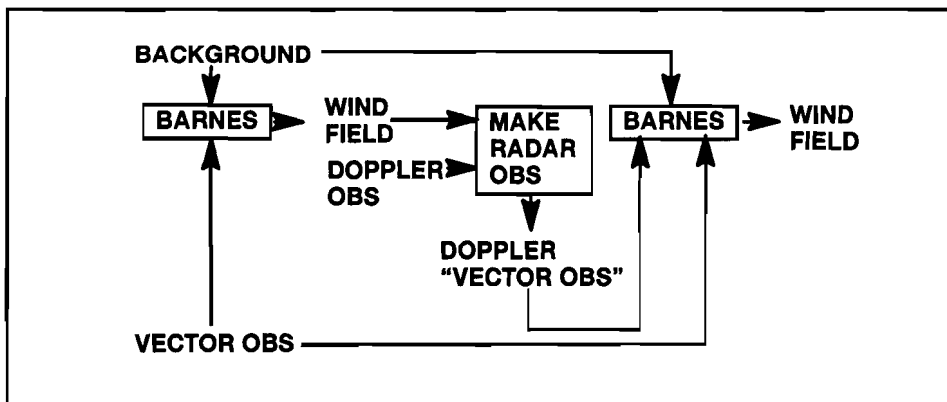


Figure A-1. Data flow for the LAPS single-Doppler analysis.

The steps used to bring Doppler observations into the analysis are as follows:

- Perform preliminary analysis (first Barnes pass)
- Construct “radar vector obs”
- Perform final analysis (second Barnes pass)

The preliminary analysis is performed as discussed in Section A.2.1 above using the background wind field and the non-radar observations.

Each “radar vector observation” is constructed from the component measured by the Doppler radar and the orthogonal component (the component not measured by the radar) from the output of the first Barnes pass. This is done by adjusting the wind estimates from the first Barnes pass at points with a Doppler wind speed estimate. At these points, the component of the wind along the radar beam is set to the Doppler value. The component perpendicular to the radar beam is unchanged. The resulting wind vectors at points with a Doppler value are considered to be “radar vector observations.”

The final analysis is computed from the original background wind field, the true vector observations, and the “radar vector observations” in the second Barnes pass as described in Section A.2.1.

A.3 Multiple Single-Doppler Analysis

The ITWS gridded winds analysis may have inputs from more than one Doppler radar, requiring the enhancement of LAPS. Two procedures for the assimilation of Doppler data from multiple radars were developed for this purpose. These procedures, which we call Multiple Single-Doppler Analysis (MSDA) techniques, are more suited for unsupervised operational analysis than traditional Dual-Doppler Analysis (DDA) (Armijo, 1969) because they are able to automatically handle such problems as incomplete data and baseline instability. The first is a simple extension of the two-pass Barnes method described above. The second method, described below, incorporates a third Barnes pass and is referred to as a three-pass Barnes. The MSDA techniques are simple extensions of the original LAPS Doppler analysis in that they differ from the original LAPS analysis only in how the “radar vector observations” are constructed. In 1992, the Orlando testbed had data available from the Melbourne NEXRAD and the Lincoln TDWR prototype, FL-2.

A.3.1 BI-2

The data flow for the two-pass Barnes MSDA method is given in Figure A-2. This figure differs from Figure A-1 only in the additional Doppler input stream into the “make radar obs” module. In the two-pass Barnes MSDA method, the “radar vector observations” are constructed from the preliminary analysis by first adjusting the wind field at points with a NEXRAD Doppler wind speed estimate. At these points, the component of the wind along the radar beam is set to the NEXRAD Doppler value. The component perpendicular to the radar beam is unchanged. Next, the resulting wind field is adjusted at points with a TDWR Doppler wind speed estimate. At these points, the component of the wind along the radar beam is set to the TDWR Doppler value. The

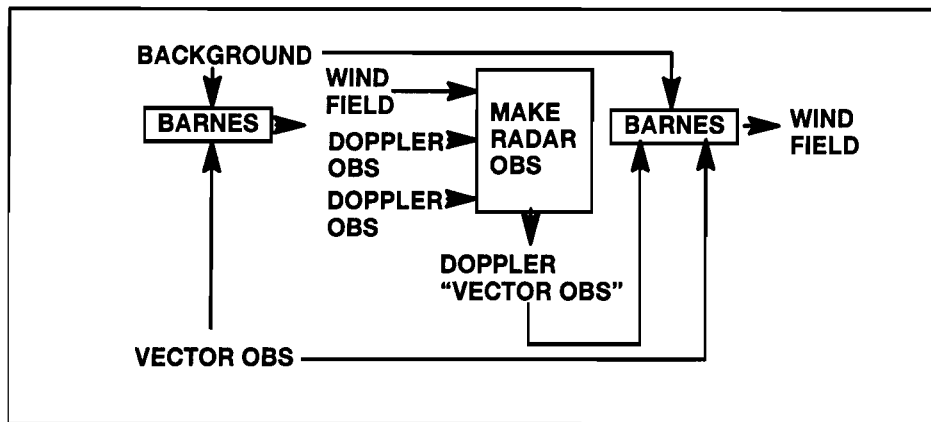


Figure A-2. Data flow for the two-pass Barnes MSDA.

component perpendicular to the radar beam is unchanged. The resulting wind vectors at points with at least one Doppler value are considered to be “radar vector observations.”

At a point with two Doppler values, the measured radial component from TDWR will equal the radial component of the “radar vector observation.” The difference between the radial component measured by NEXRAD and the corresponding radial component of the “radar vector observation” depends on the acute angle formed by the two radar beams. When the angle is 90°, the difference is zero; the “radar vector observation” agrees exactly with both Doppler values. As the angle decreases to 0°, the difference increases to the difference between the TDWR and NEXRAD measurements, and at 0°, a “radar vector observation” is equal to the single-Doppler “radar vector observation” computed from only the TDWR data. The TDWR data were chosen to follow the NEXRAD data in the MSDA process since the TDWR is located closer to the Orlando International Airport, where the most accuracy is desired.

A.3.2 BI-3

In the three-pass Barnes MSDA method, an intermediate Barnes pass is inserted between the first and second Barnes passes used in the BI-2 method as shown in Figure A-3. The first and second Barnes passes in BI-3 are used only to construct “radar vector observations.” The third Barnes pass produces the final analysis from the background field, vector observations, and all the “radar vector obs.” The first Barnes pass combines the background field with the true vector observations and is used to build the “radar vector obs” only at points with multiple-Doppler values using the process described above. These “radar vector obs” can be thought of as “multiple radar vector obs.” The new second Barnes pass takes in data from the background field, vector observations, and the “multiple radar vector obs.” The resulting wind field is then used to construct “radar vector obs” at points with only a single-Doppler observation.

Only the “radar vector observations” at points with a single-Doppler observation differ between BI-2 and BI-3. At these points, BI-2 estimates the missing component from the background field and the vector observations. In BI-3 however, the estimate of the missing component is derived from the background field, the vector observations, and the “radar vector observations”

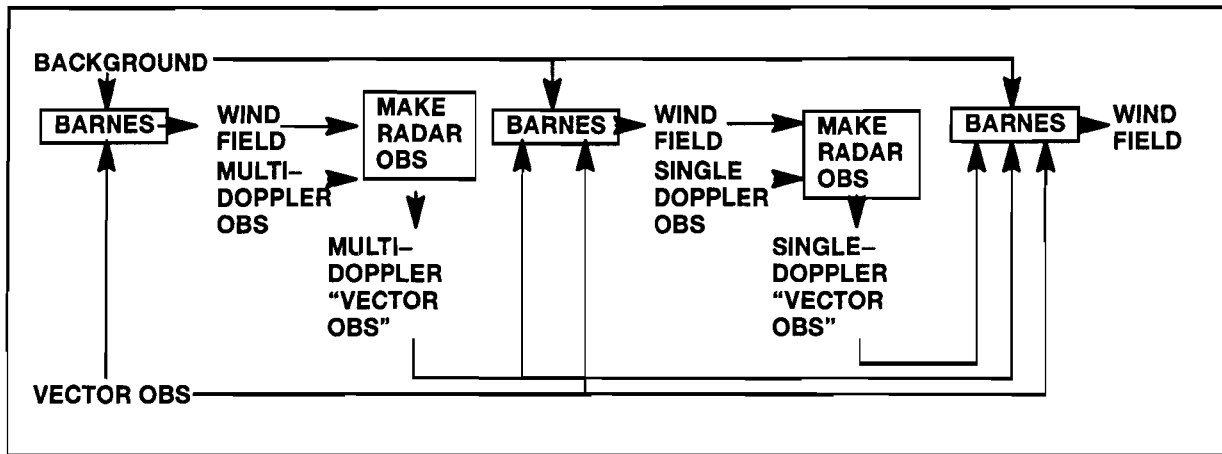


Figure A-3. Data flow for the three-pass Barnes MSDA

at points with multiple-Doppler observations. This additional data generally results in better estimates of the missing component in the single-Doppler “radar vector observations.” However, when there are only a few multiple-Doppler “radar vector observations” the final analysis can be very sensitive to them, as seen in case study 5.3 of the report. This is discussed in more detail below.

A.4 Consequences of the T-LAPS Analysis

T-LAPS produces a very smooth analysis on each horizontal level. This is the result of the weights in the Barnes analysis; in particular, the minimum value of K_2 and the use of a data window with infinite horizontal extent. This was a design decision for the original LAPS which did not have the abundance of Doppler data available to T-LAPS. The degree of smoothing inherent in T-LAPS may not be appropriate for an analysis with 2km horizontal resolution dominated by Doppler data.

From Equation A-1, Section A.2 we see that the weights used to analyze the Δ obs are normalized to sum to one. From Equation A-2 we see that the weights, before normalization, decrease exponentially with the square of the distance between the observation location and the analysis location, where the rate of decrease is controlled by the local data density. It is worth noting three consequences of these facts.

The first consequence relates to the normalization of the weights. Because of the normalization, if there is only one observation that is used at a given analysis level, that observation is given weight one at each analysis location regardless of the distance between the observation and analysis point. When data are scarce, such as aloft at times when there are few aircraft entering the airspace enclosed by the analysis region, this can lead to temporal and vertical discontinuities. This is also problematic when there are only a few observations, as in case study 5.3 of the report.

The second consequence arises from the interaction between the exponential die off and the normalization when data are scarce. For example, consider the case of two observations located 40 grid points apart. We will look at the weights assigned to each observation at analysis points lo-

cated on the line between the two observations. That is, we look at cases where the analysis point is n grid points from observation 1 and $40-n$ grid points from observation 2. The normalized weights for both observations as a function of the distance from observation 1 to the analysis point are given in Figure A-4. From these normalized weights we see that the observation closest to the analysis location gets substantially more weight than the more distant observation unless the observations are nearly equidistant to the analysis location. This is the situation shown in case study 5.2 of the report.

A third consequence also arises from the normalization of the weights in the BI-3 analysis when there are very few “multiple radar vector obs” produced for a given horizontal level and no vector observations near them. The “multiple radar vector obs” are given full weight over the entire horizontal analysis grid in the second Barnes pass that is used to estimate the missing component in the single Doppler “radar vector obs.” If the “multiple radar vector obs” do not agree with the background field, the second Barnes pass produces wind estimates that are dominated by the few “multiple radar vector obs” so that the single Doppler “radar vector obs” are very heavily influenced by these few data. This can result in the behavior seen in case study 5.3 of the report.

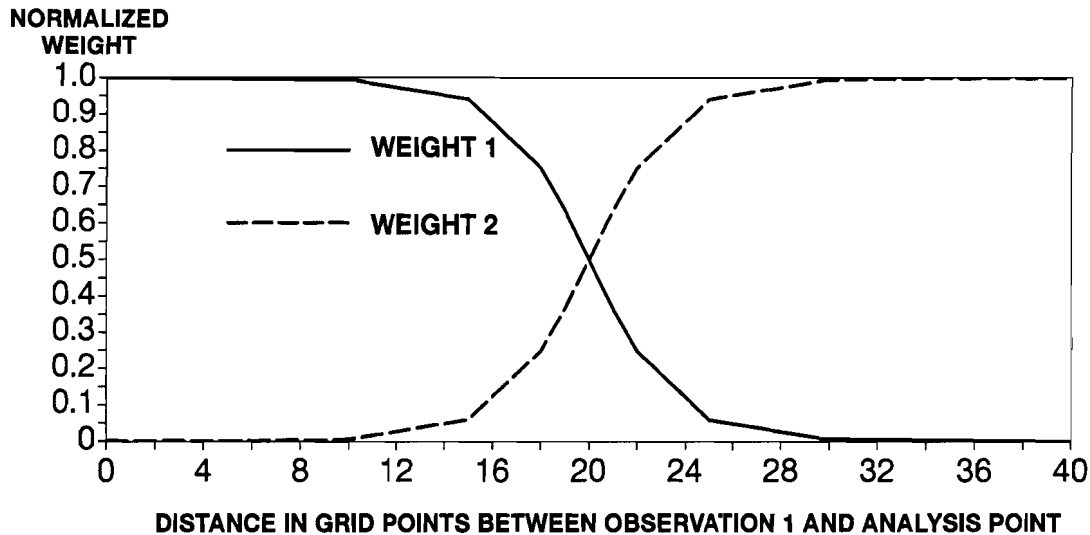


Figure A-4. Weights vs. distance to analysis location.

A.5 Cascade of Scales

The ACARS reports tend to be widely spaced, spatially and temporally. Additionally, the ACARS reports have a significant data latency. Some of the surface data are hourly observations. In contrast to these data, the Doppler radars provide data with a much higher spatial and temporal resolution in the region of return, as does the LLWAS anemometer network at the airport. These different types of data support different scales of analysis. This situation is handled by an analysis “cascade of scales.”

The data flow for the cascade of scales is shown in Figure A-5. First, an analysis is performed with a 10 km horizontal resolution, a 50 mb vertical resolution, and 30-minute update rate utiliz-

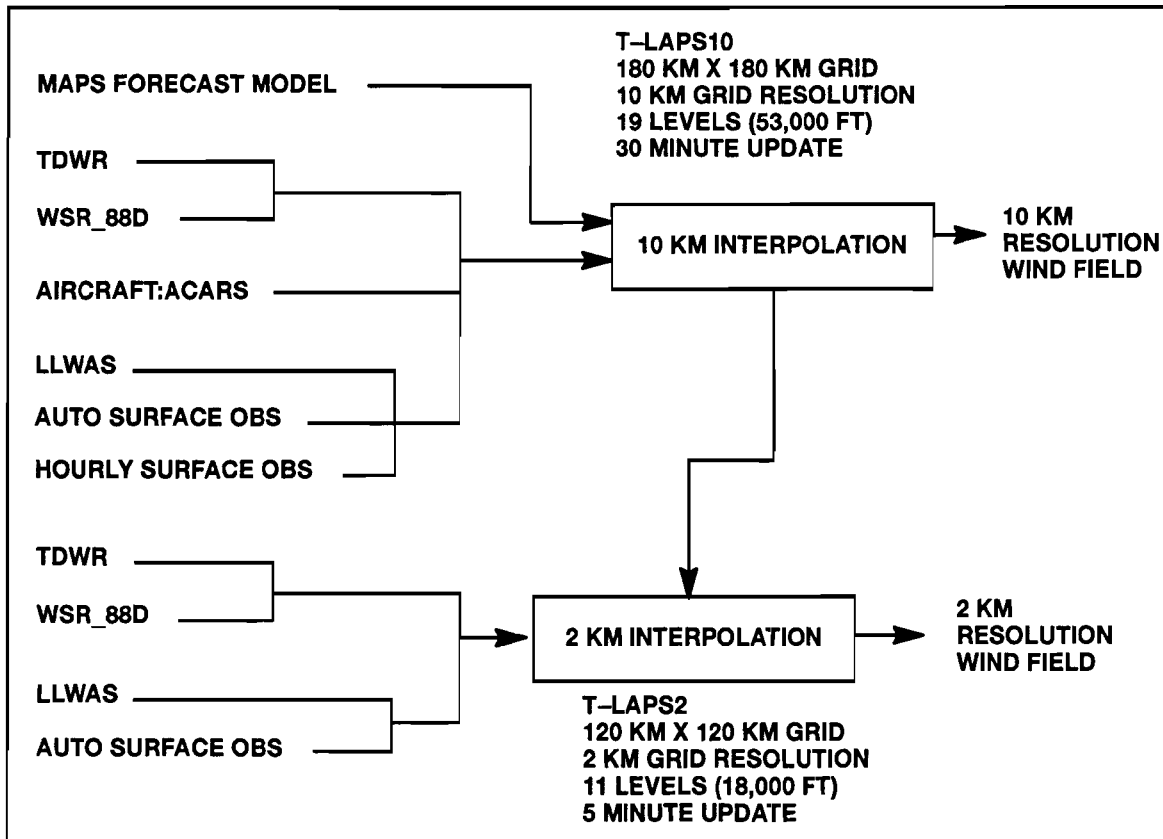


Figure A-5. Data flow for T-LAPS cascade of scales.

ing all of the data sources. This is very similar to the traditional LAPS winds analysis. The current 10 km analysis is then used as the background field for an analysis with a 2 km horizontal resolution, a 50 mb vertical resolution, and an update rate of five minutes. Only Doppler radar data and recent surface data are used in the 2 km analysis. The aircraft reports and other surface data are not used due to data latency. The analysis domains used for the cascade of scales at the Orlando test bed are shown in Figure A-6. The 10 km and 2 km analysis regions are shown as squares centered on the airport. The dimensions are 180 km x 180 km and 120 km x 120 km, respectively. The background field for the 10 km analysis is derived from the wind estimates on the 6x6 sub-domain of the MAPS grid shown. The TDWR radar is located near the center of the 2 km domain, and the NEXRAD radar is located near the southeast corner of the 2 km domain. Aircraft reports were available primarily along arrival and departure routes.

The 10 km analysis uses a background derived from MAPS. The background field is produced by linear interpolation in all four dimensions between the two MAPS forecasts that bracket the analysis time. The Doppler data are smoothed by applying a median filter with a 1 km² footprint to the base data, then resampled to the 10 km grid. All data are required to have collection times within 90 minutes of the analysis time. This gives a reduction in spatial and temporal scales of 6:1 from background.

The background for the 2 km analysis is the most recent 10 km analysis. The Doppler data are smoothed by applying a median filter with a 1 km² footprint to the base data and resampled to the

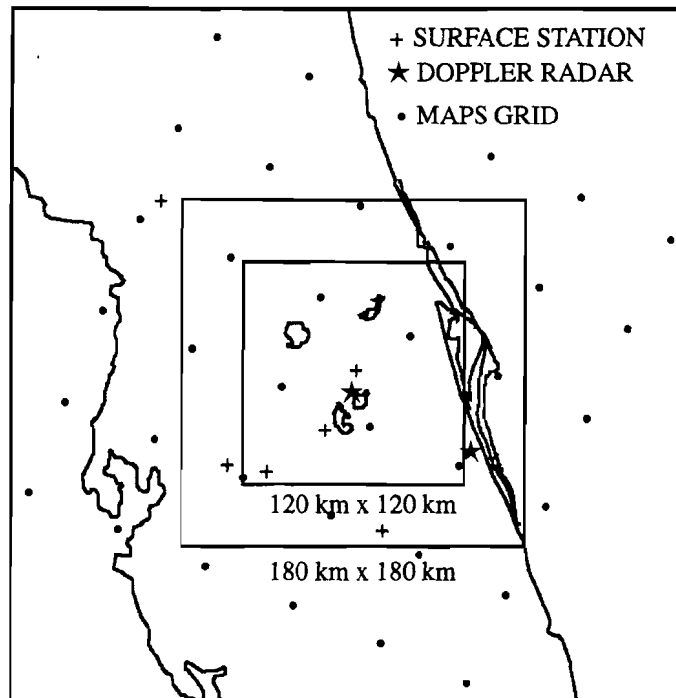


Figure A-6. T-LAPS domain and sensor locations.

2-km grid. Currently, the only surface data in the 2 km analysis come from the Low Level Wind Shear Alert System (LLWAS)(Wilson and Gramzo, 1991) anemometer network located at the airport. On grid levels with no observations (surface or Doppler), the analysis is the 10 km analysis. This gives a further reduction in spatial scale of 5:1 and temporal scale of 6:1 from background.

APPENDIX B. RADAR DATA ANALYSIS

Stephen Kim and F. Wesley Wilson

B.1 Introduction

Three issues related to radar data are discussed: (1) automatic analysis techniques for monitoring data quality, (2) the process by which the radar data are interpolated from radar coordinates to the regular T-LAPS grids, and (3) the dual-Doppler analysis that is used to compute the dual-Doppler values that are used as a comparison set in this evaluation study. The first two issues apply to preprocessing of the radar data for both the T-LAPS analysis and for the dual-Doppler analysis. This dual use is an important consideration for the issue of error correlation between the analyzed winds and the dual-Doppler winds.

B.2 Radar Data Quality

There are three major types of error in meteorological Doppler radar data:

- Type 1–Echoes from objects whose velocity is not similar to the wind velocity
- Type 2–Velocity values that are misrepresented by velocity folding
- Type 3–Echoes that are improperly synchronized with the pulse timing of the radar.

Type 1 errors are usually the result of the intersection of the radar beam or its sidelobes with objects on the ground (*ground clutter*) or with flying objects such as birds or aircraft (*point targets*). Aircraft are an especially likely problem for operations near an airport. The two radars, whose data are used in T-LAPS, have different capabilities for dealing with these problems. Type 2 errors result from the insufficient sampling rate in the Doppler velocity calculation. Given a sampling rate or the pulse repetition frequency (PRF), the unambiguous velocity range is determined by Equation B-1

$$v_n = \frac{c \text{ PRF}}{4f} \quad (\text{B-1})$$

where f is the radar frequency and c is the speed of light. When the velocity falls outside of this range, it is folded back into the range of representable velocities (*velocity folding*). Both TDWR and NEXRAD have algorithms which attempt to correct for velocity folding. Type 3 errors result from echoes from very distant and bright reflectors, usually large storms, that are received after a subsequent pulse has been transmitted (*second trip* or *range folding*). As a result of hardware characteristics and more sophisticated data quality processing, TDWR usually has fewer data errors than NEXRAD.

B.3 Radar Data Resampler

Resampling is the process by which information is moved from radar coordinates to the Cartesian coordinates of T-LAPS. The radar reflectivity and radial velocity data are collected in contiguous

ous, equal-width gates along one-degree radials. Both radars scan sectors of the region with all beams at the same elevation angle. A maximum collection of beams which are contiguous in time and which have the same elevation angle is called a tilt. All NEXRAD tilts cover a full 360-degree sector. NEXRAD has several different scan strategies, which are realized by varying the tilt elevations. TDWR can either scan with 360-degree sectors (monitor mode) or with two 360-degree surface tilts and an intense pattern of approximately 120-degree sectors at various elevations over the airport. The elevations for the TDWR tilts are preset for each airport installation, so there are only two TDWR scan strategies for each airport. Each radar also interrupts its standard velocity scanning to make long-range (low PRF) scans that are used to detect the possibility of range folding. These data are not used in the T-LAPS analysis. They provide an artificial temporal partition of the tilts into volume scans. T-LAPS does not make use of this volume structure. Instead, at each analysis time, it composes a "natural" (most up to date) volume out of the most recent tilts. This design also accommodates the fact that the scan strategies of these radars can change during operations and that there is no definition of the scan strategy in the data stream. By constructing its own volumes from the most recent tilts, T-LAPS uses the most current data and is able to continue processing during changes in the radar scan strategy.

The resampling process includes two sub-processes:

- Tilt Resampling – the process by which the radar tilt information is moved in a tilt to the (x,y) positions of the T-LAPS grid.
- Volume resampling – the process by which the output information from the tilt resampling is moved vertically to the T-LAPS analysis levels.

The tilt resampling is processed immediately after each tilt is scanned and is an asynchronous process since it is controlled by the radar scan strategy. Volume resampling is processed at the beginning of each T-LAPS analysis cycle and hence is a synchronous process.

B.4 Dual-Doppler Analysis

The T-LAPS analysis at MCO uses two Doppler radars: TDWR at Kissimee and NEXRAD at Melbourne. Each radar measures the component of wind velocity in the direction of the radar beam. This measured radial velocity is represented mathematically as the dot product of the wind velocity vector and the beam direction vector. Given the two independent measurements, mathematically, the wind velocity vector can be recovered using Equation B-2:

$$\begin{bmatrix} \sin \theta_1 & \cos \theta_1 \\ \sin \theta_2 & \cos \theta_2 \end{bmatrix} \begin{bmatrix} u \\ v \end{bmatrix} = \begin{bmatrix} V_1 \\ V_2 \end{bmatrix} \quad (\text{B-2})$$

where u and v are the components of the horizontal wind velocity to the east and north, respectively; V_1 and V_2 are the radial velocity measurements from the two radars; and θ_1 and θ_2 are the azimuths of radar beam.

The dual-Doppler analysis output equation is numerically unstable when the direction of the beams are nearly dependent. For the 1992 T-LAPS dual-Doppler analysis, the angle between the two radar beams is constrained to lie between 30 degrees and 150 degrees. This constraint, in turn,

defines the analysis region to be the union of two circular regions minus the intersection of two circular regions as shown in Figure B-1.

The resampled volume data were used as inputs for the dual-Doppler analysis. The resampling algorithm used for the wind analysis allowed tilt elevation angles as high as twenty degrees, and the vertical extrapolation parameter was set to be one full analysis layer width. However, the resampling algorithm parameters for the dual-Doppler analysis were more stringent to minimize the deviation from the true wind. Specifically, the tilt elevation angle was restricted to be less than ten degrees, and the vertical extrapolation parameter was set to be half of the analysis layer width. The vertical velocity component was assumed to be zero in both the wind analysis and the dual-Doppler analysis.

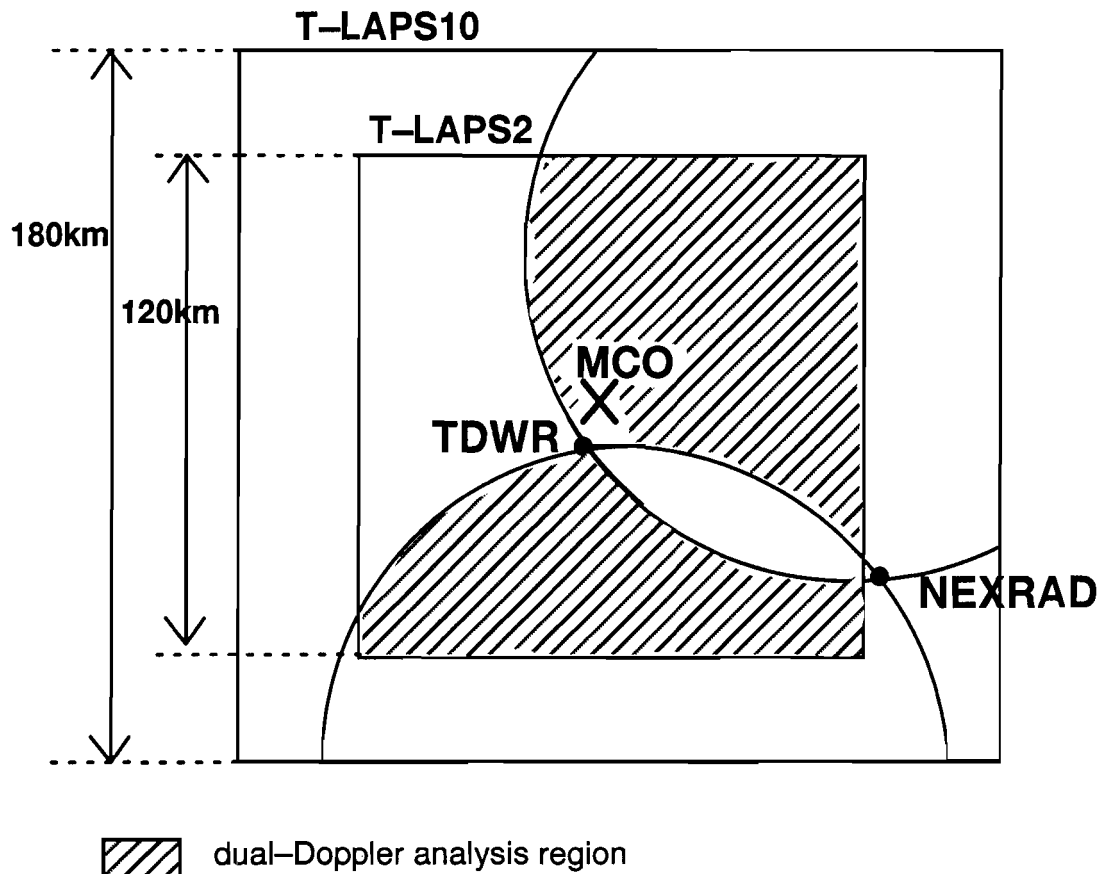


Figure B-1. T-LAPS dual-Doppler analysis region.

APPENDIX C. DETAILED EVALUATION STATISTICS

Steven R. Finch

Sections C-1 to C-15 contain detailed statistical outputs of the T-LAPS evaluation. The fifteen sections are:

C-1:	T-LAPS2 BI2 – ACARS data
C-2:	T-LAPS2 BI3 – ACARS data
C-3:	T-LAPS10 BI2 – ACARS data
C-4:	T-LAPS10 BI3 – ACARS data
C-5:	MAPS – ACARS data
C-6:	T-LAPS2 BI2 – CLASS sounding data
C-7:	T-LAPS2 BI3 – CLASS sounding data
C-8:	T-LAPS10 BI2 – CLASS sounding data
C-9:	T-LAPS10 BI3 – CLASS sounding data
C-10:	MAPS – CLASS sounding data
C-11:	T-LAPS2 BI2 – dual-Doppler data
C-12:	T-LAPS2 BI3 – dual-Doppler data
C-13:	T-LAPS10 BI2 – dual-Doppler data
C-14:	T-LAPS10 BI3 – dual-Doppler data
C-15:	MAPS – dual-Doppler data

Each section contains plots of:

- histogram for u wind differences (gridded analysis – observational dataset)
- histogram for v wind differences
- histogram for wind speed differences
- histogram for wind direction differences
- histogram for norm of wind vector differences
- cumulative distribution function (cdf) for norm of wind vector differences

and relevant statistics. For the sake of being definite, we will explain the plots and statistics in Section C-1 in detail. We shall also present a few other evaluation outputs in Section C-1 not contained in the other fourteen sections for reasons of space.

The histograms depicted in Section C-1 are discrete step-functions with 1-m/s increments for wind speed and 15-degree increments for wind direction. Each histogram has been normalized so that the area between it and the horizontal axis is 1. Wind speed plots are uniformly scaled from -15 to 15 m/s, with the exception of the norm of wind vector plot, which is scaled from 0 to 15 m/s. The vertical scales have not been uniformized (since they characterize probability density), with the exception of the cdf plot, which is scaled from 0 to 1 (characterizing probability).

The smooth curves depicted in Section C-1 are two-moment Gaussian distribution fits to the histograms, i.e., the Gaussian curves with matching mean and standard deviation. These curves are

included to provide an informal visual data check for normality. If error distributions are significantly non-normal, this suggests a trend or dependence in the errors. More sophisticated curve fits or formal hypothesis tests are possible but are beyond the purpose of this report. The exception is for the norm of wind vector difference. In this case, we plotted the density function of the non-central Rayleigh distribution which would result if the u wind differences and v wind differences were both Gaussian and statistically independent. The relevant formula for the non-central Rayleigh curve is found in Papoulis, 1965.

We generally see an excellent fit between the empirical histograms and the theoretical densities in the analysis comparisons against ACARS and CLASS. Against dual Doppler, the MAPS histograms agree well with the fitted curves. Against dual Doppler, however, the T-LAPS histograms are more sharply peaked than the fits due to the dependence between dual Doppler and T-LAPS.

A number of statistics are included with each plot, such as the RMS differences and percentiles used to create Figures 5 to 8. We comment on two other statistics. The skewness and kurtosis excess coefficients (Zar, 1974) quantify the departure of a distribution from symmetry and mesokurtic shape, respectively. The coefficient values observed here are almost always close to zero, which is additional evidence for normality. The exceptions are the T-LAPS to dual-Doppler difference densities, which possess sharp peaks and long tails and thus have large kurtosis. This is because dual Doppler and T-LAPS are highly dependent.

Means, sigmas and RMS differences for wind direction were estimated using circular distribution moment formulas in Zar, 1974. The reason standard moment formulas fail for wind direction is the wrap-around phenomena ($-180 \text{ deg} = +180 \text{ deg}$) for circular data. Analogous formulas for skewness and kurtosis excess coefficients have not been implemented and such estimates do not appear in any of the wind direction histogram plots.

Wind direction differences were computed only when the observed (ACARS, CLASS or dual-Doppler) wind speeds were greater than 5 m/s. This is required so angles between analysis vectors and observed vectors are physically relevant. As a consequence, the sample sizes indicated on the wind direction plots are appreciably smaller than the sample sizes indicated on the wind speed plots.

Two other comments about sample sizes are needed. The number of data points reported on each plot is the number of differences which contributed to the histogram as pictured. For wind speed plots, the number of data points is always 368 for ACARS, 833 for CLASS, but somewhat varying ($>70,000$) for dual Doppler. This is due to outliers in the dual-Doppler dataset, which gave rise to differences falling outside of the $[-15.0, 15.0]$ m/s range of the horizontal axes. The number of times a u wind difference (analysis u wind - dual-Doppler u wind) exceeds 15.0 m/s is not the same as the number of times a v wind difference exceeds 15.0 m/s, for example. Moment and percentile estimates, however, reflect the dataset in full.

The other comment about sample size is as follows. CLASS sounding observations are separated by merely 10 seconds and hence are significantly temporally correlated. We reported in the relevant plots not just the number of data points but also the effective number of data points, by which is meant the number of independent observations which achieve the same estimation accuracy as the original observations. Formulas in Thiebaut and Zwiers, 1984, coupled with a first-order autoregressive modeling assumption, predict effective sample size reduction as indicated. No attempt

was made to apply such formulas or models to the (temporally and spatially correlated) dual-Doppler data.

Section C-1 additionally contains

- u wind difference boxplots
- v wind difference boxplots
- wind speed difference boxplots
- wind direction difference boxplots
- norm of wind vector difference boxplots

stratified by atmospheric level,

- wind rose plot (capturing the joint distribution of wind speed differences and wind direction differences)

and

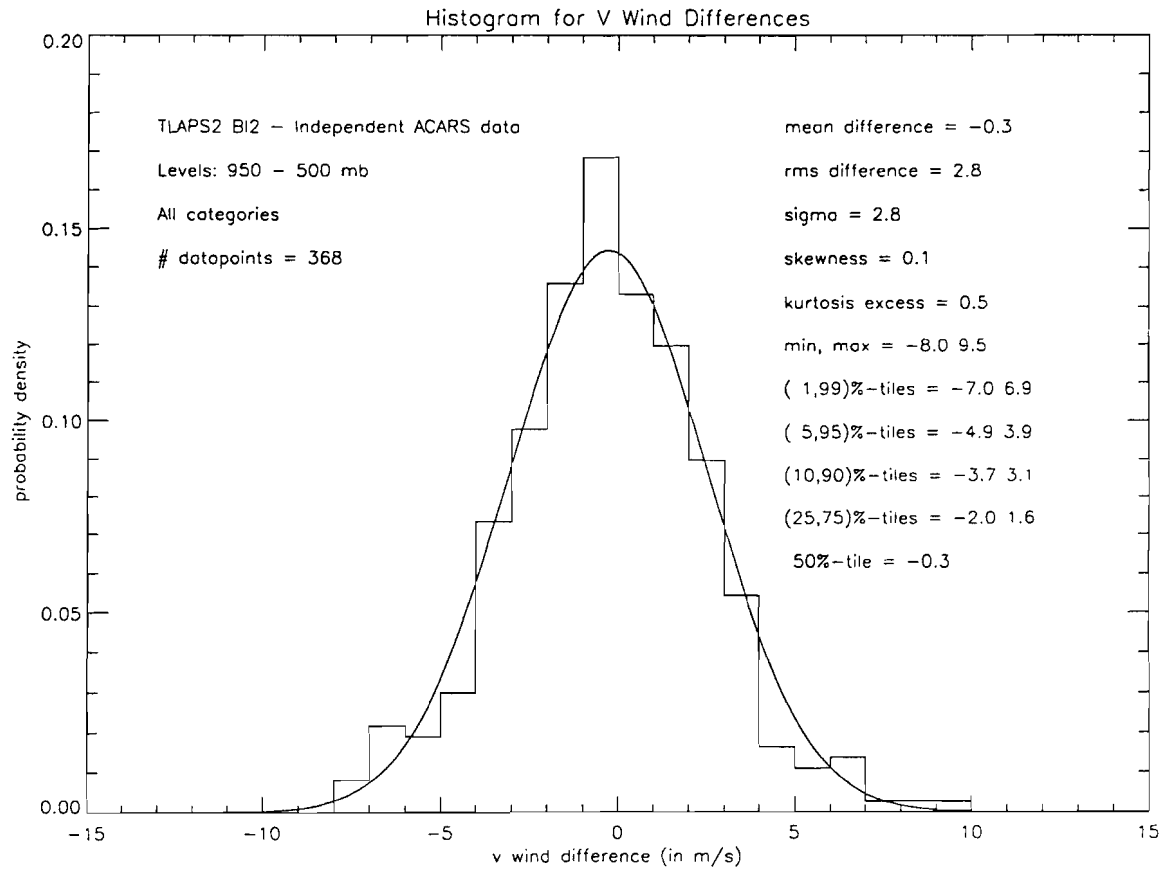
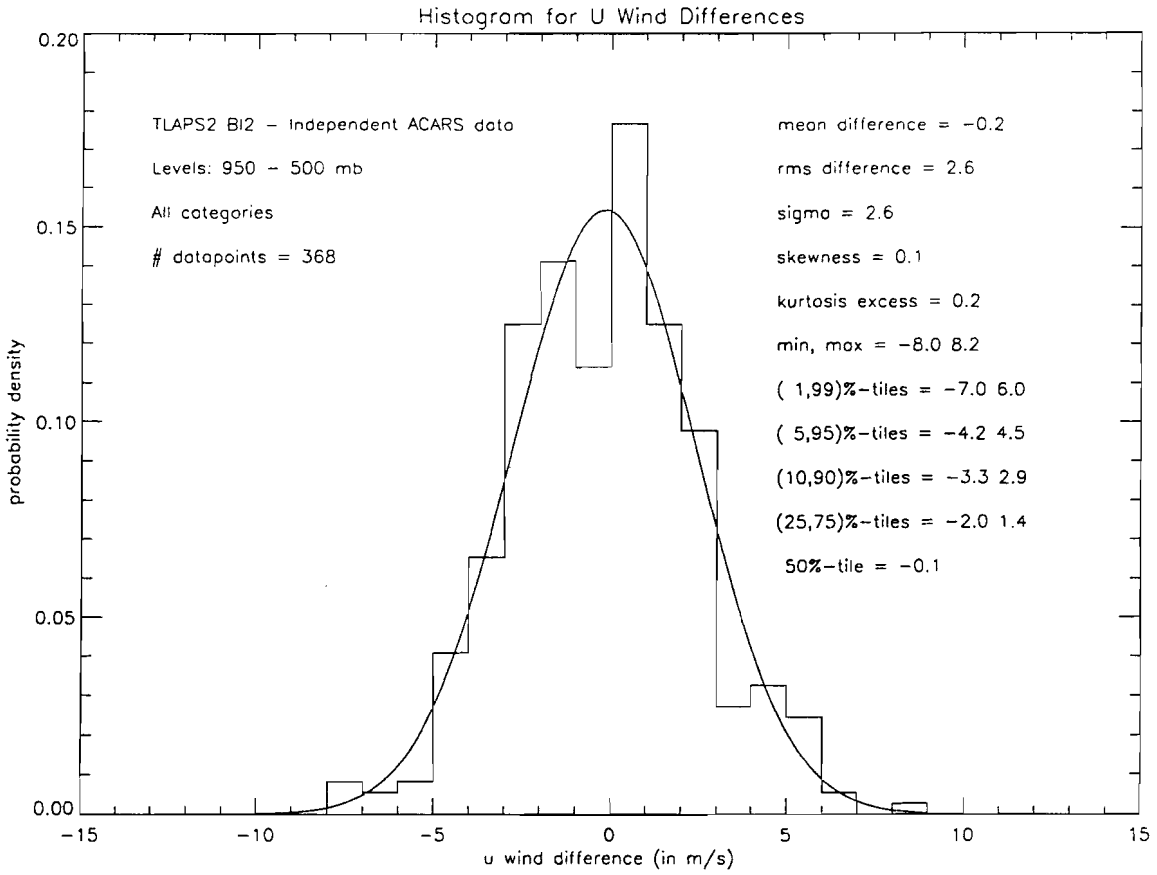
- wind uv plot (capturing the joint distribution of u wind differences and v wind differences).

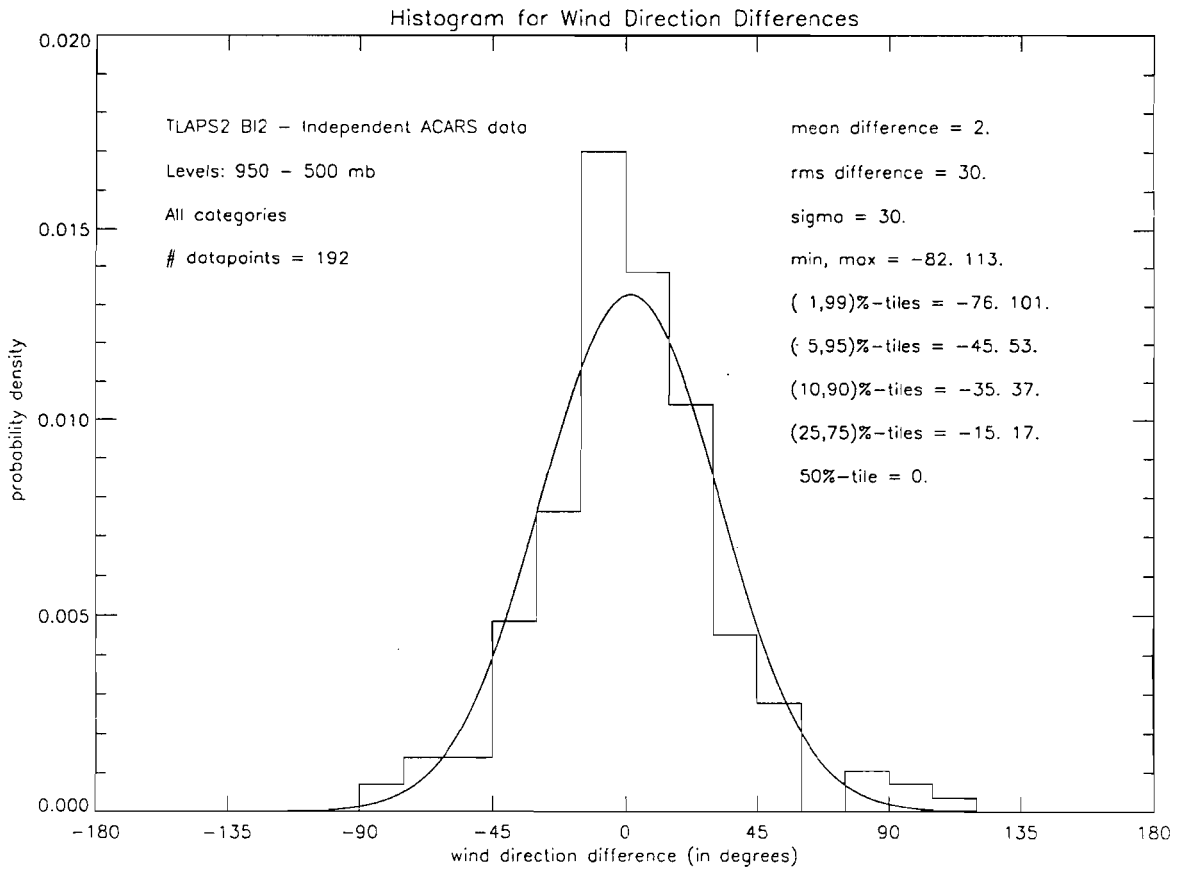
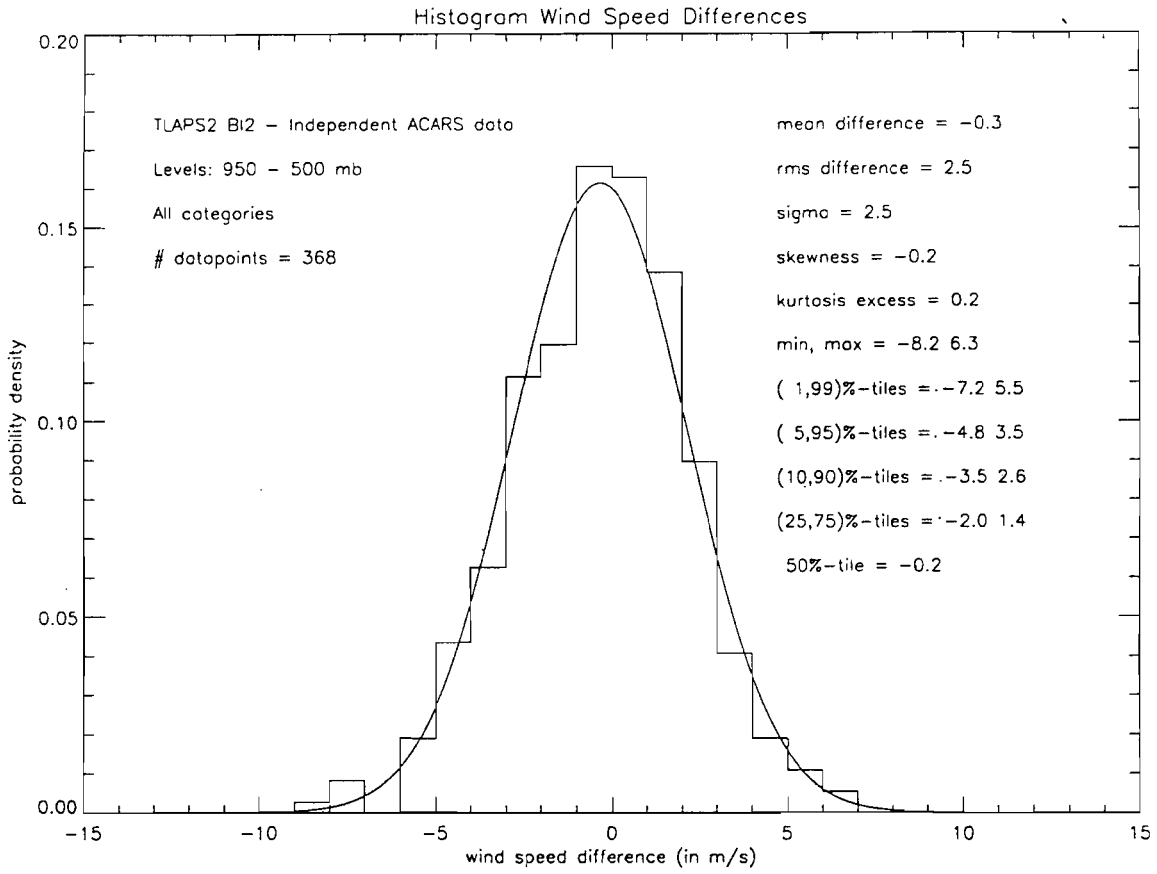
The boxplots contain the same percentile information as in Figure 4, except for each analysis level (note that sample size, as a function of level, is provided to the right of the picture). Starting from the left, the box plots show the 1st, 5th, 10th, 25th, 50th, 75th, 90th, 95th, and 99th percentile values. At the topmost level, the boxes were discarded (because of small sample) and replaced by actual difference values.

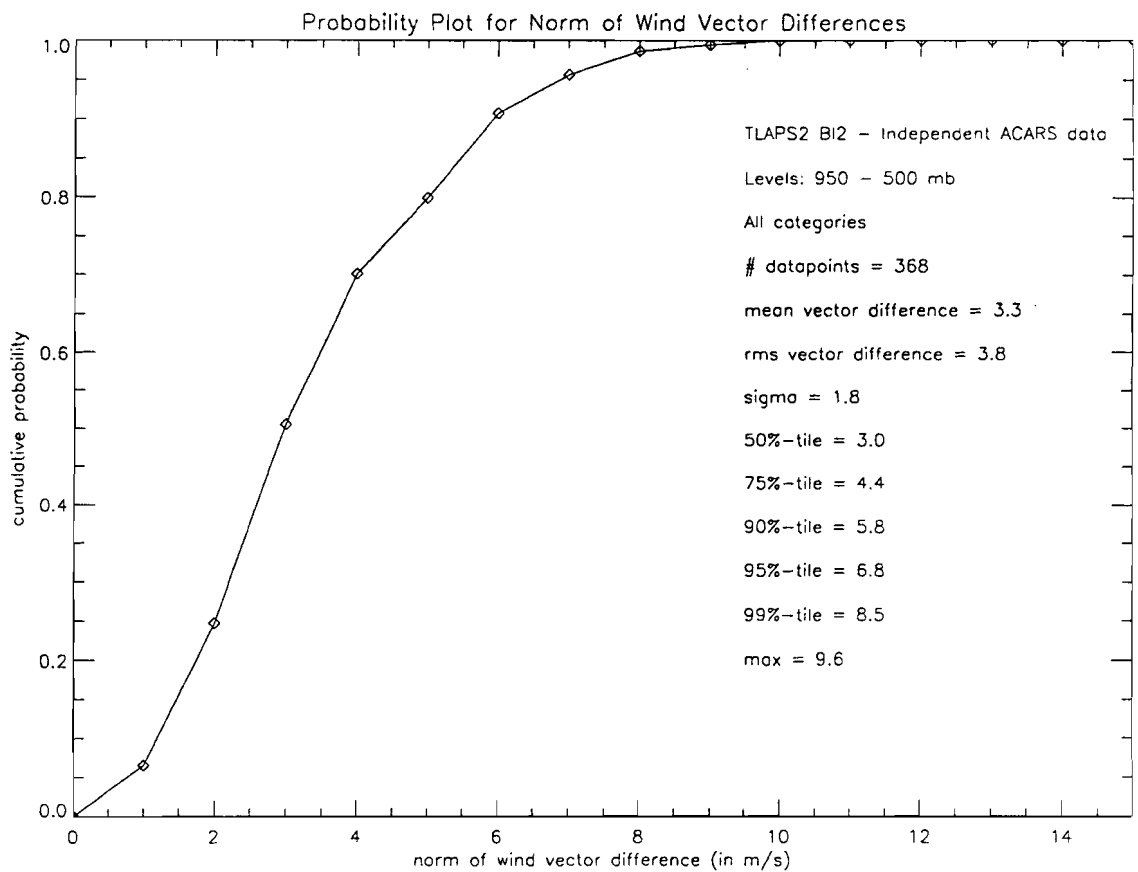
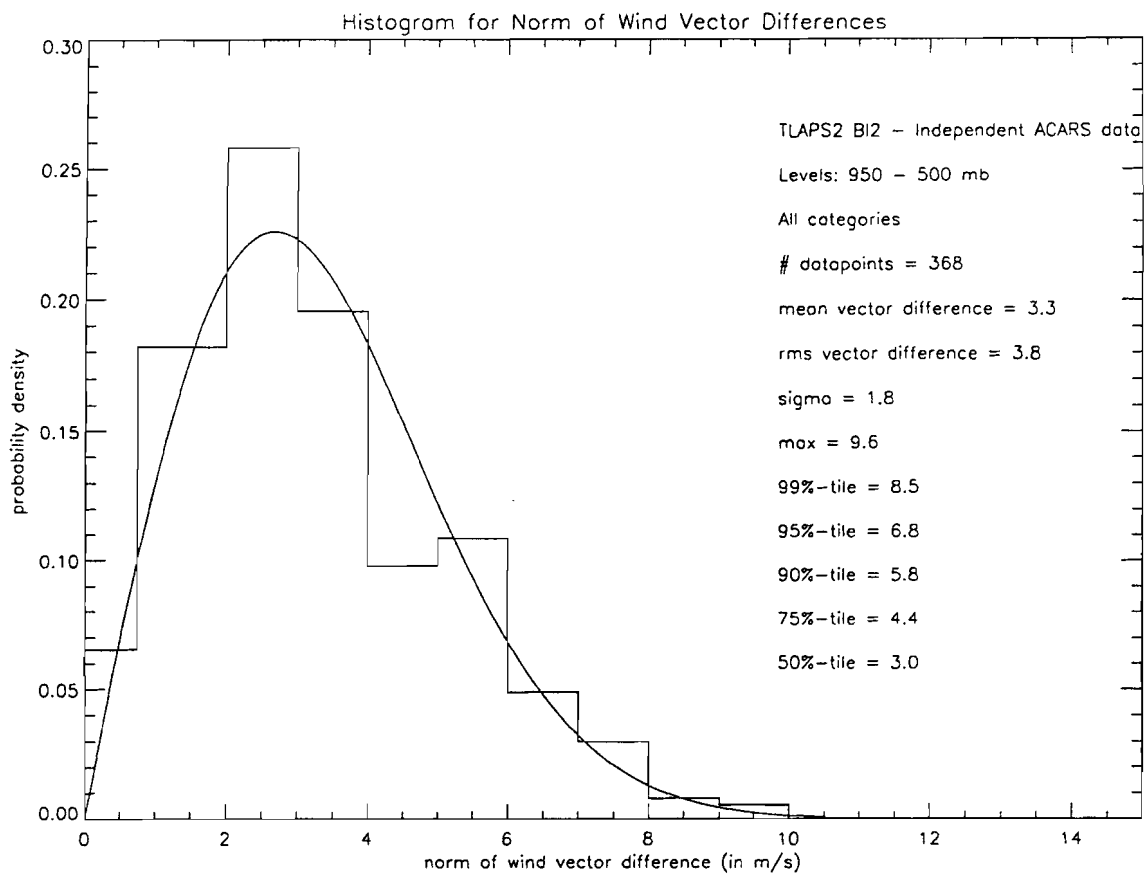
The wind rose plot is fairly self-explanatory: the topmost wedge contains counts of (analysis wind vector, observed wind vector) pairs whose difference in wind direction is between -22.5 degrees and $+22.5$ degrees and whose absolute speed difference is between 1 and 9 m/s. The central circle contains the count of ordered pairs with absolute speed difference less than 1 m/s, regardless of the difference in wind direction. The uv wind plot is also fairly self-explanatory, with one outlier (a single v difference of 9.5 m/s) depicted by an asterisk just above the checkerboard.

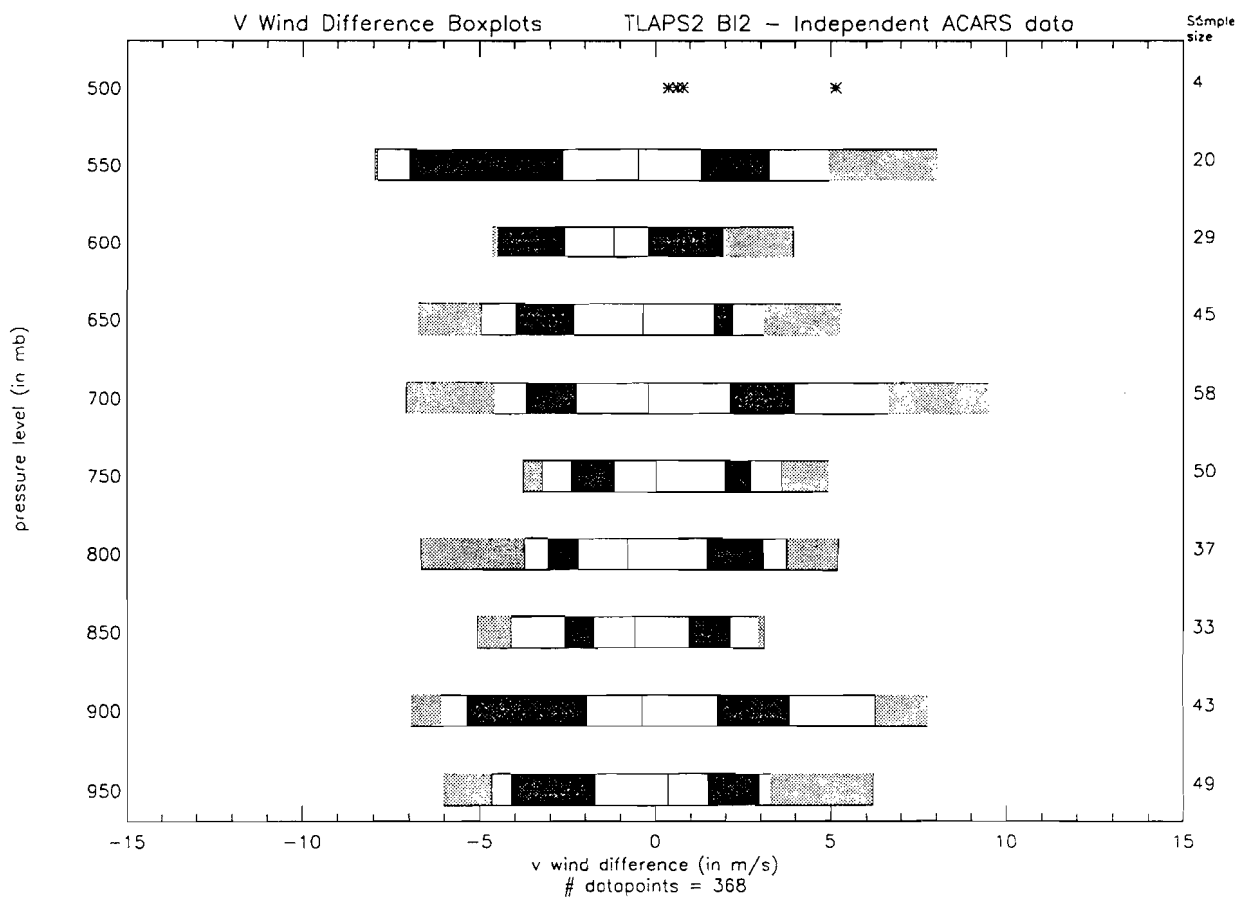
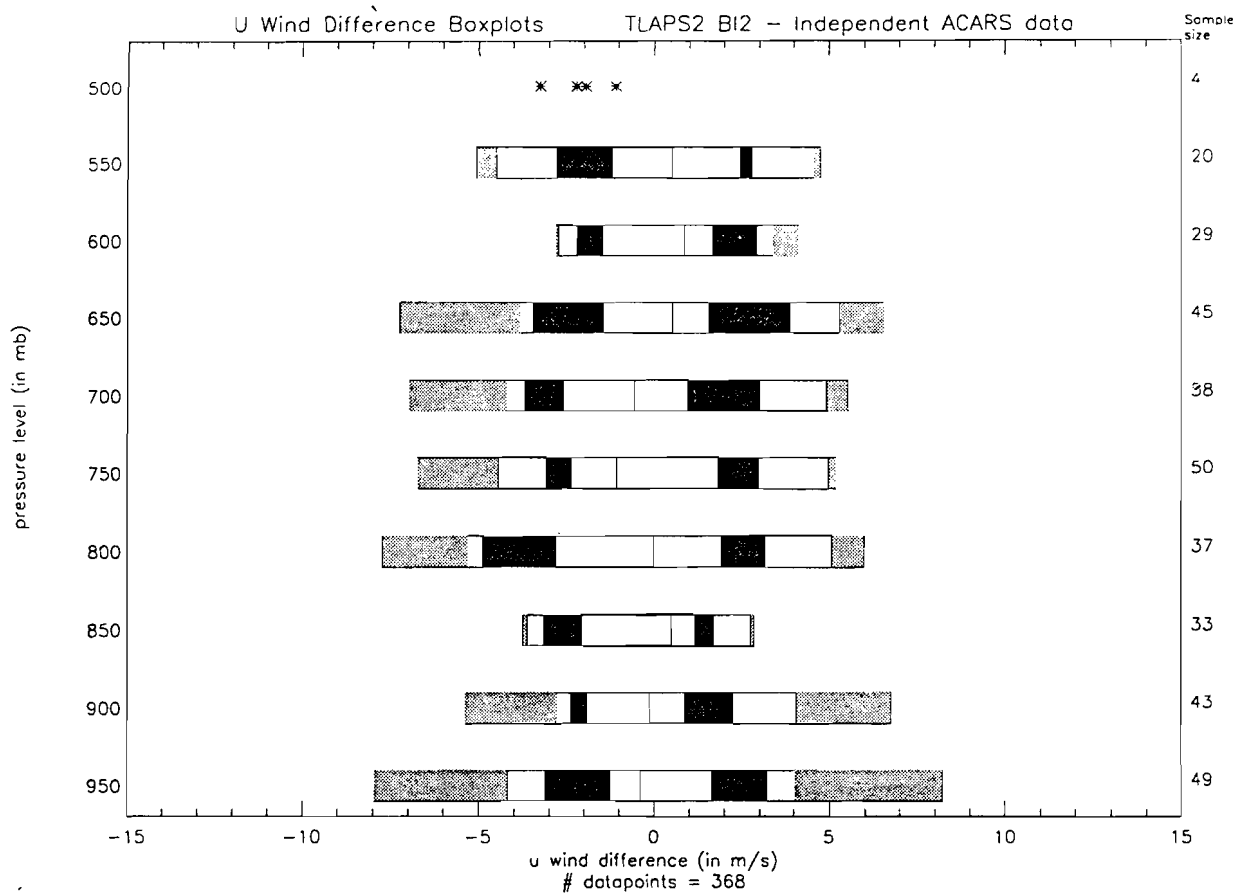
No surprising data features are seen in these additional plots. No trends are apparent in the boxplots, rose plot, or uv plot; the data appear to be distributed symmetrically about zero. Corresponding plots in Sections C-2 to C-15 have been examined and show no surprising data features.

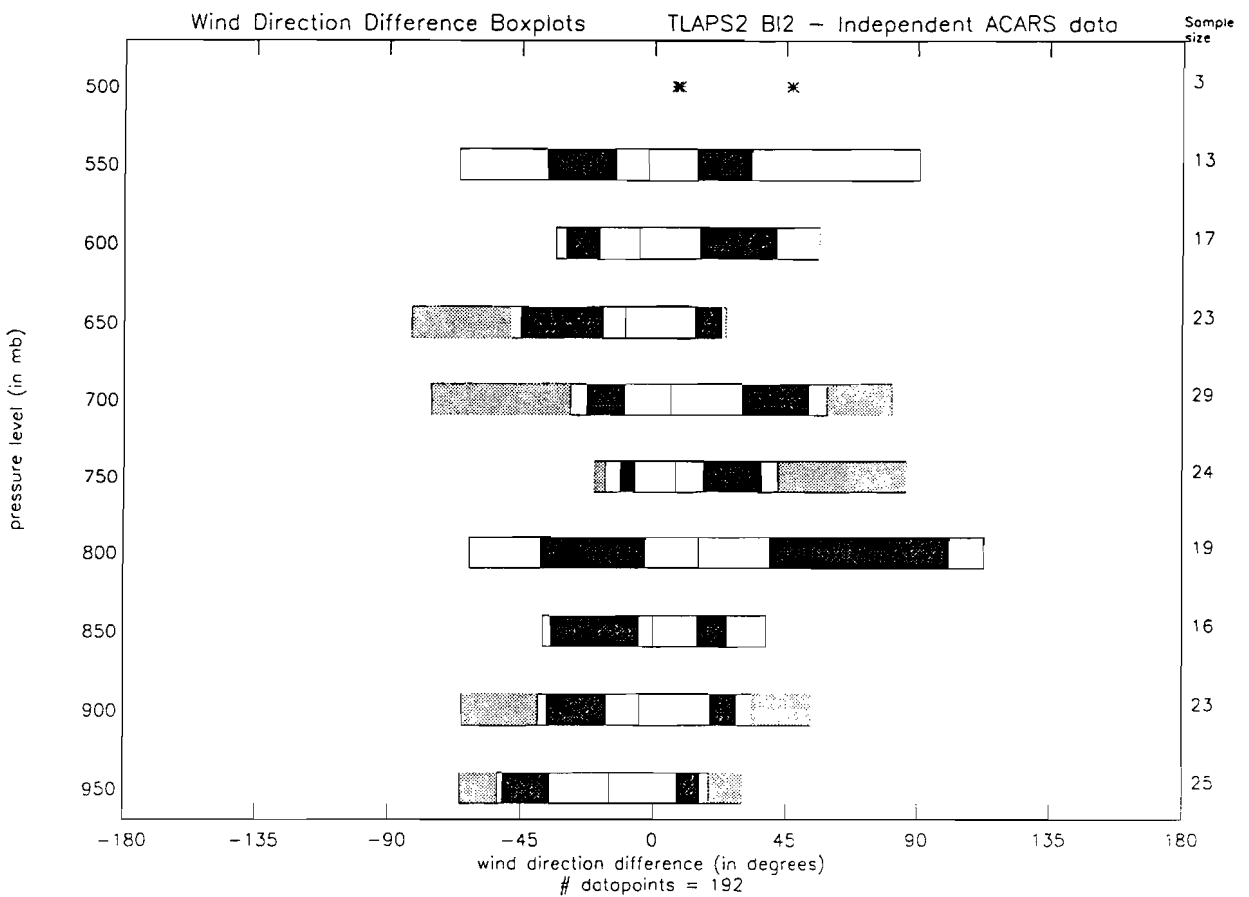
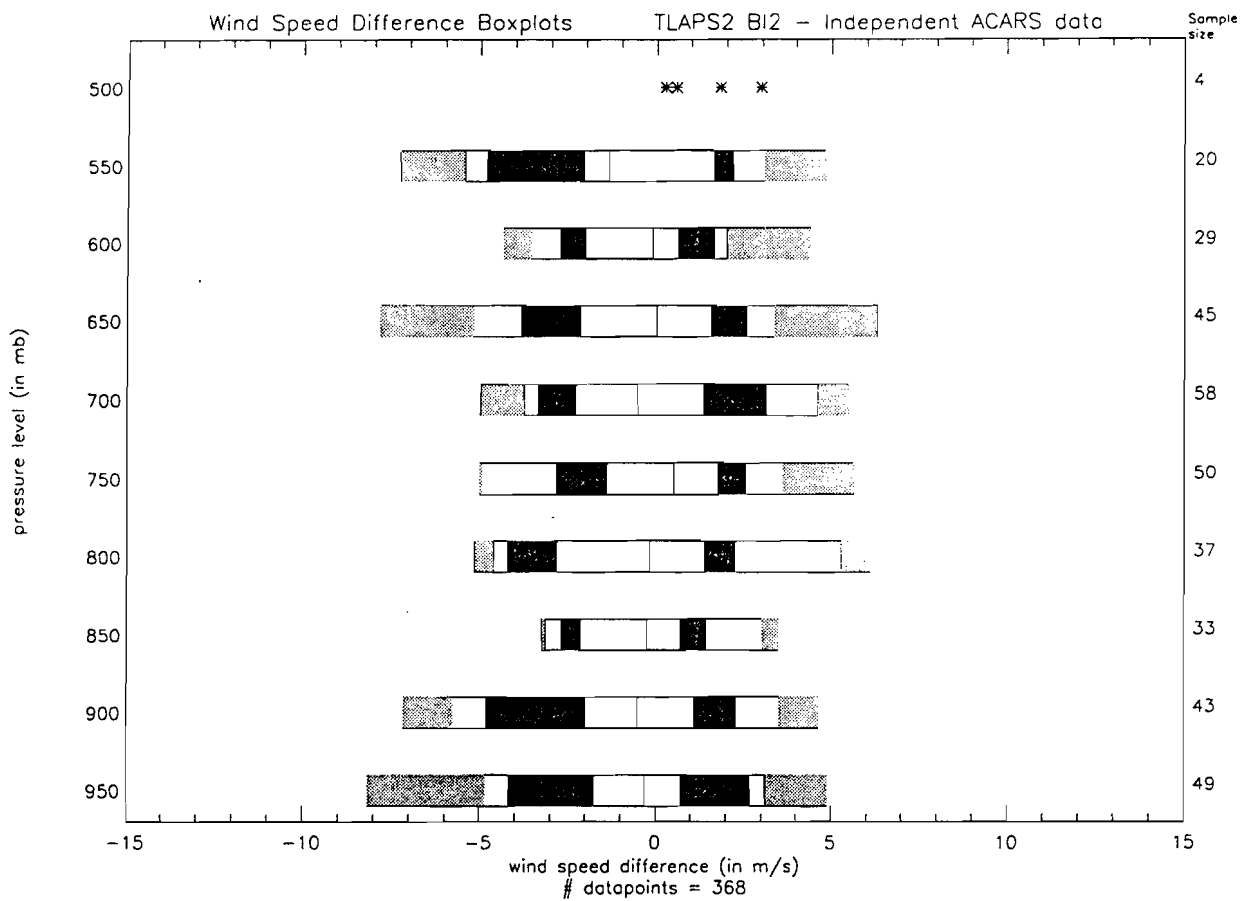
SECTION C-1



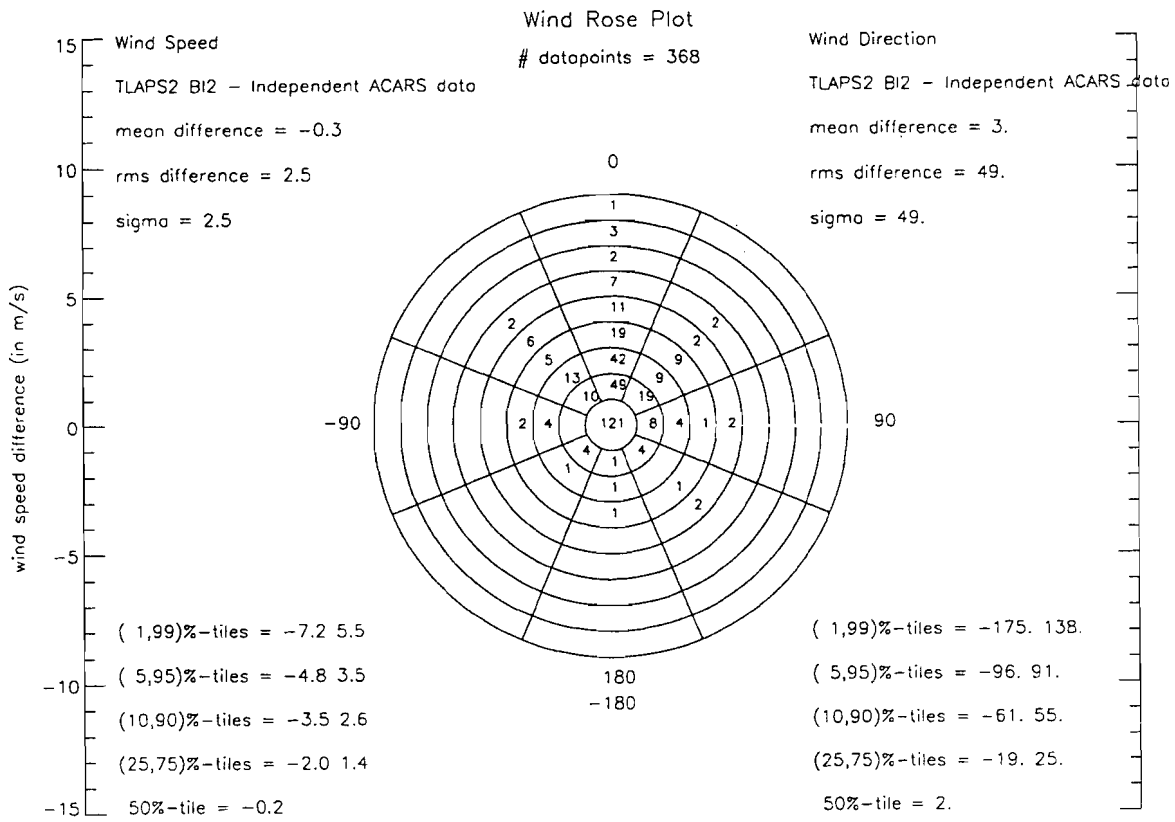
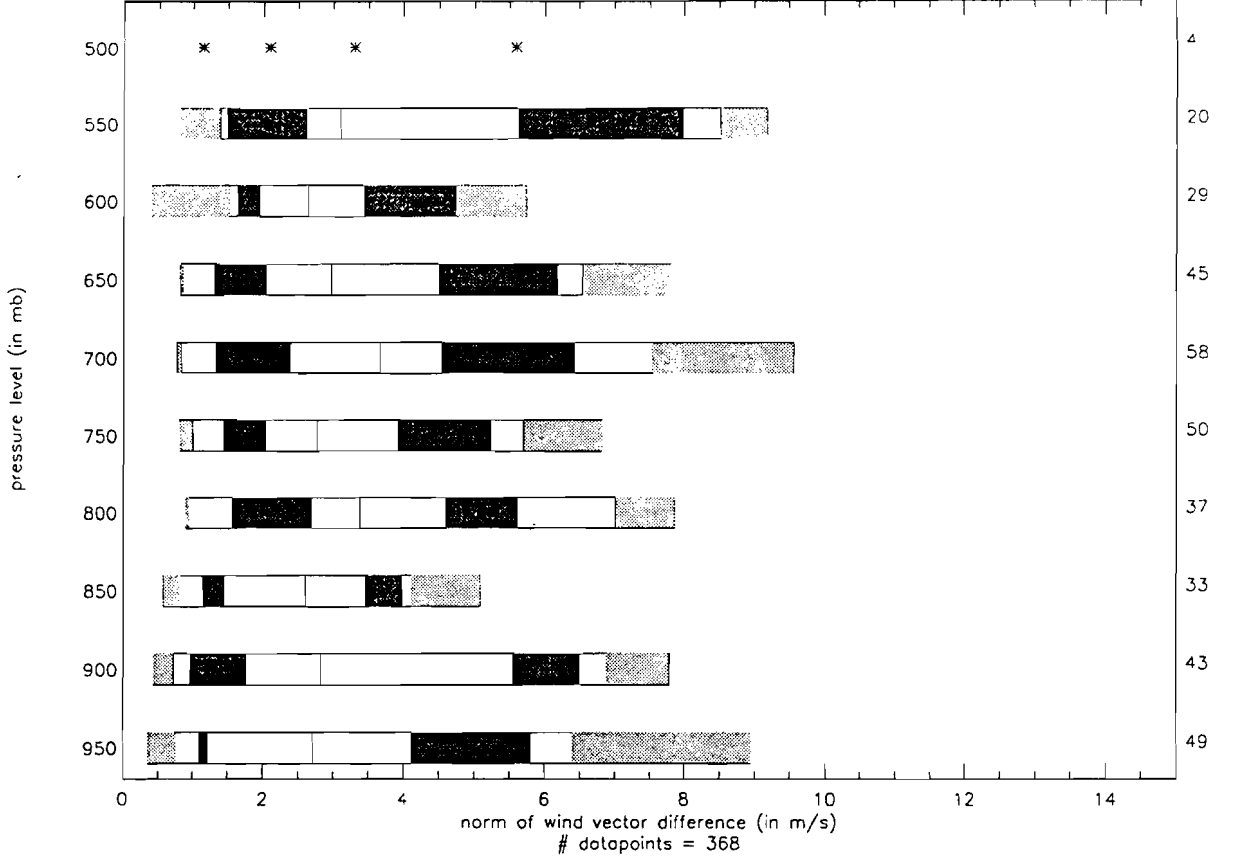




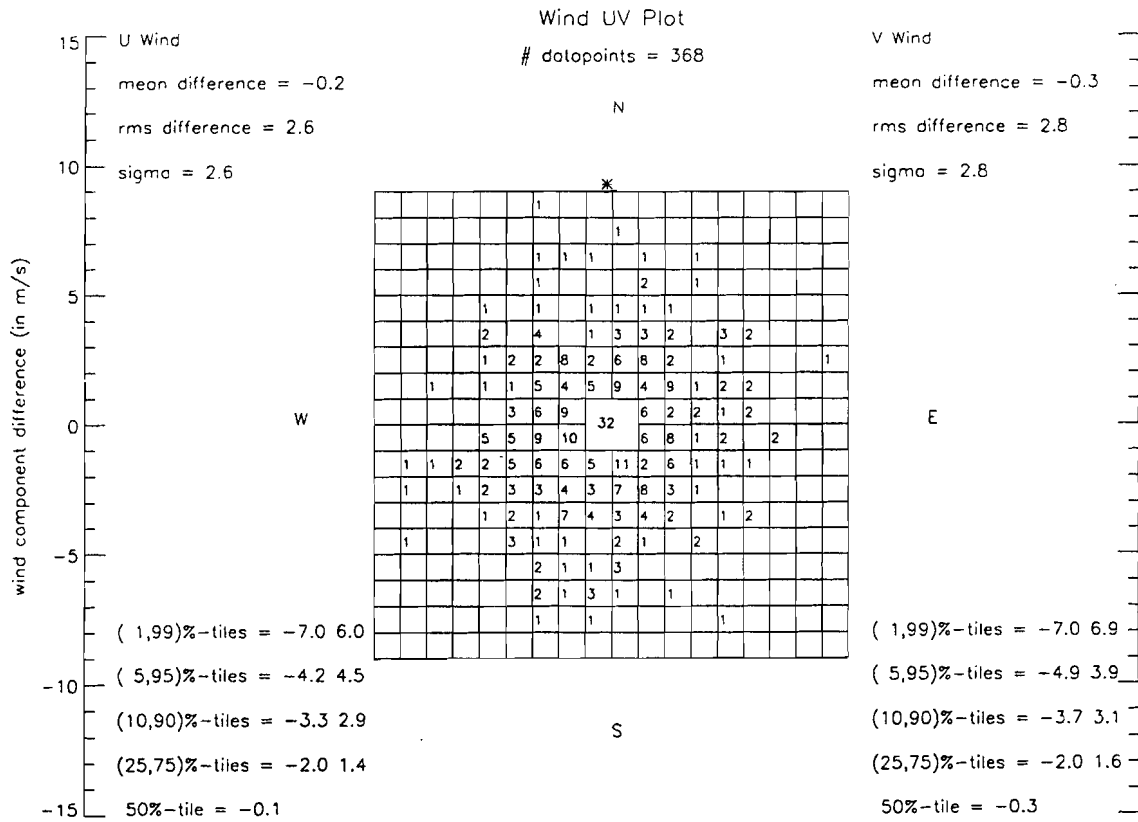




Norm of Wind Vector Difference Boxplots TLAPS2 BI2 - Independent ACARS data

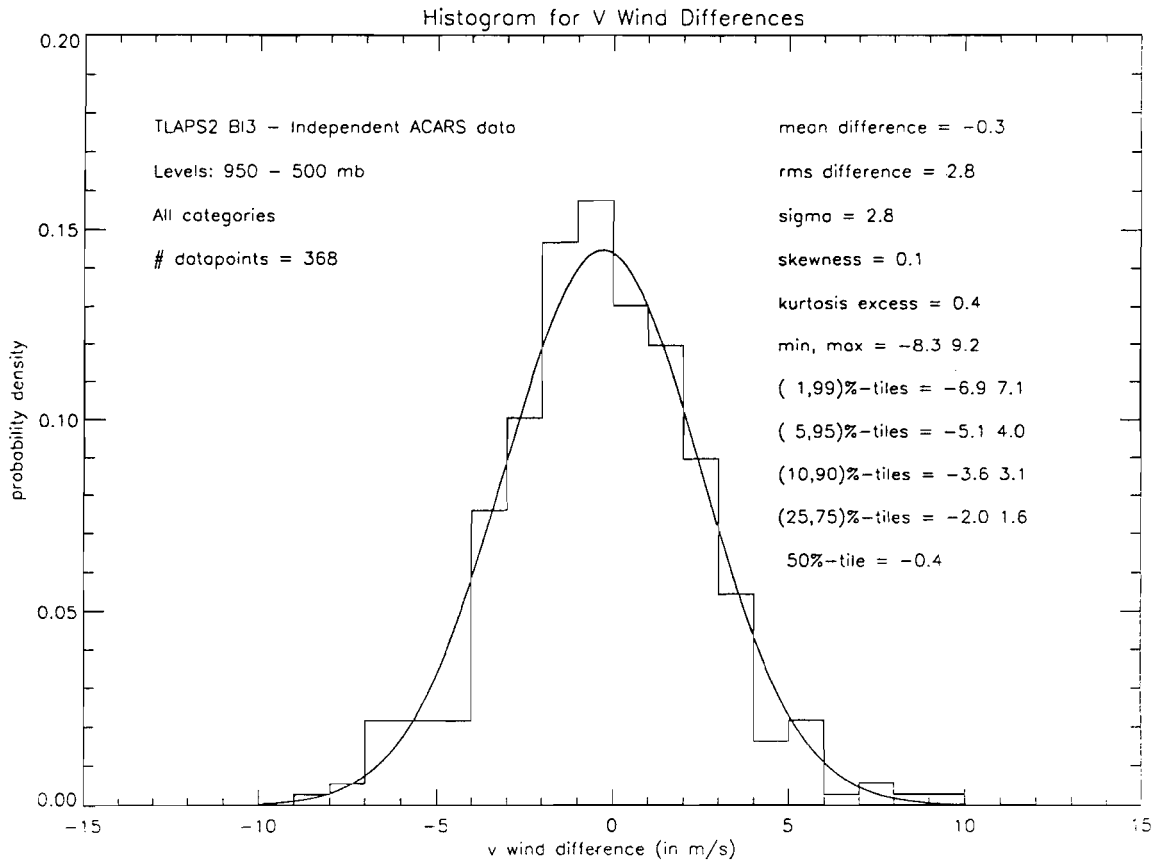
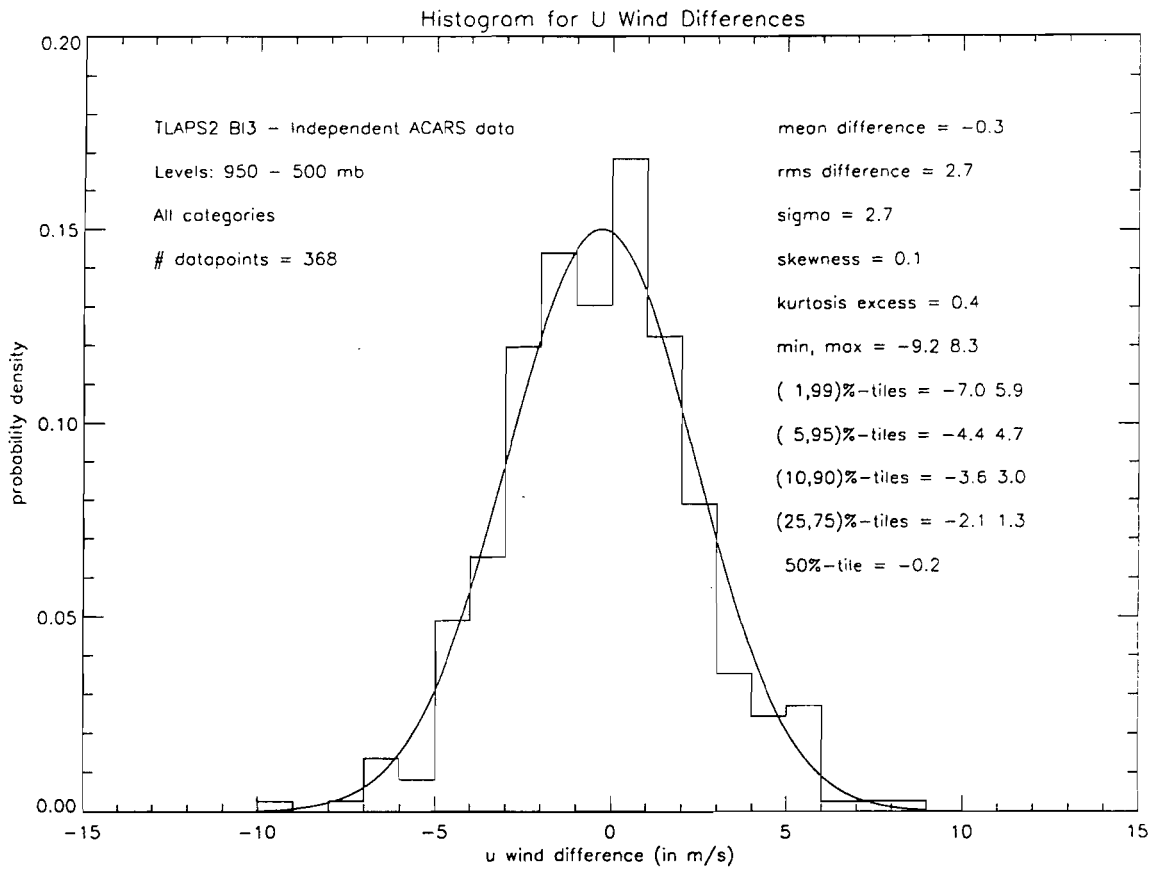


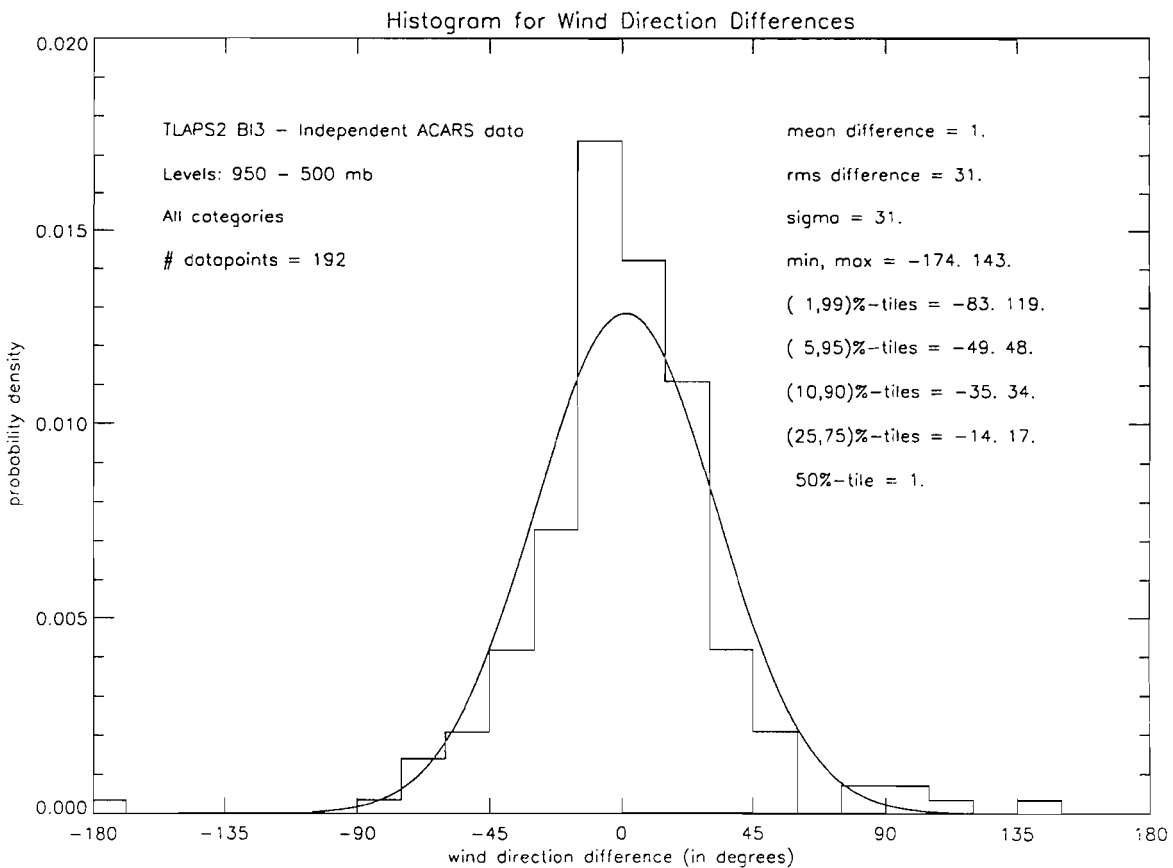
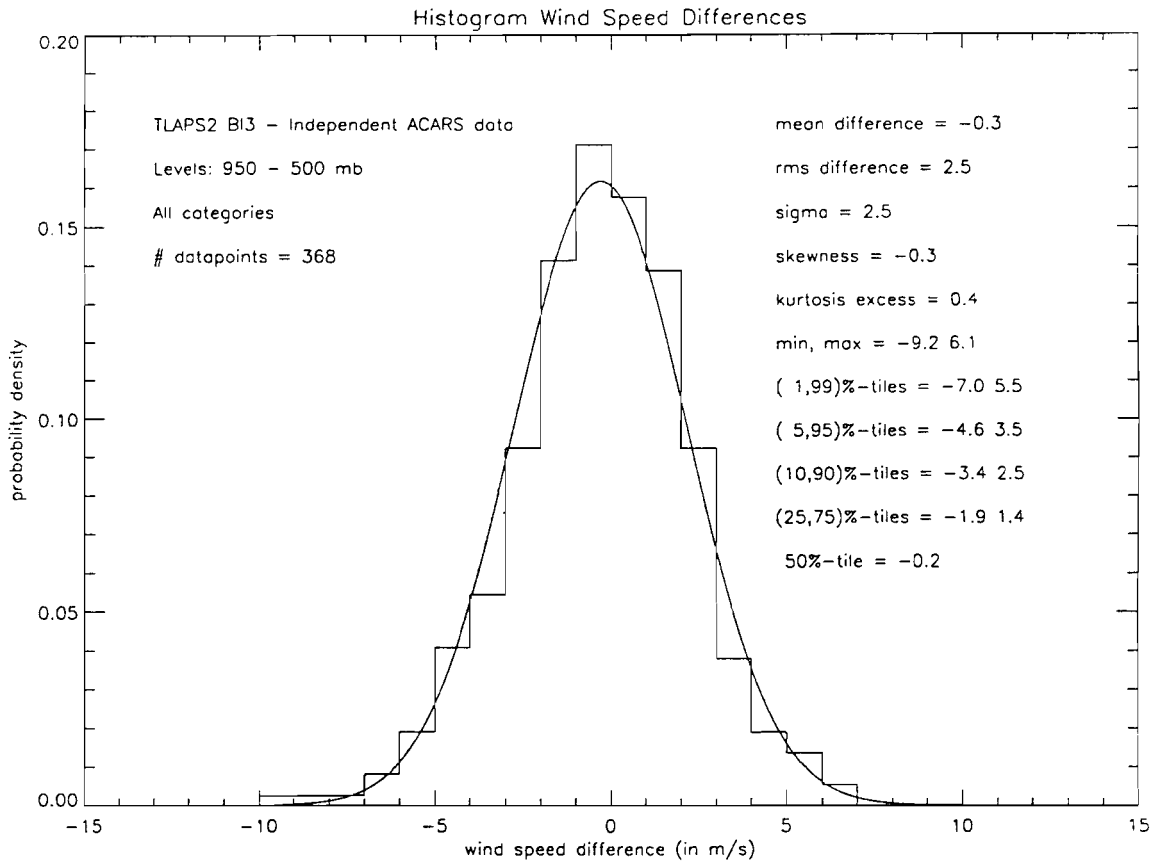
orientation: top of plot = 0 deg
note: only absolute values of wind speed differences are plotted

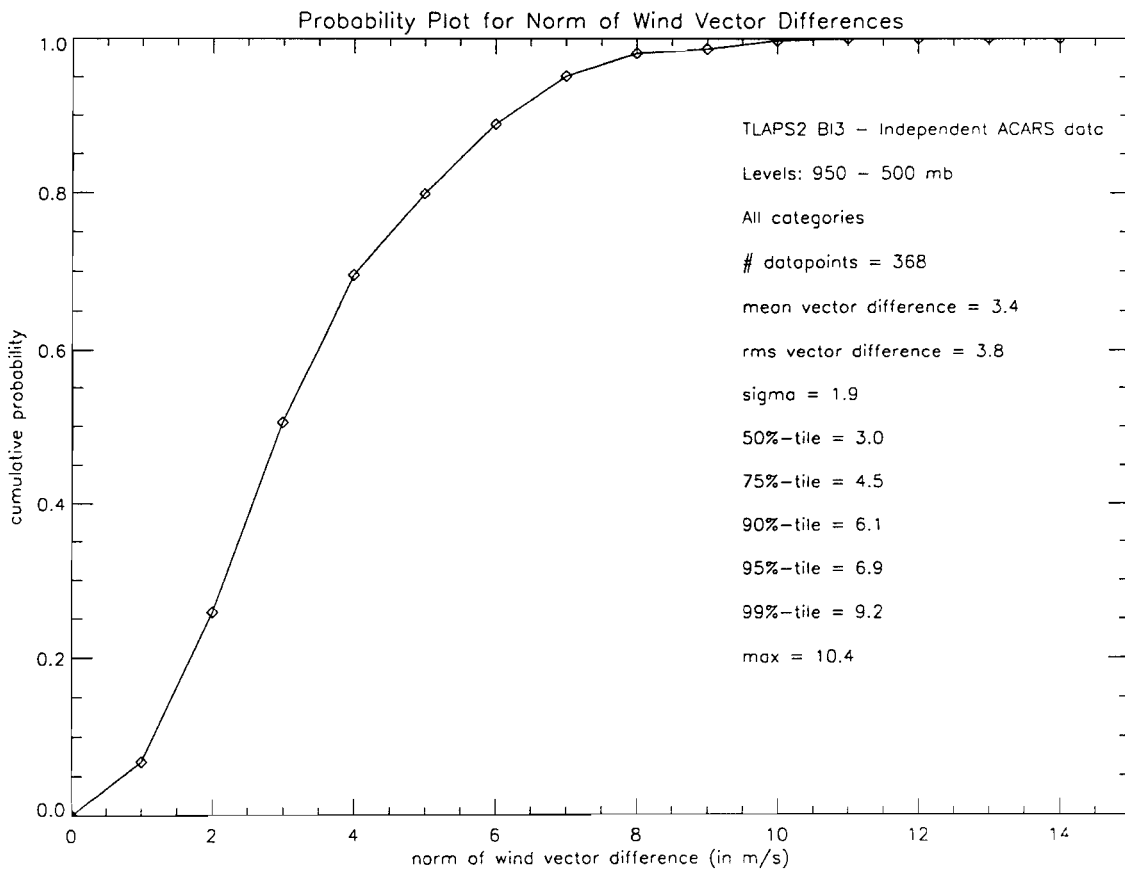
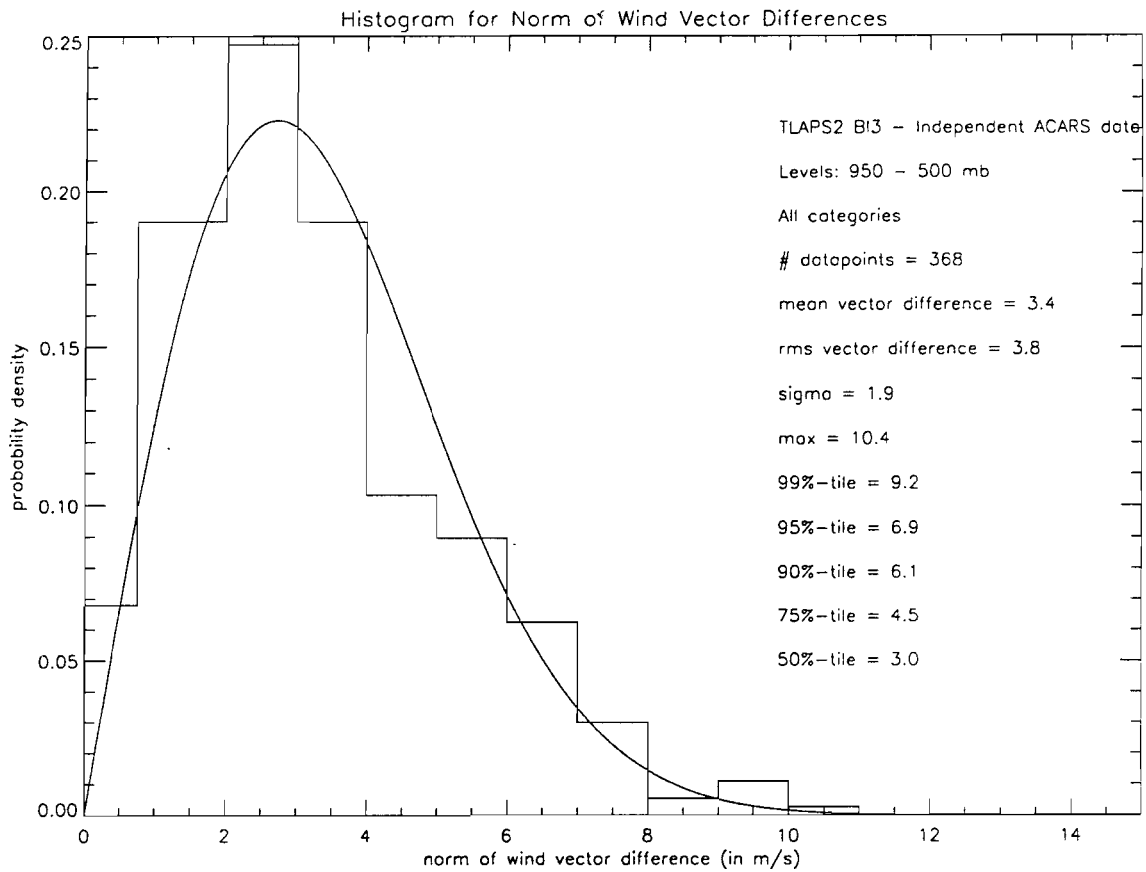


TLAPS2 BI2 - Independent ACARS data

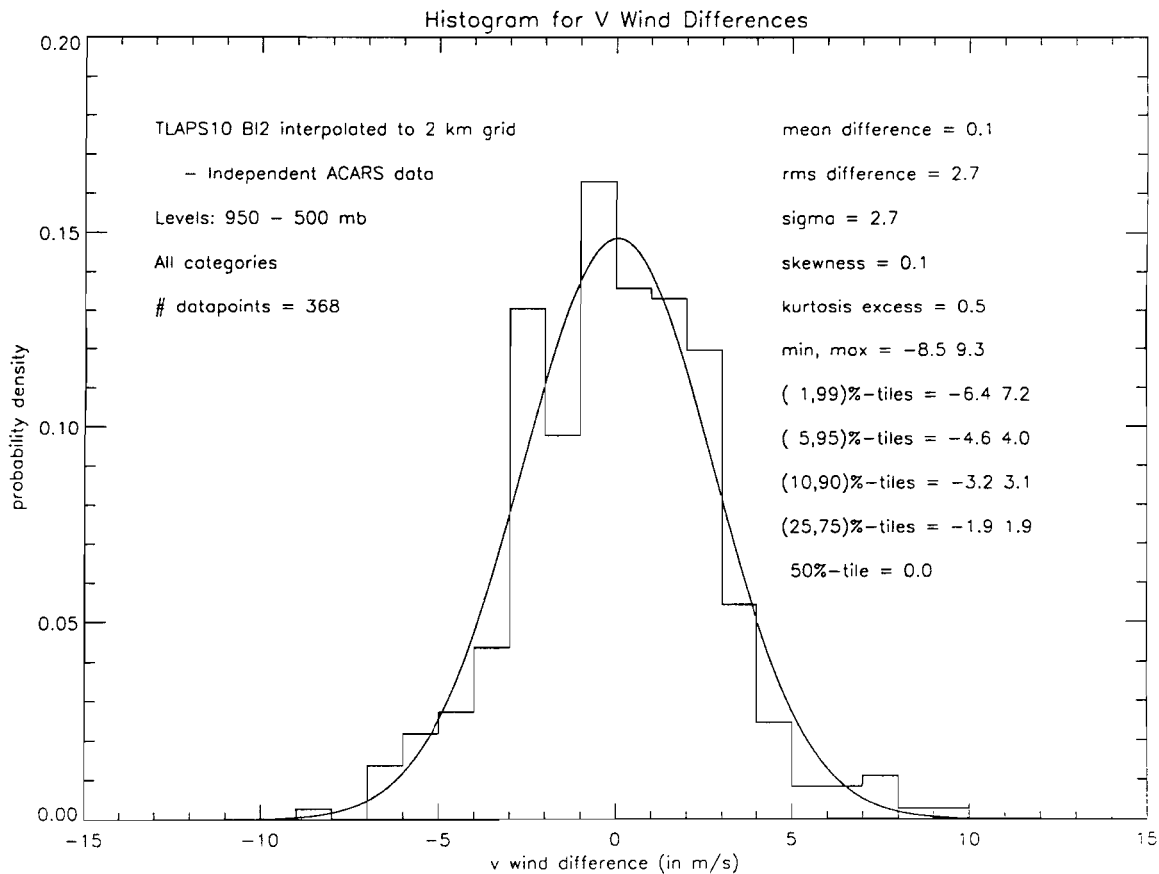
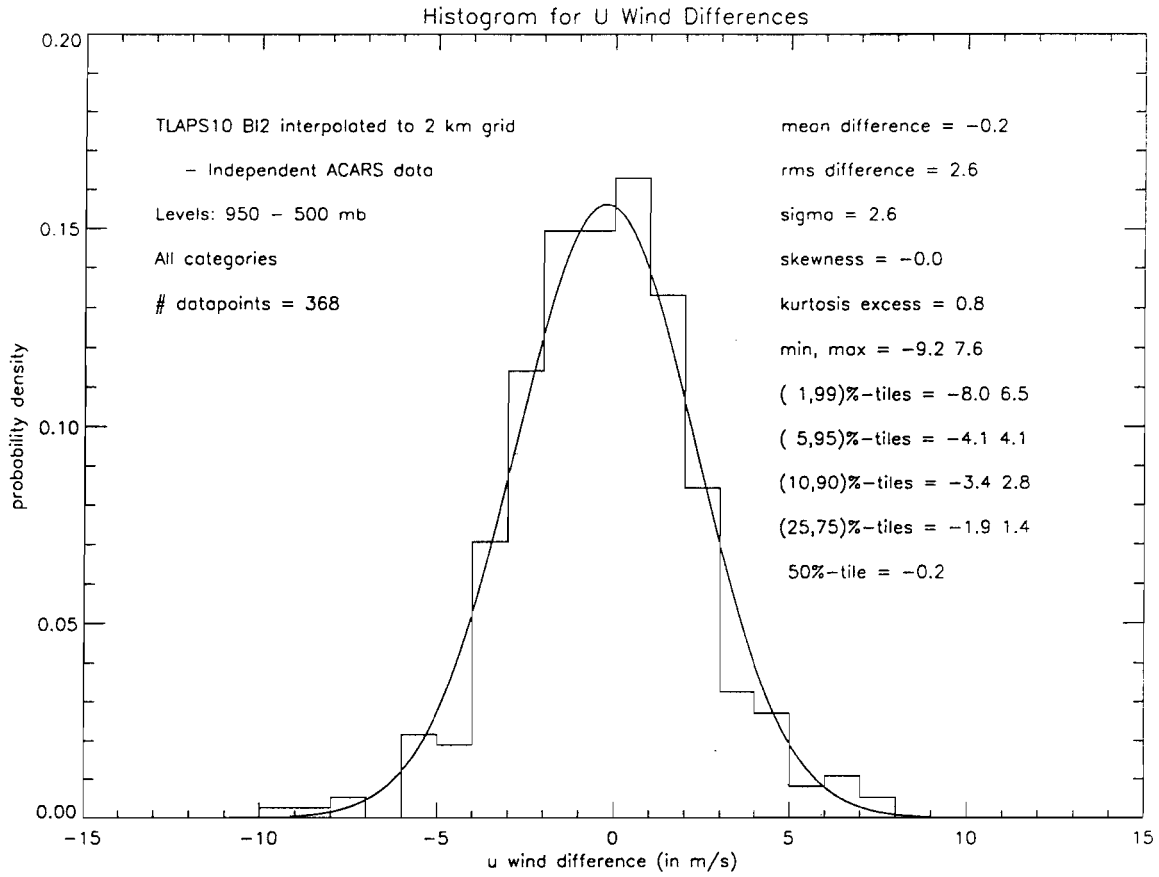
SECTION C-2



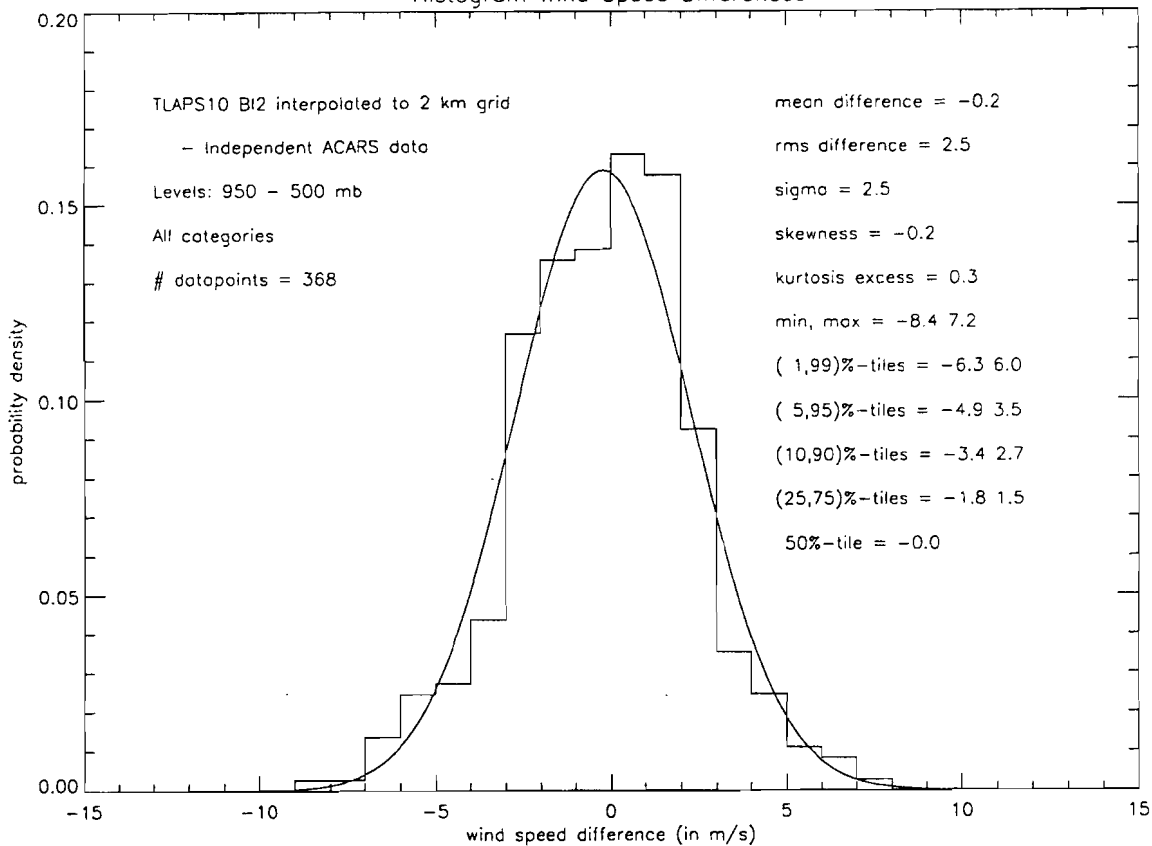




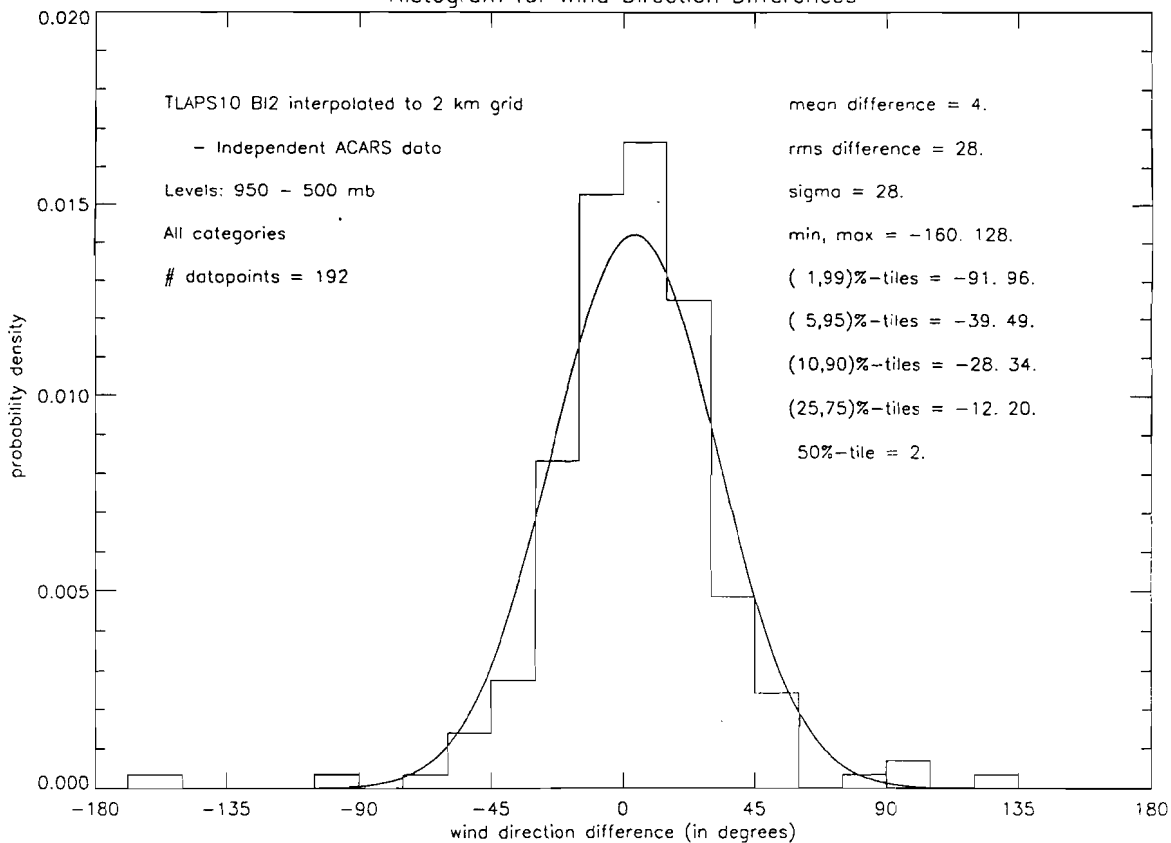
SECTION C-3

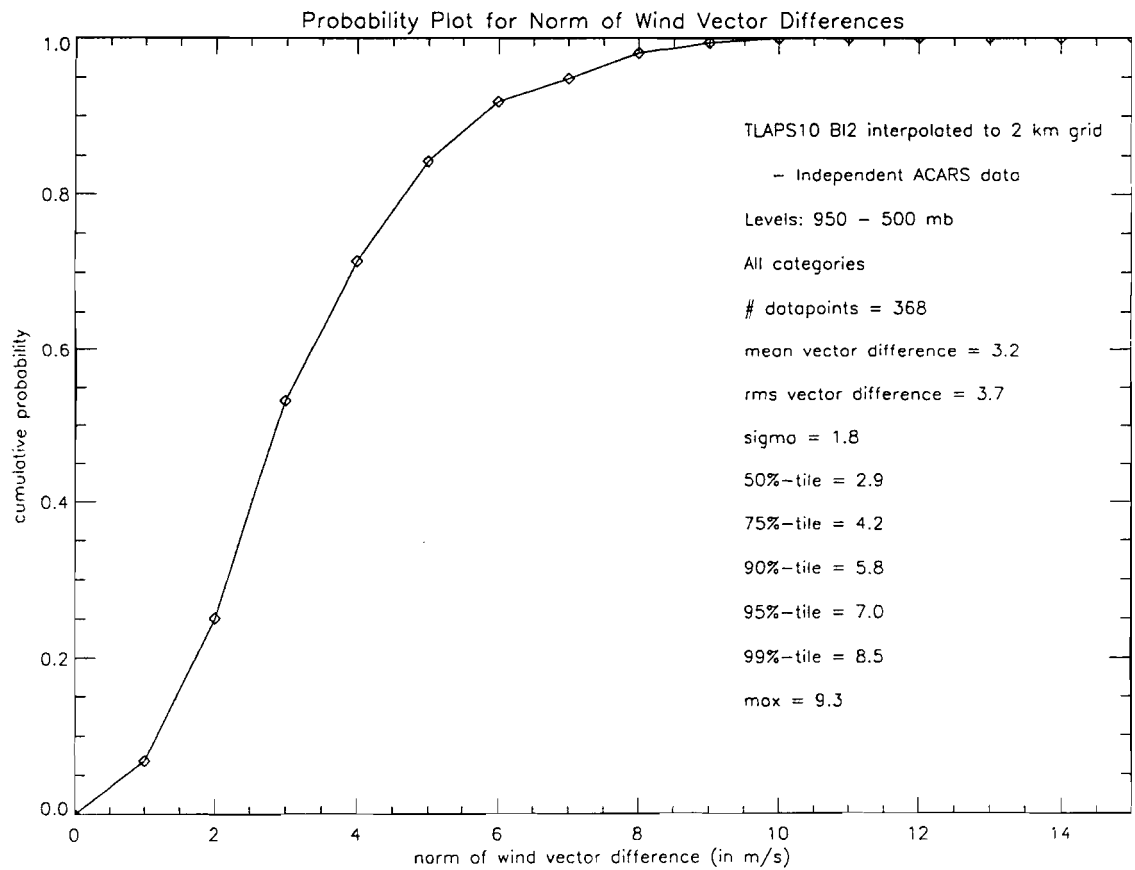
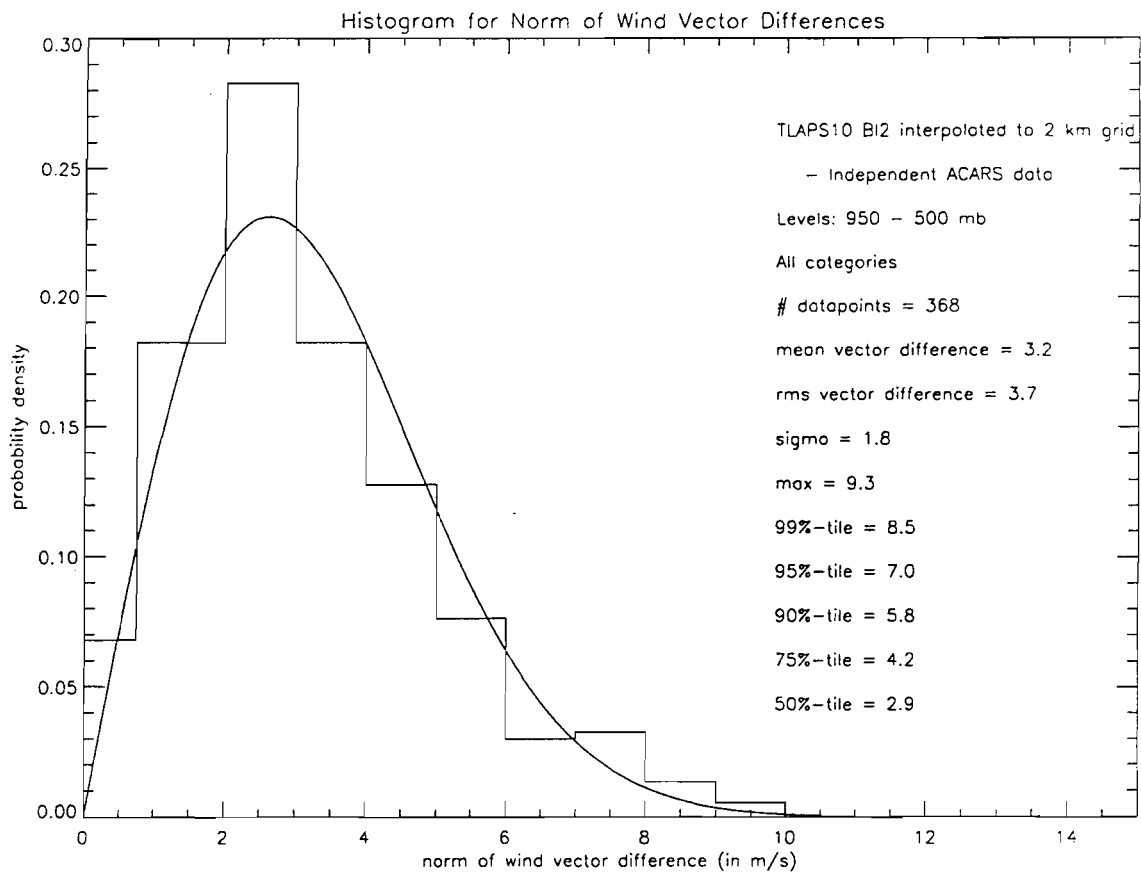


Histogram Wind Speed Differences

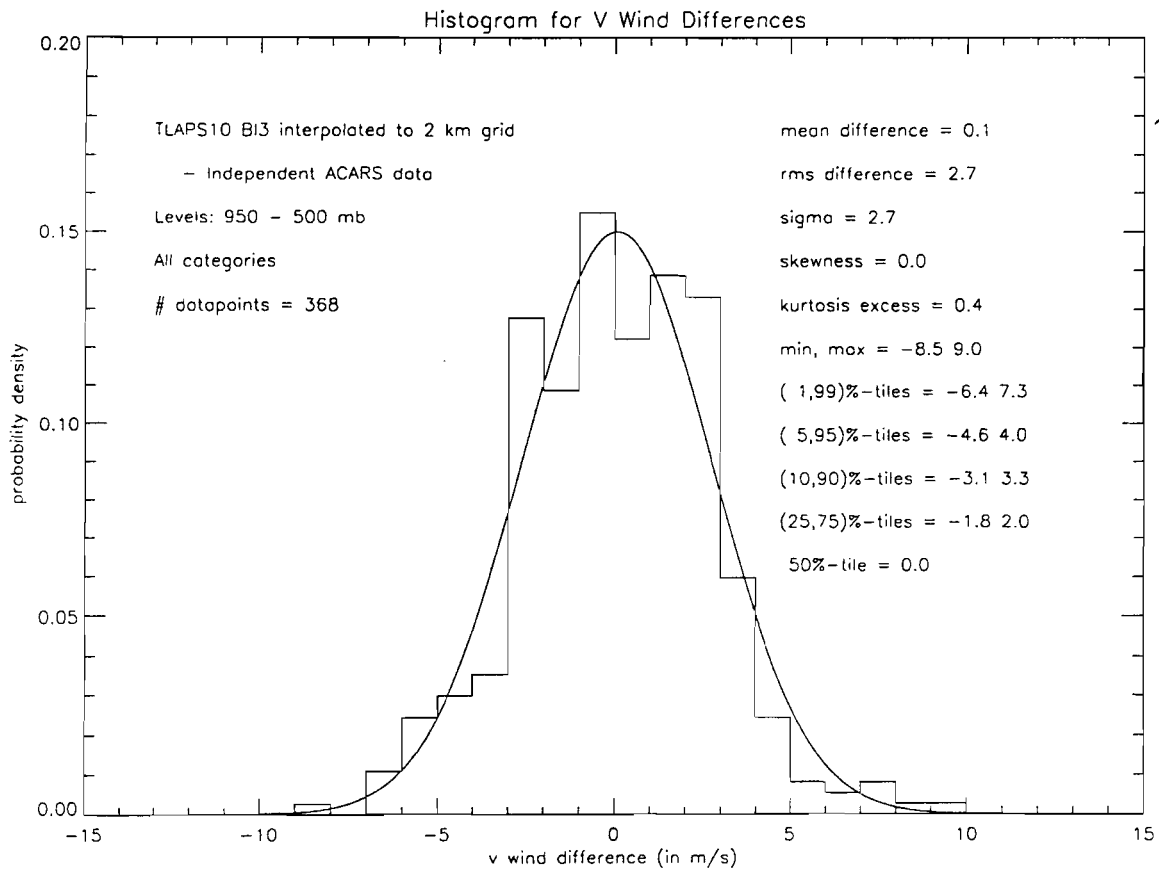
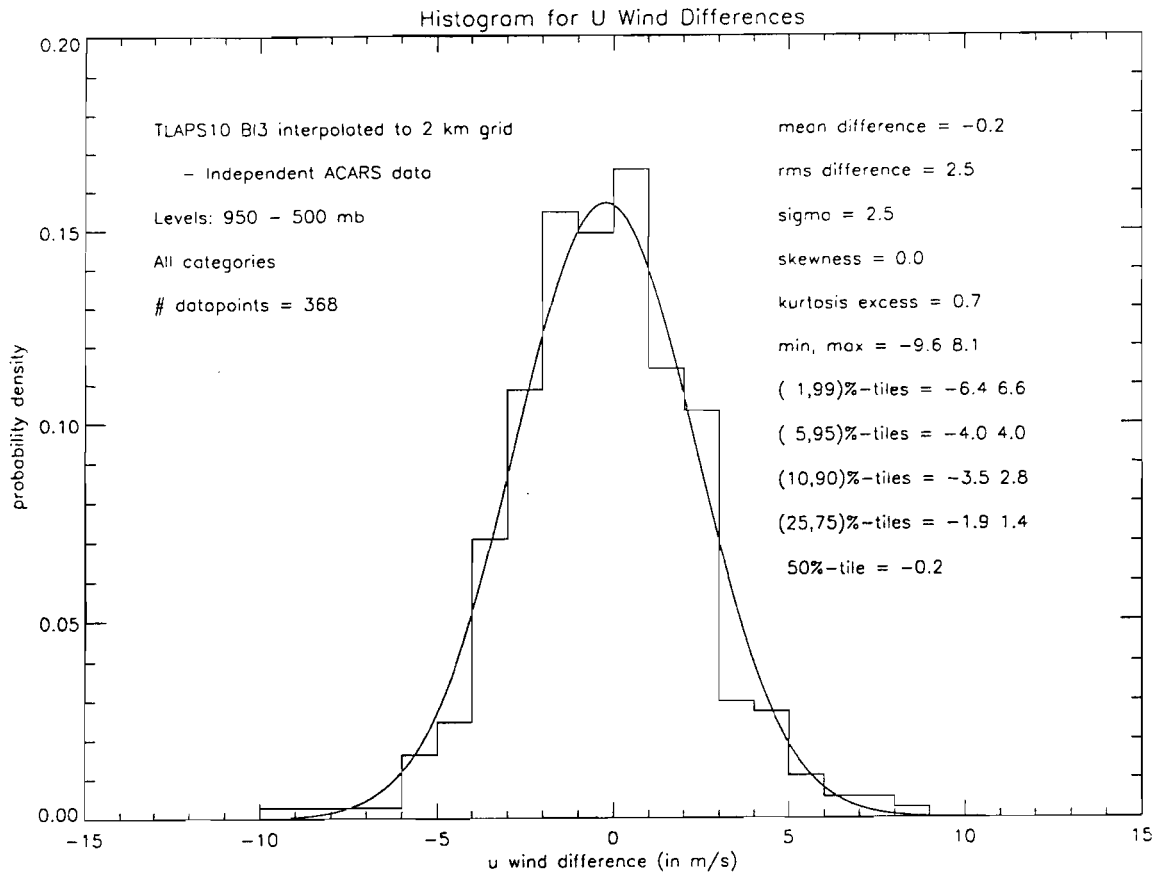


Histogram for Wind Direction Differences

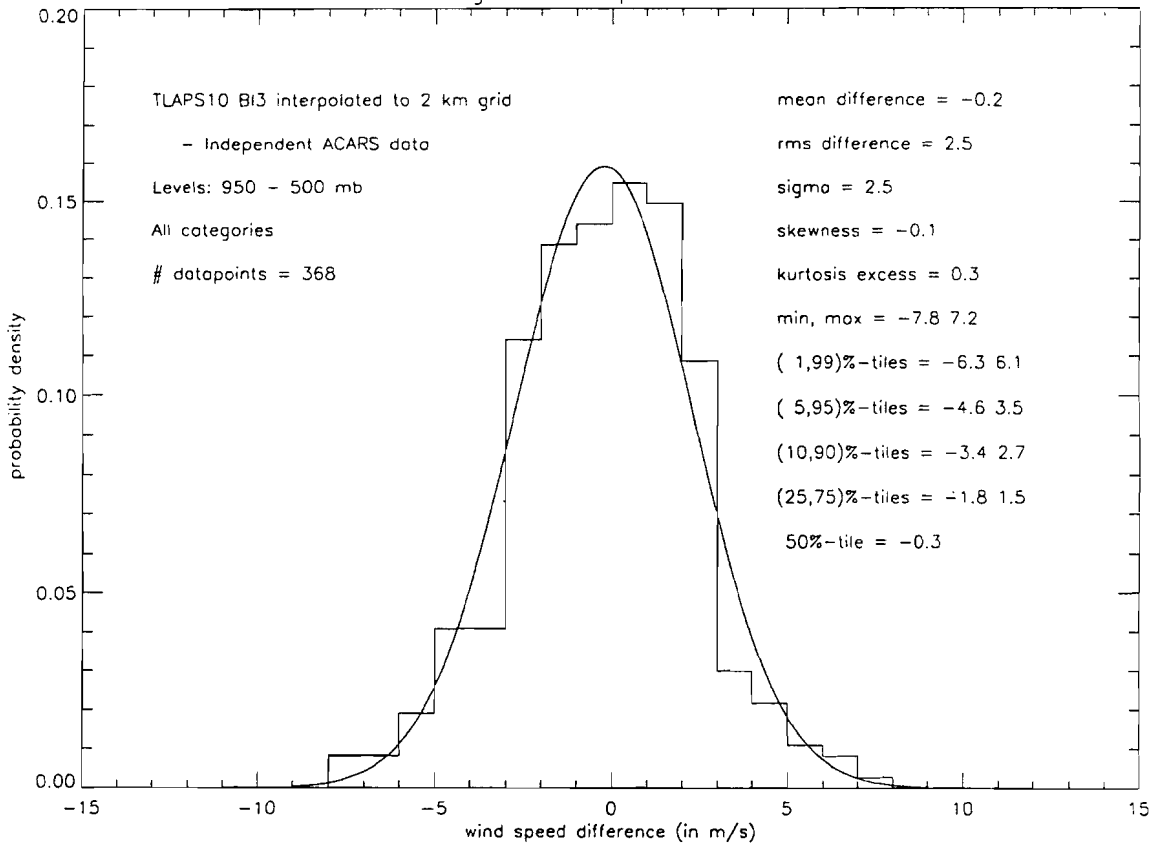




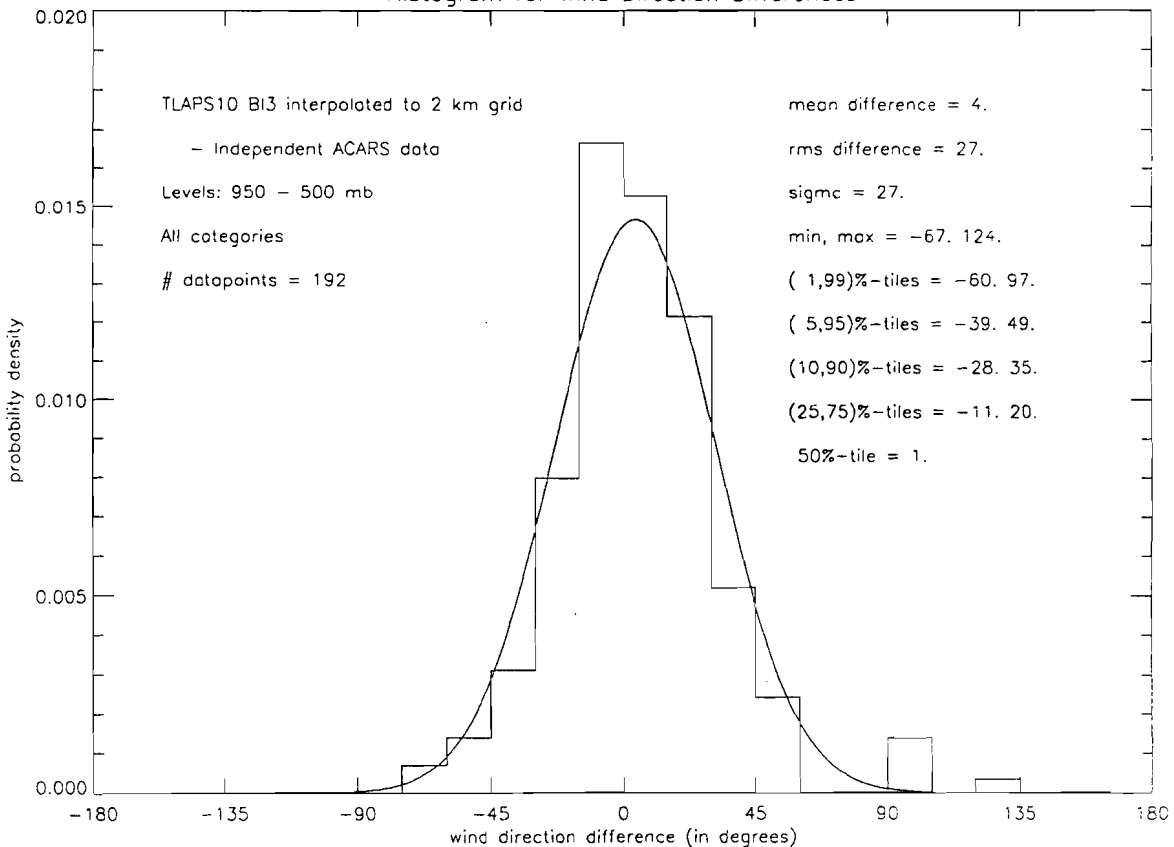
SECTION C-4

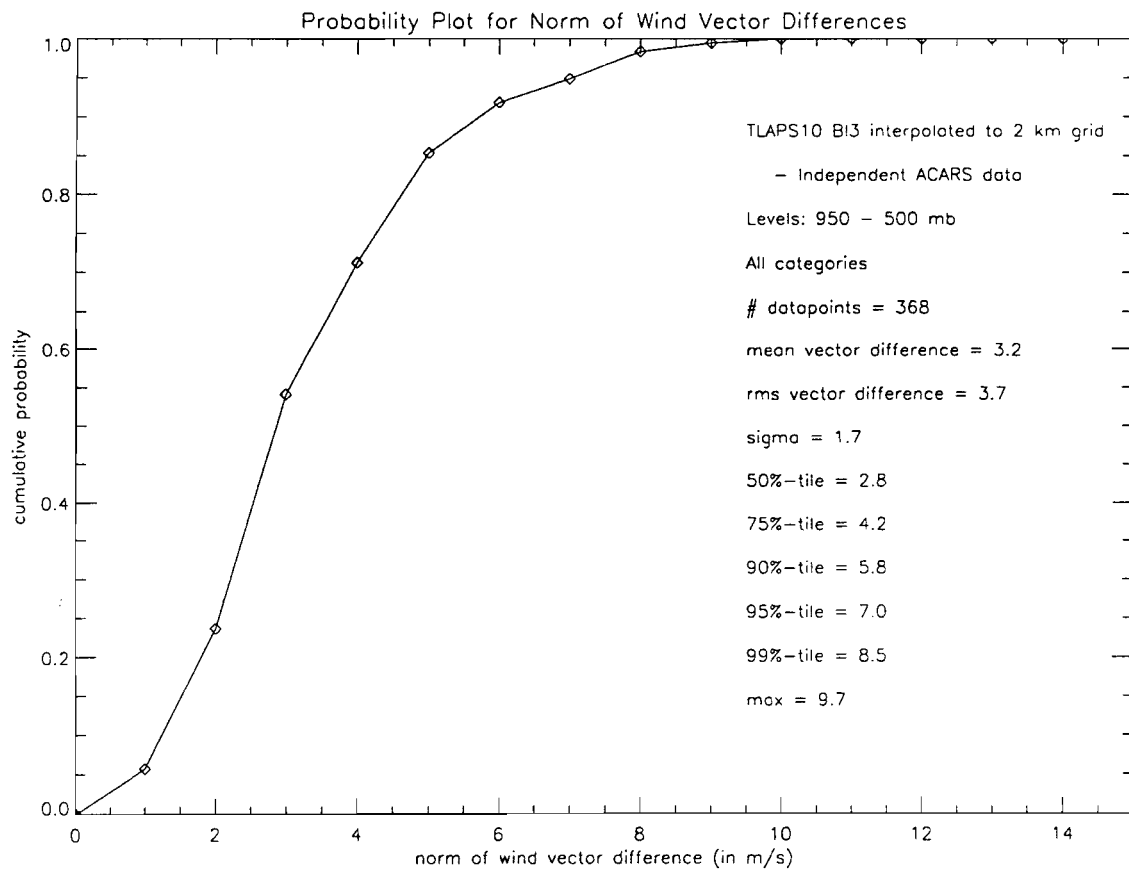
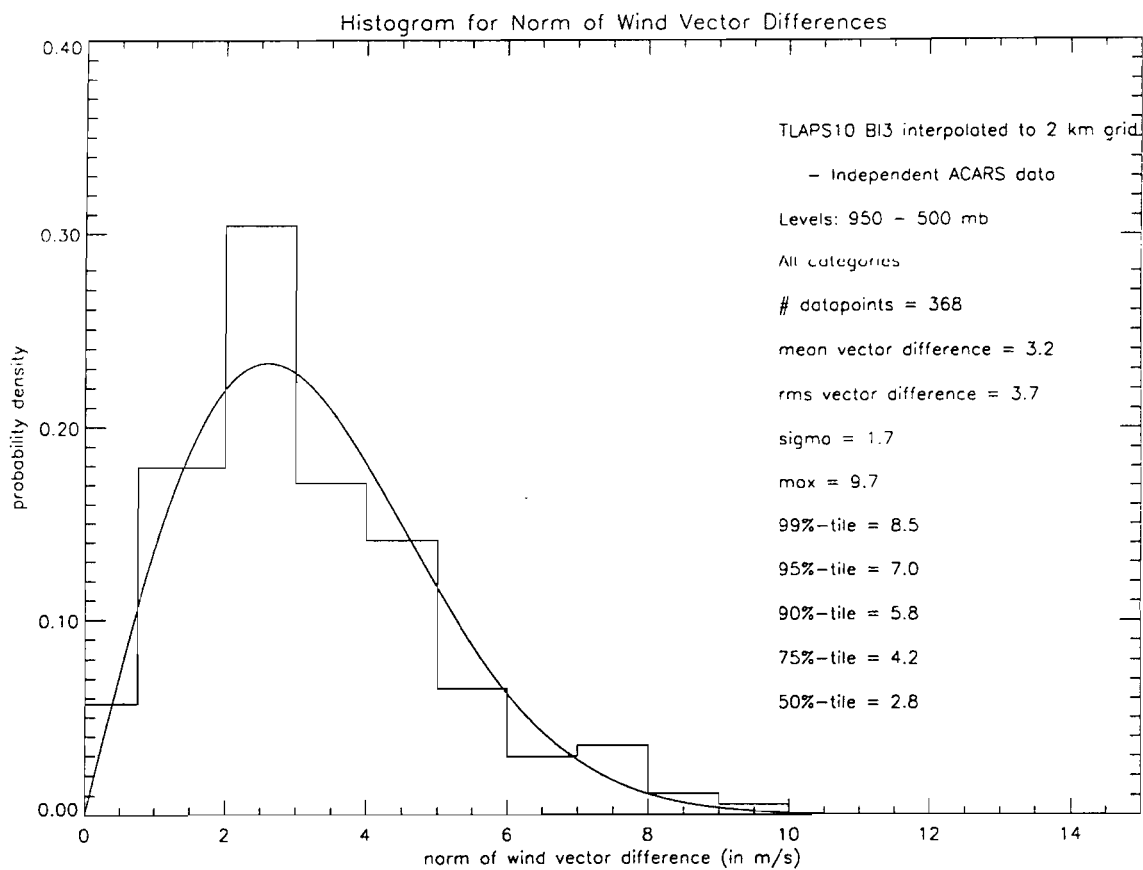


Histogram Wind Speed Differences

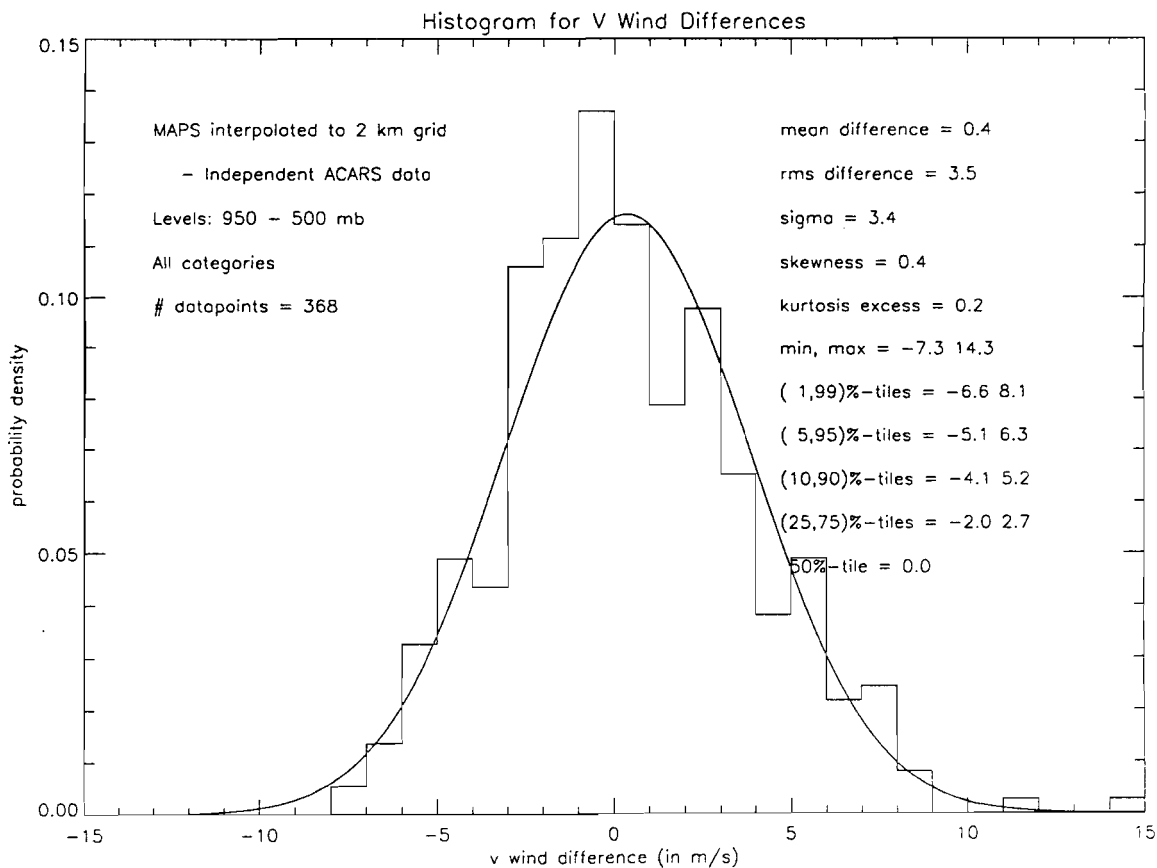
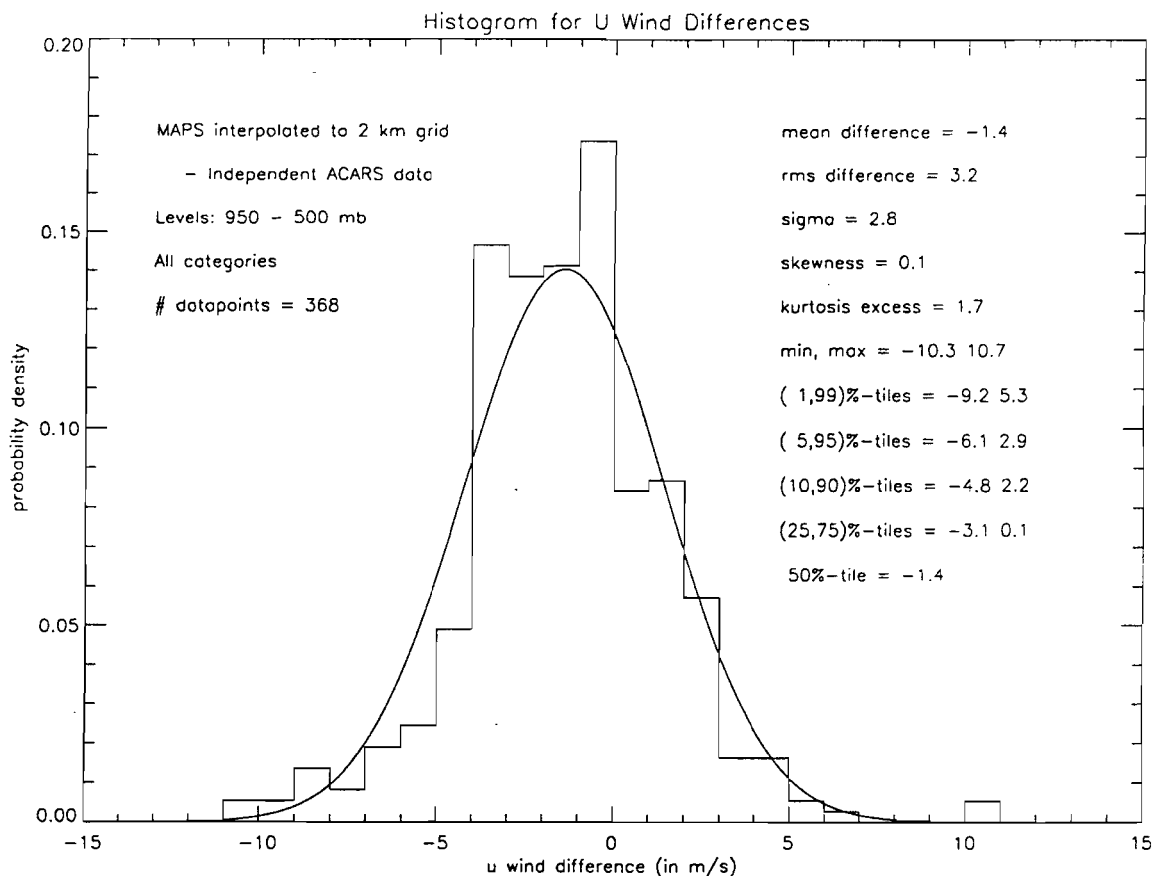


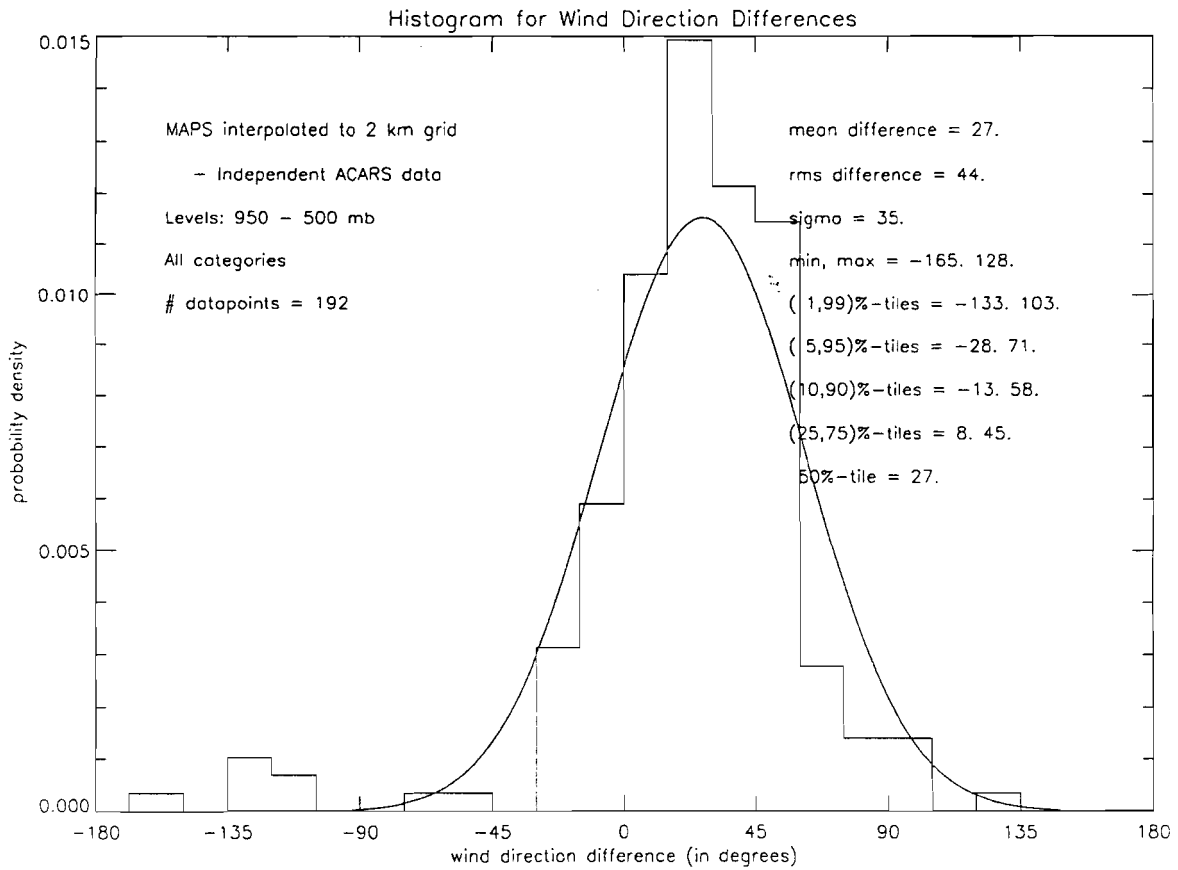
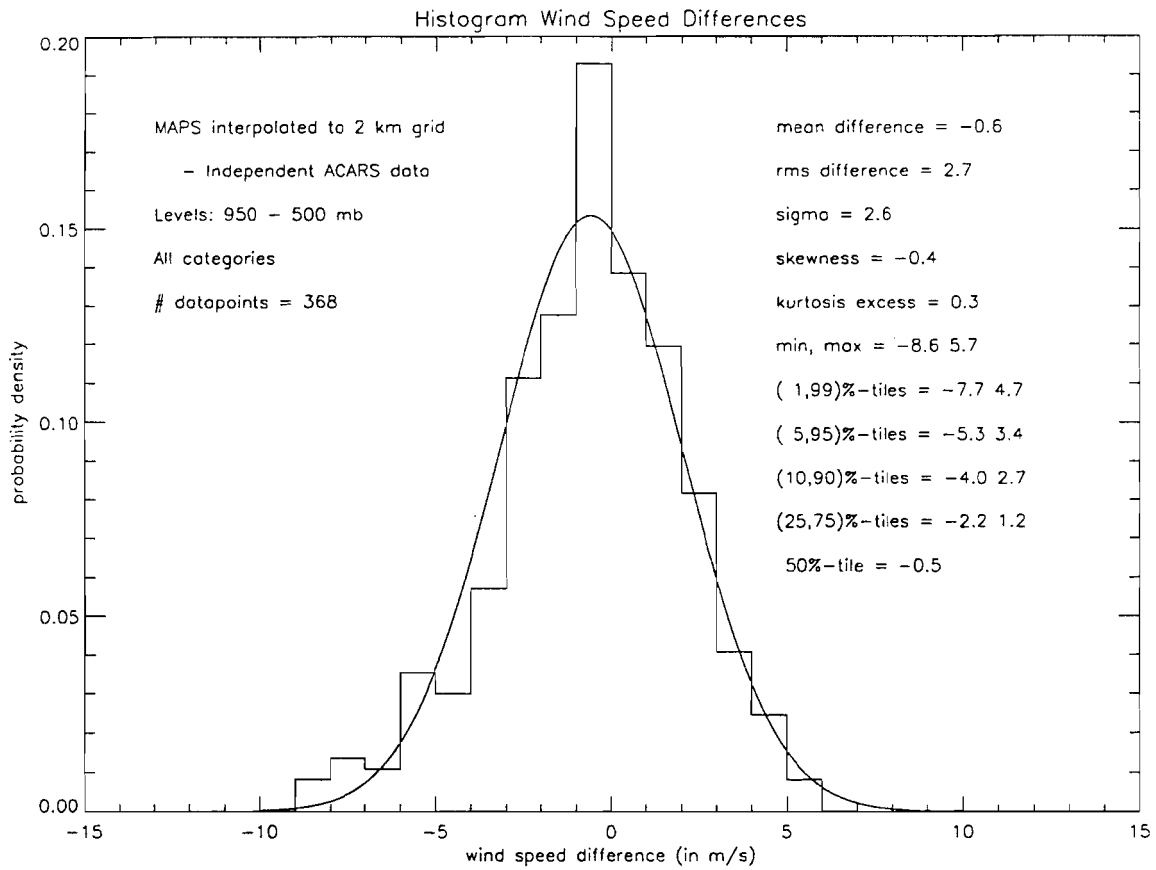
Histogram for Wind Direction Differences

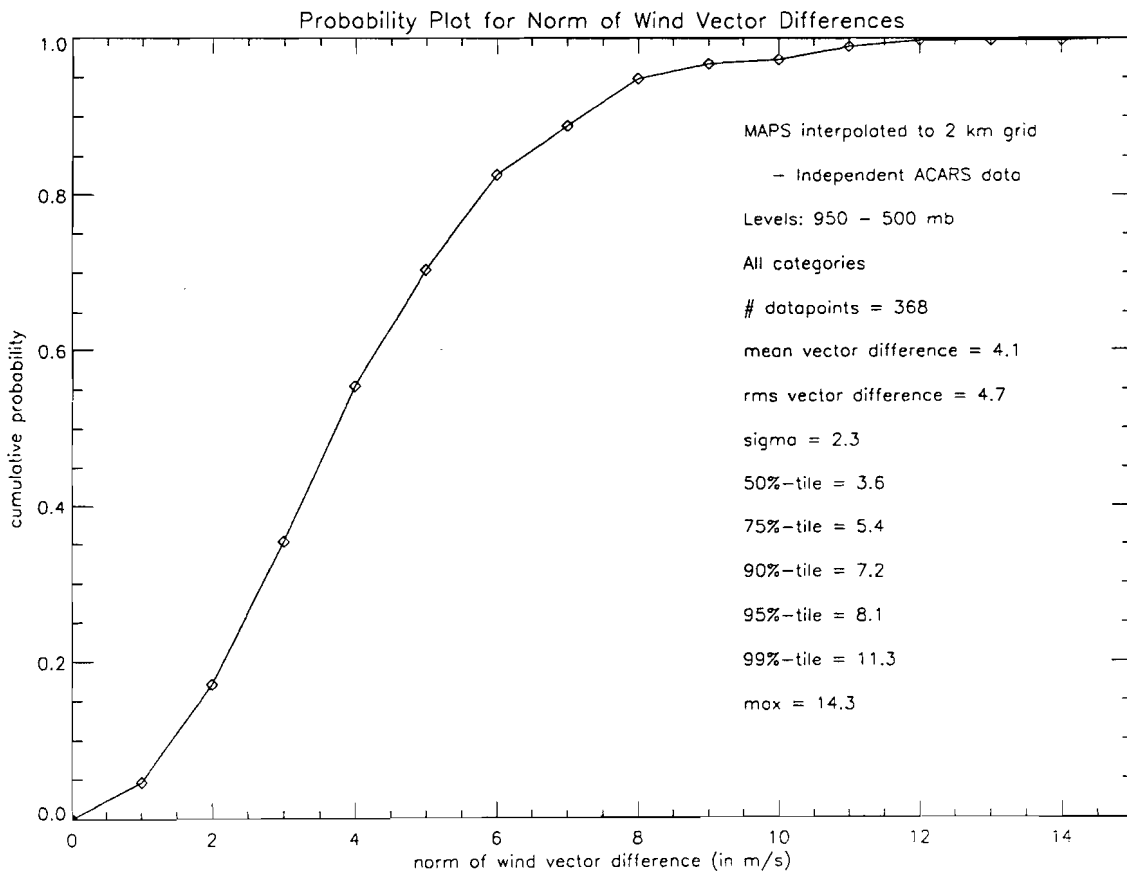
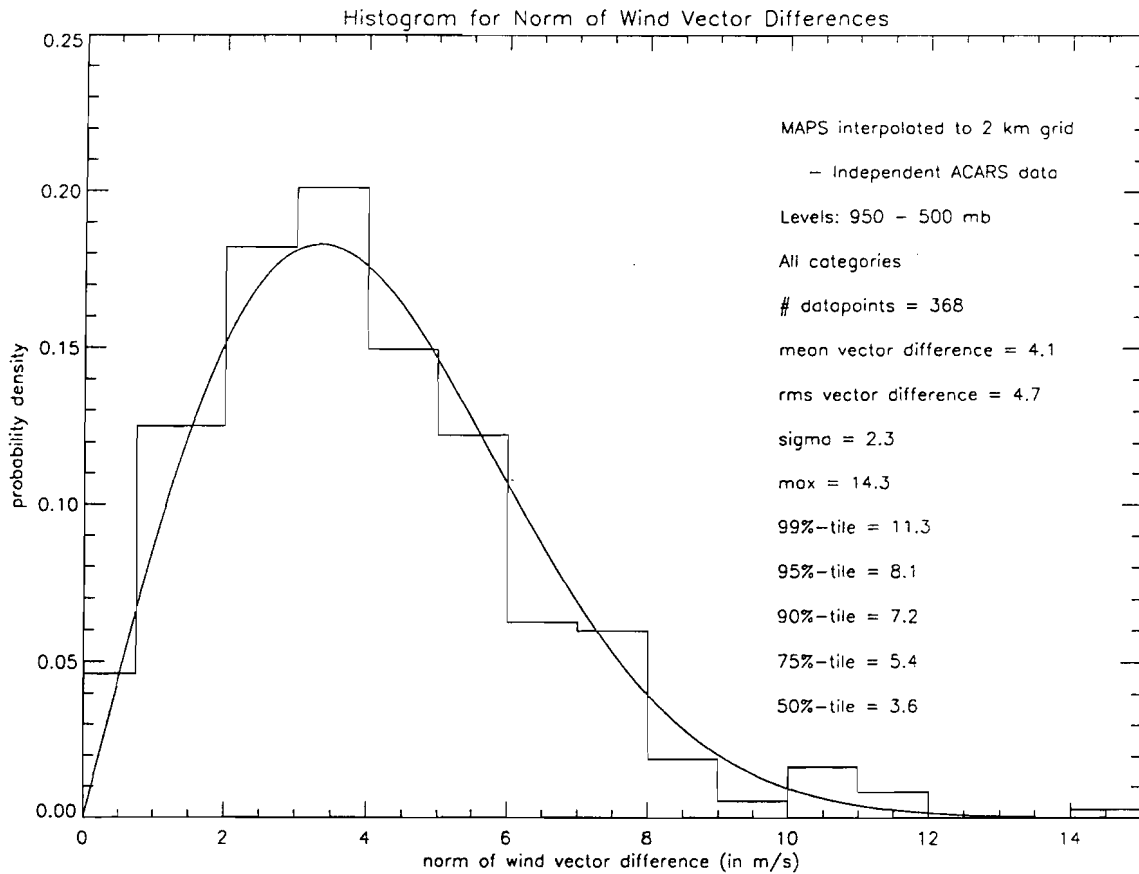




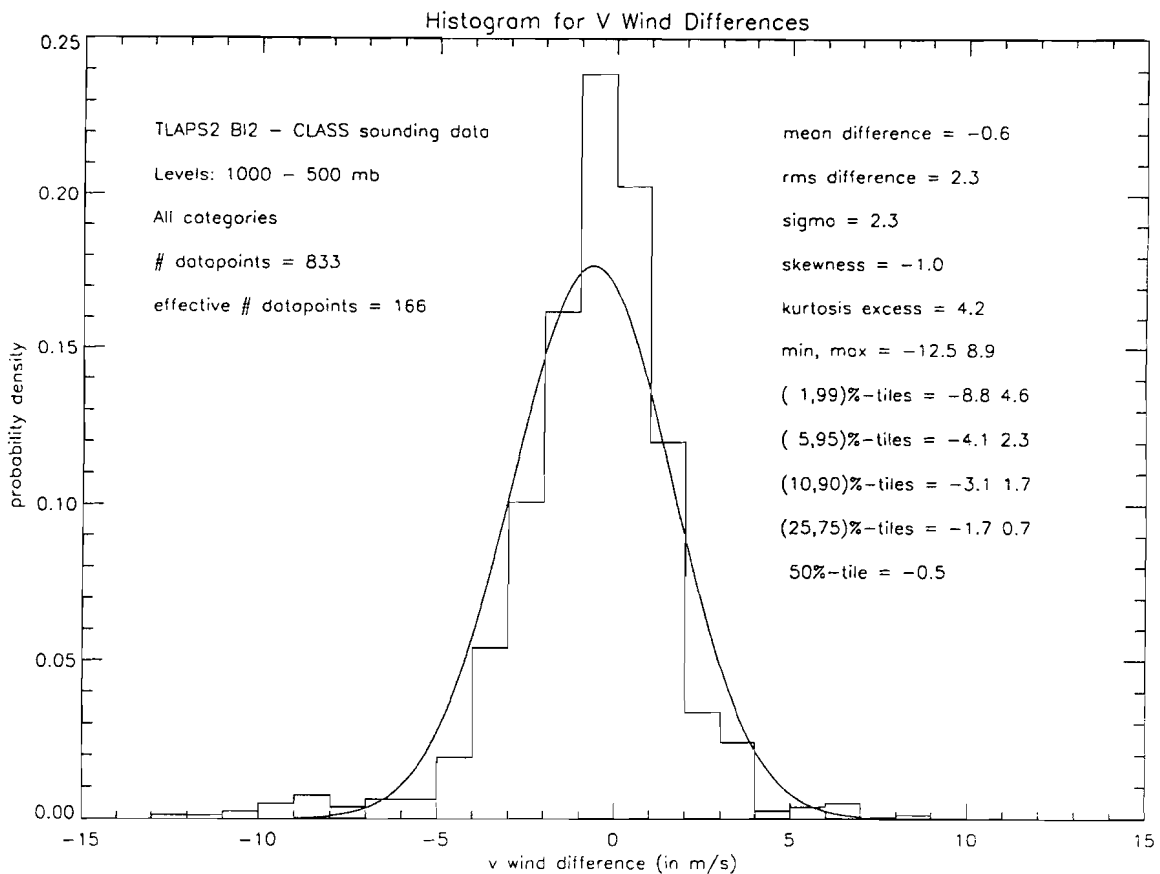
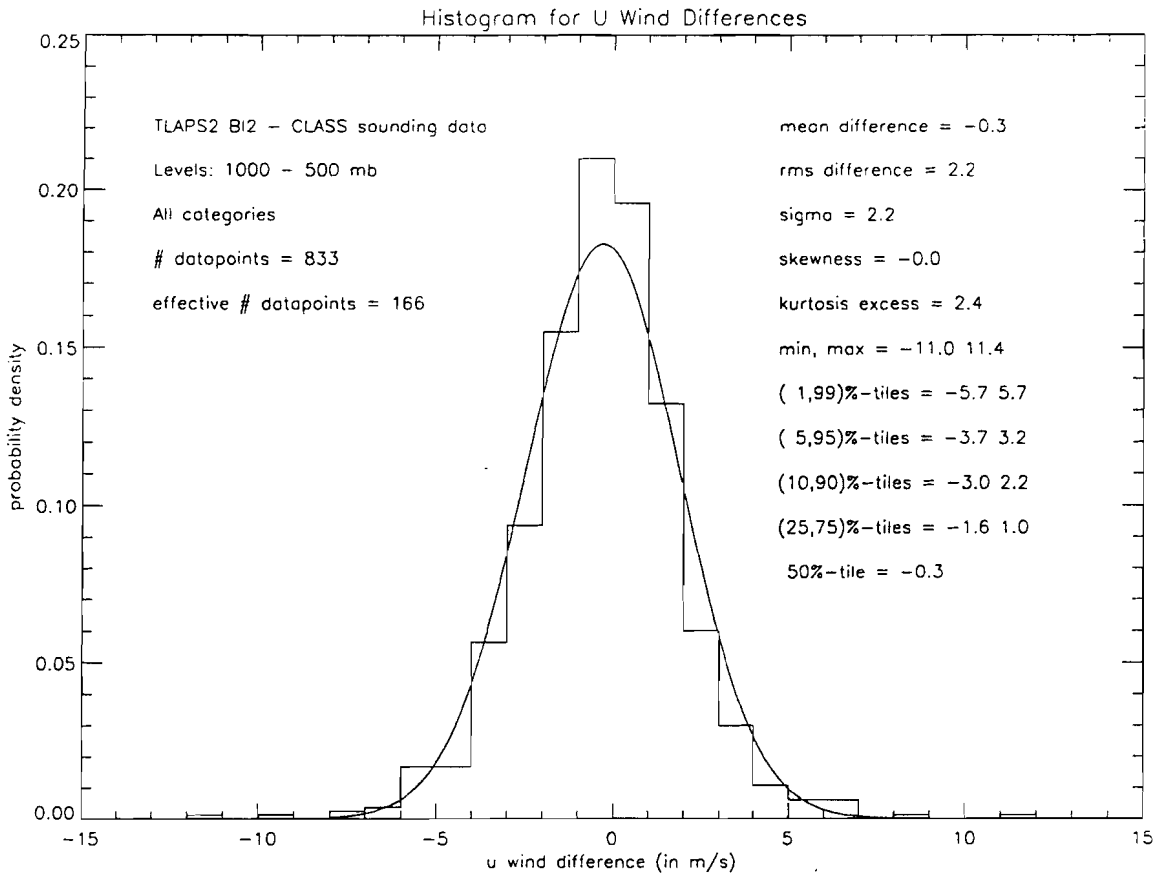
SECTION C-5



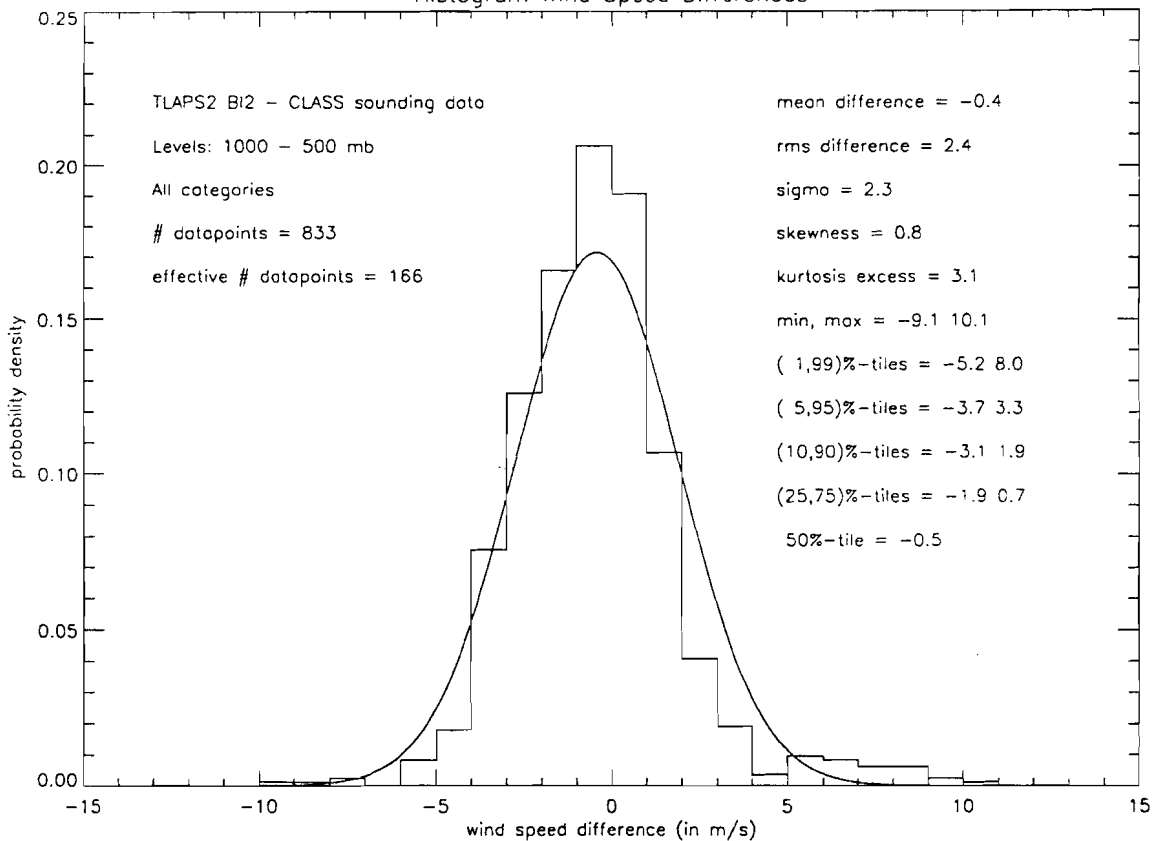




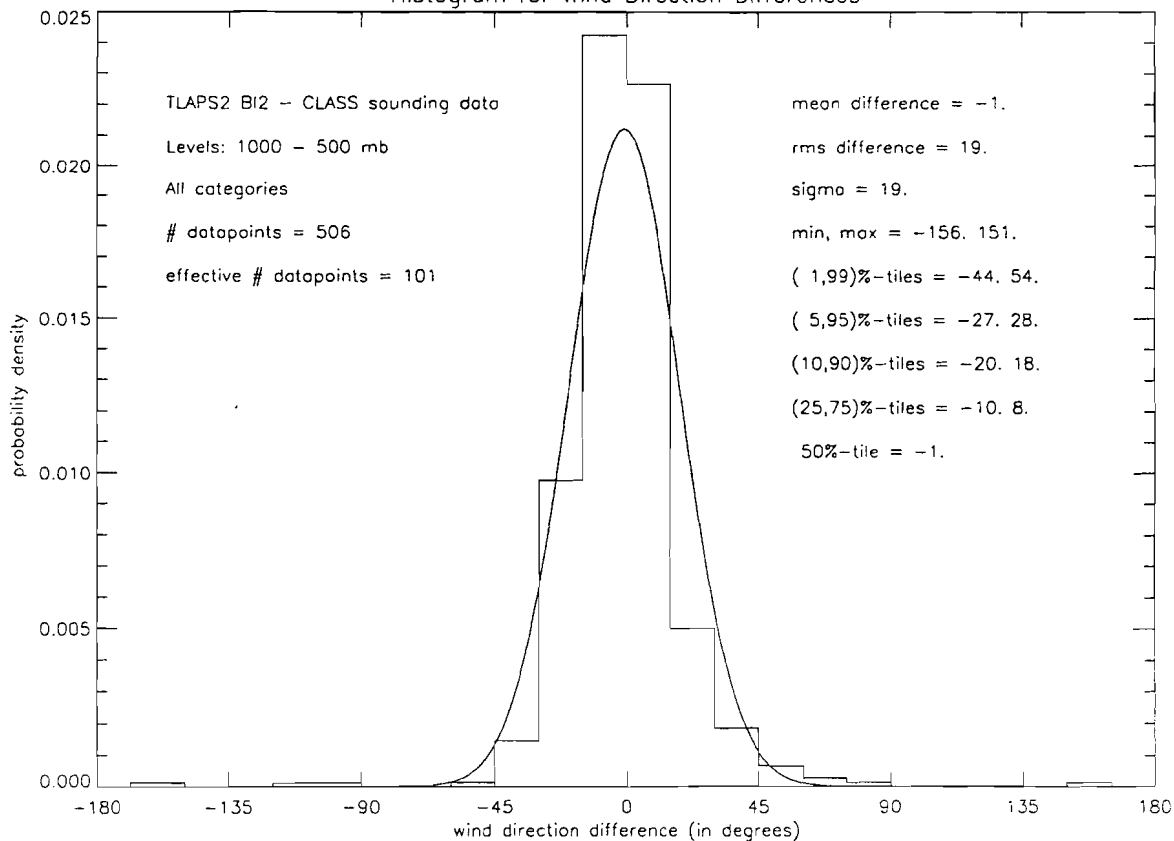
SECTION C-6

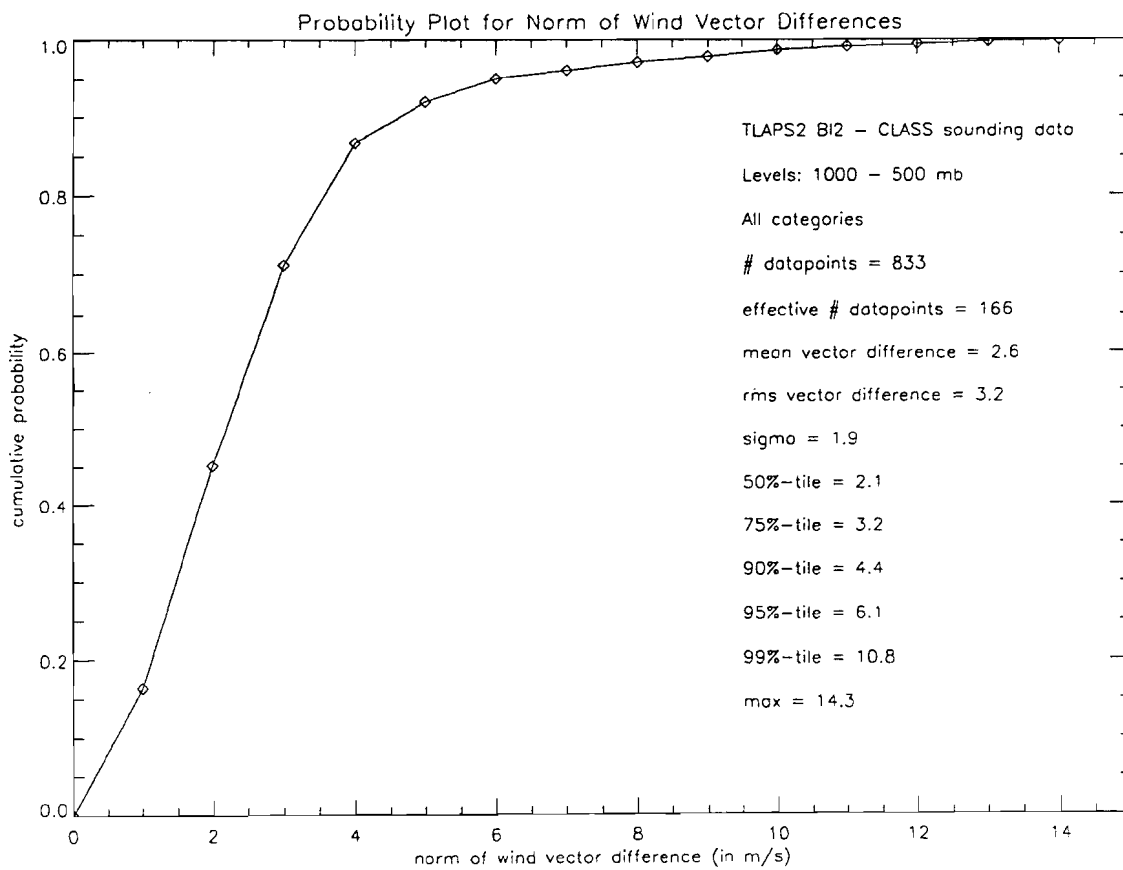
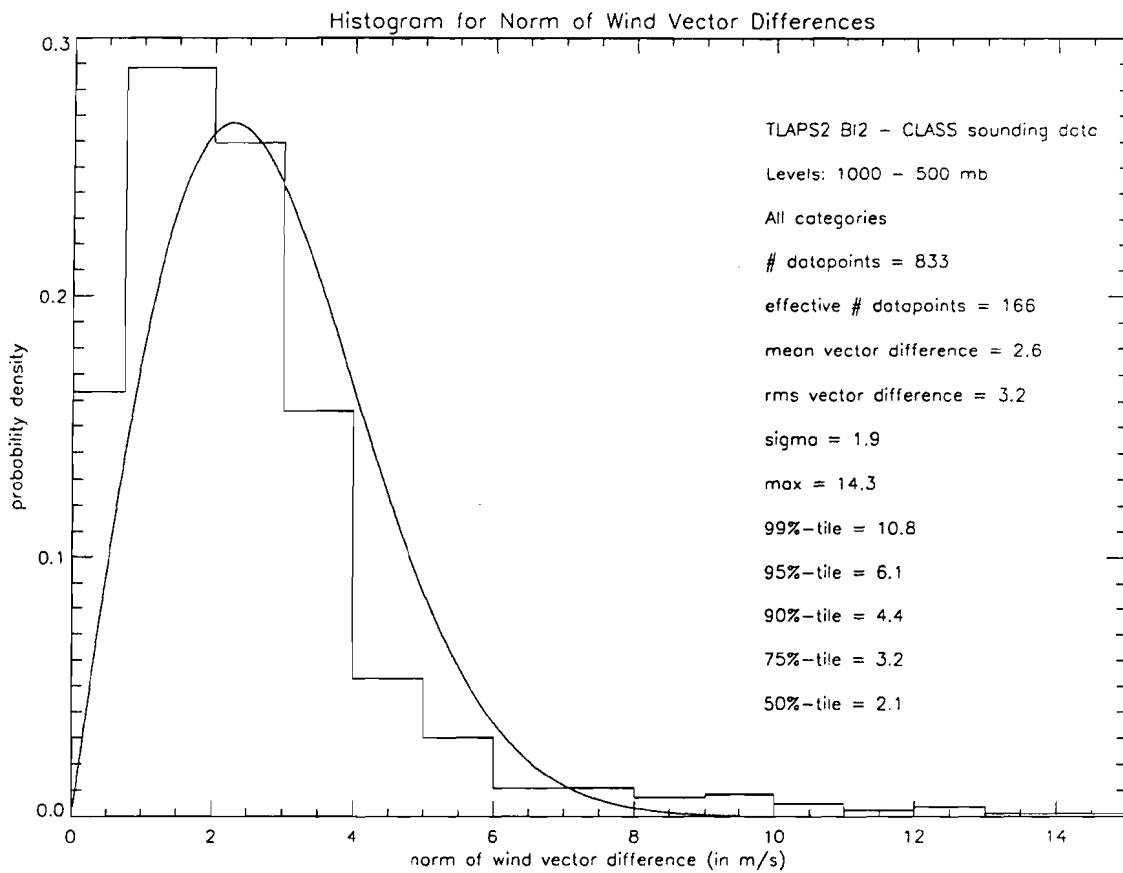


Histogram Wind Speed Differences

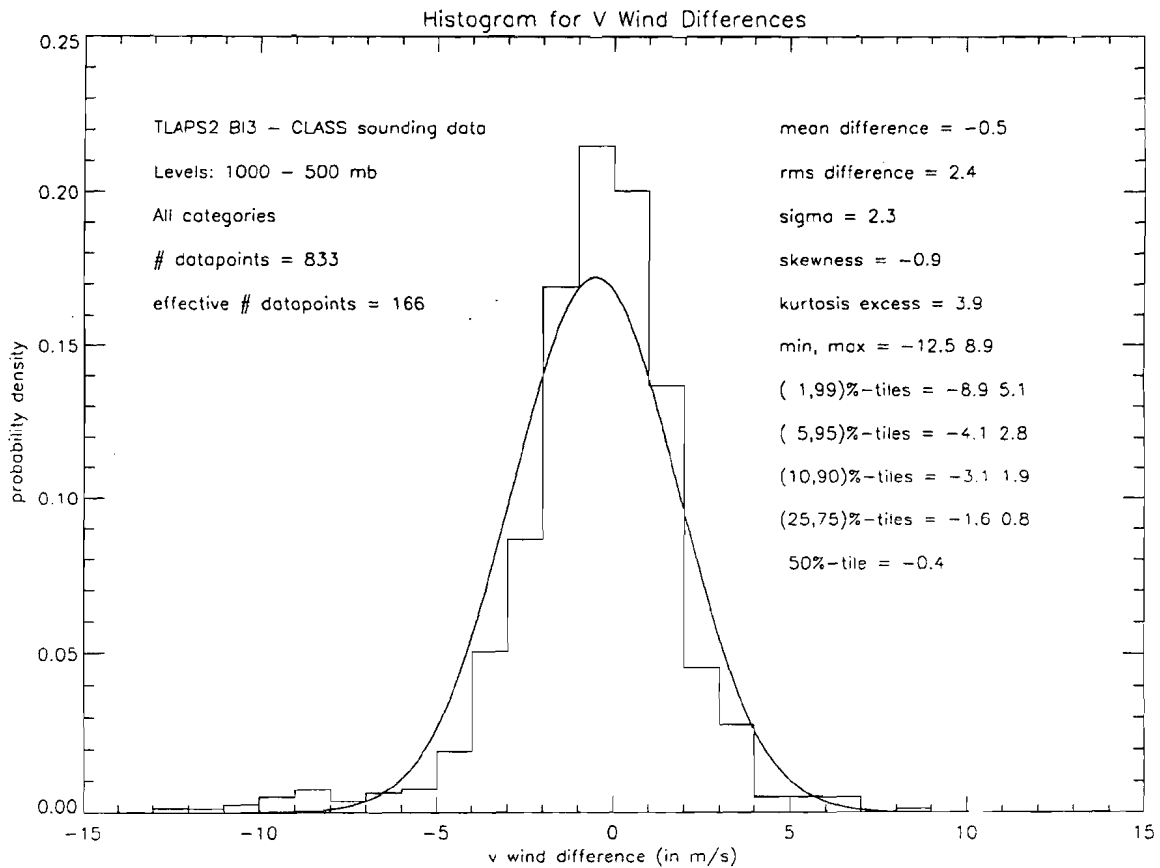
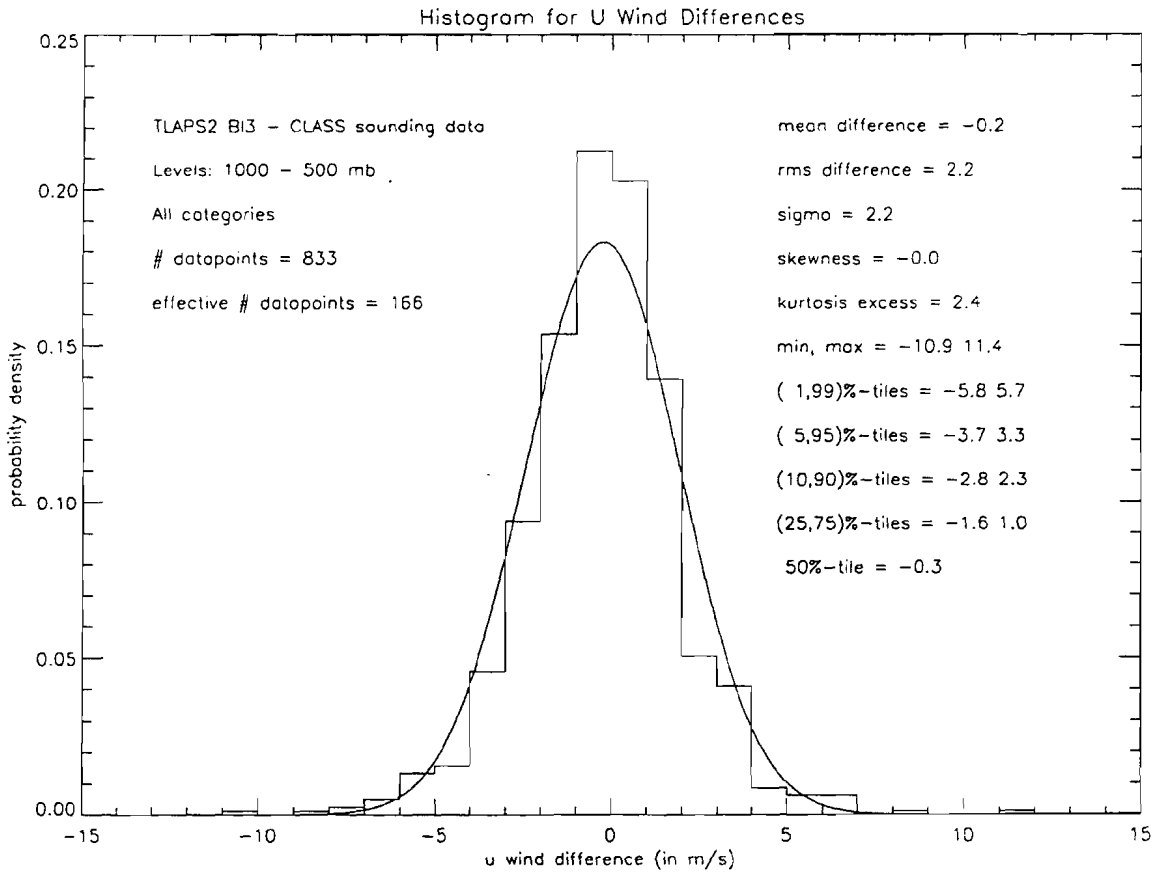


Histogram for Wind Direction Differences

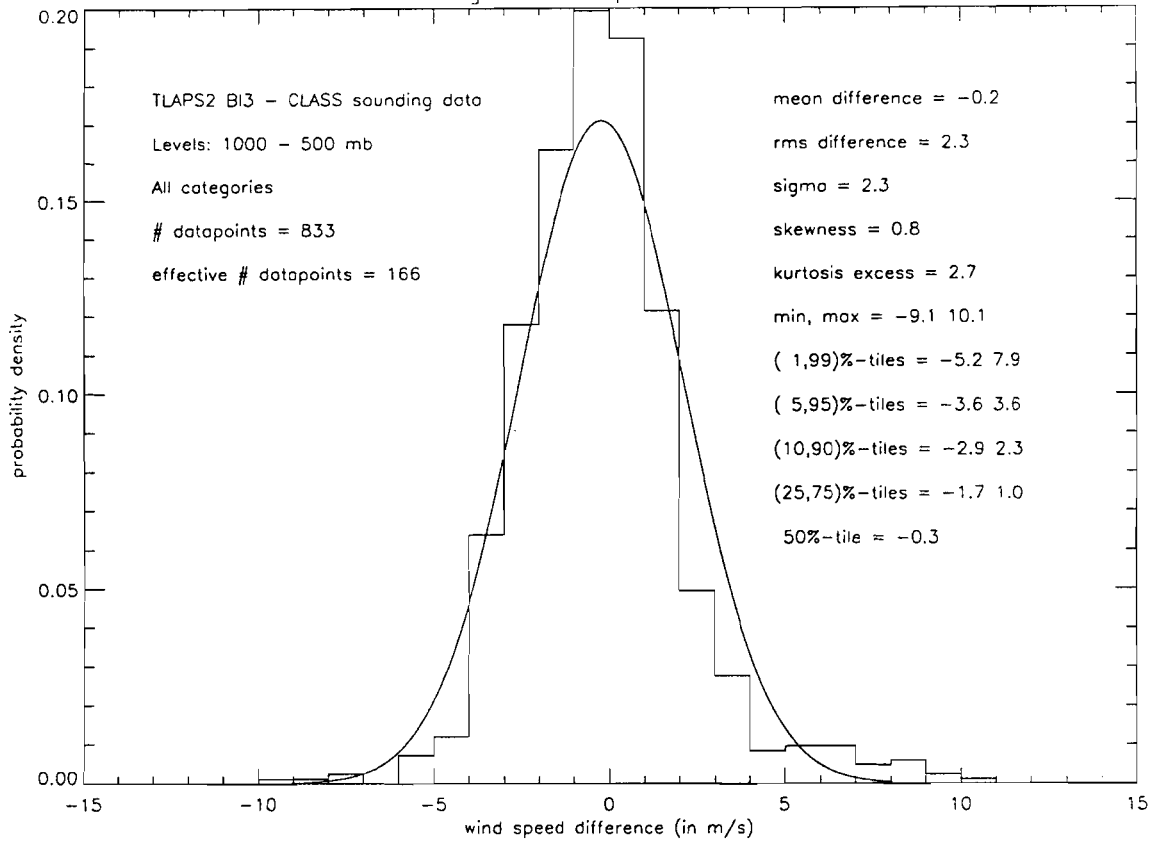




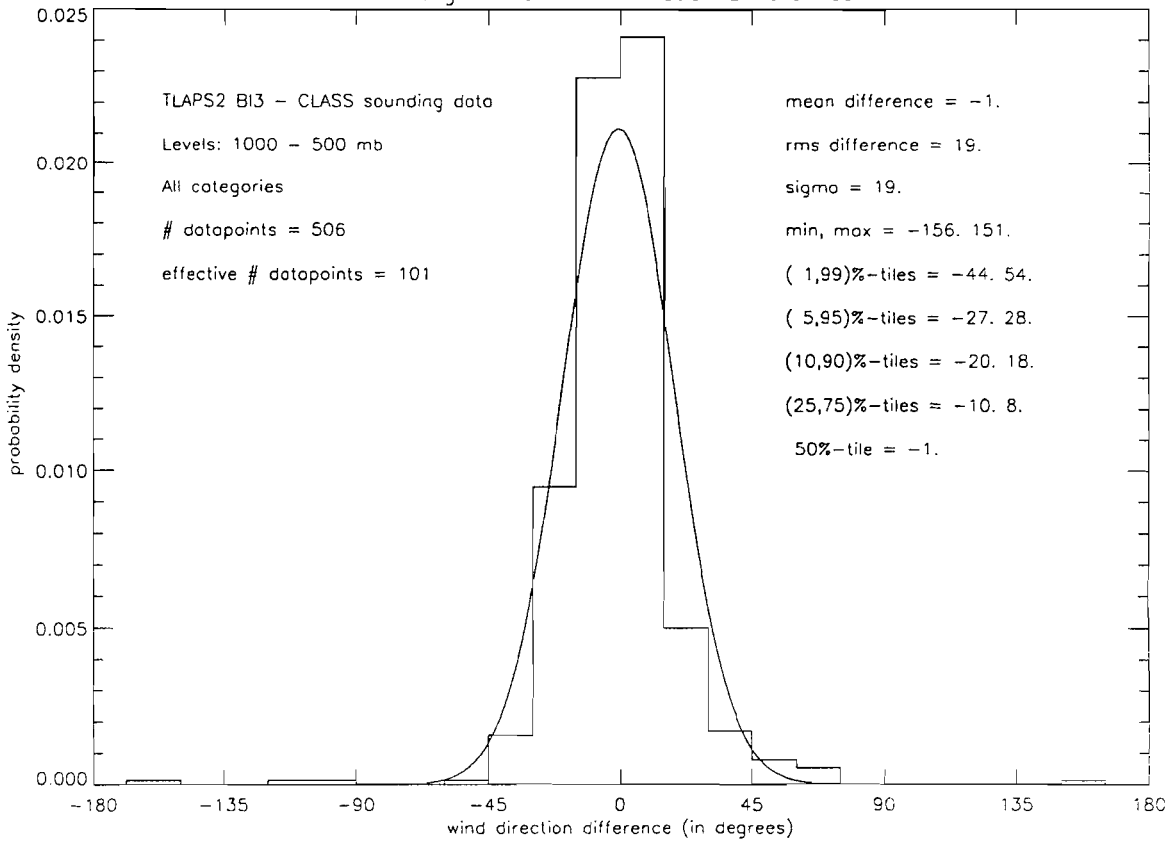
SECTION C-7

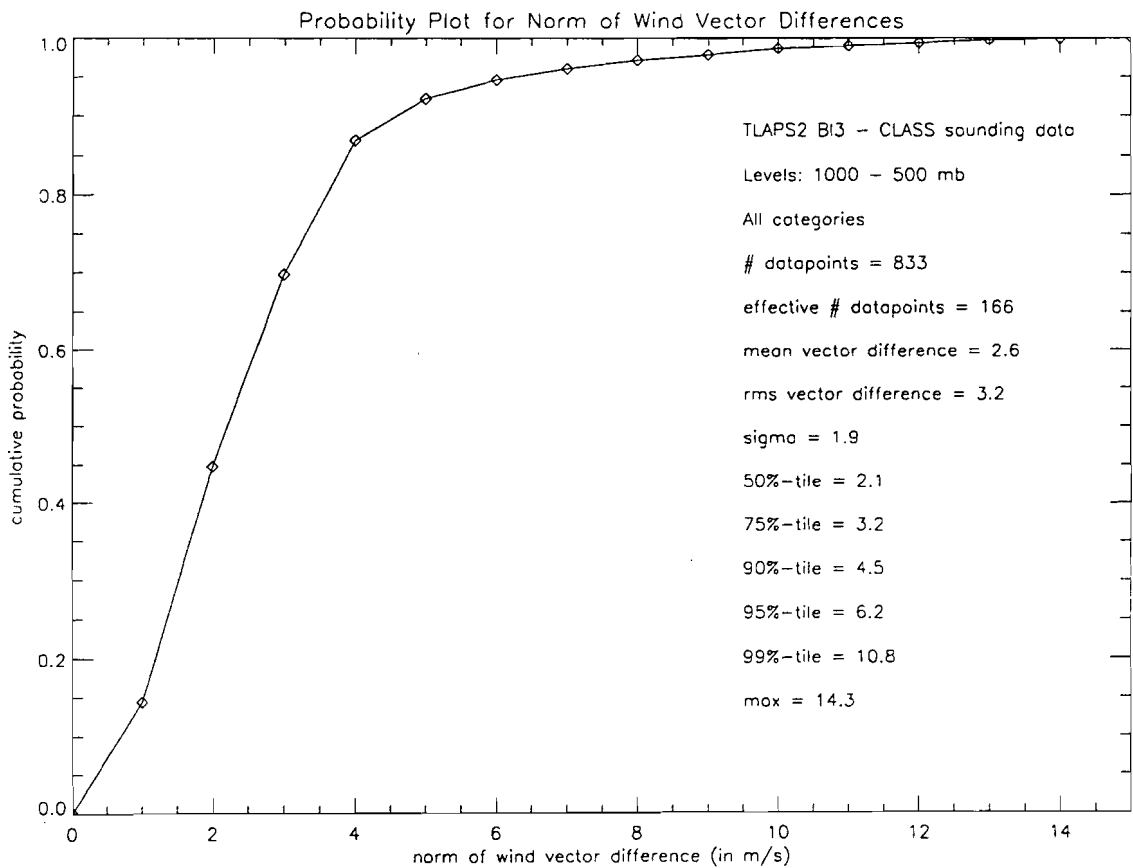
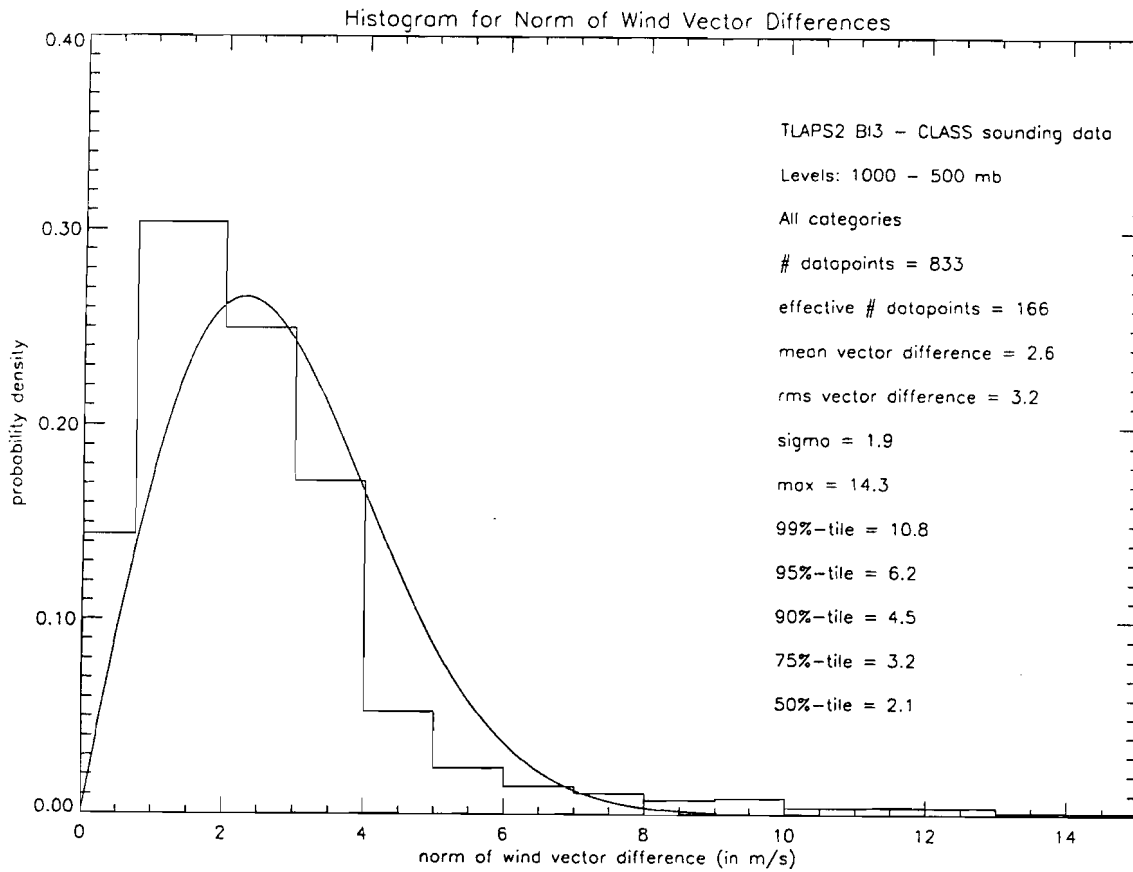


Histogram Wind Speed Differences

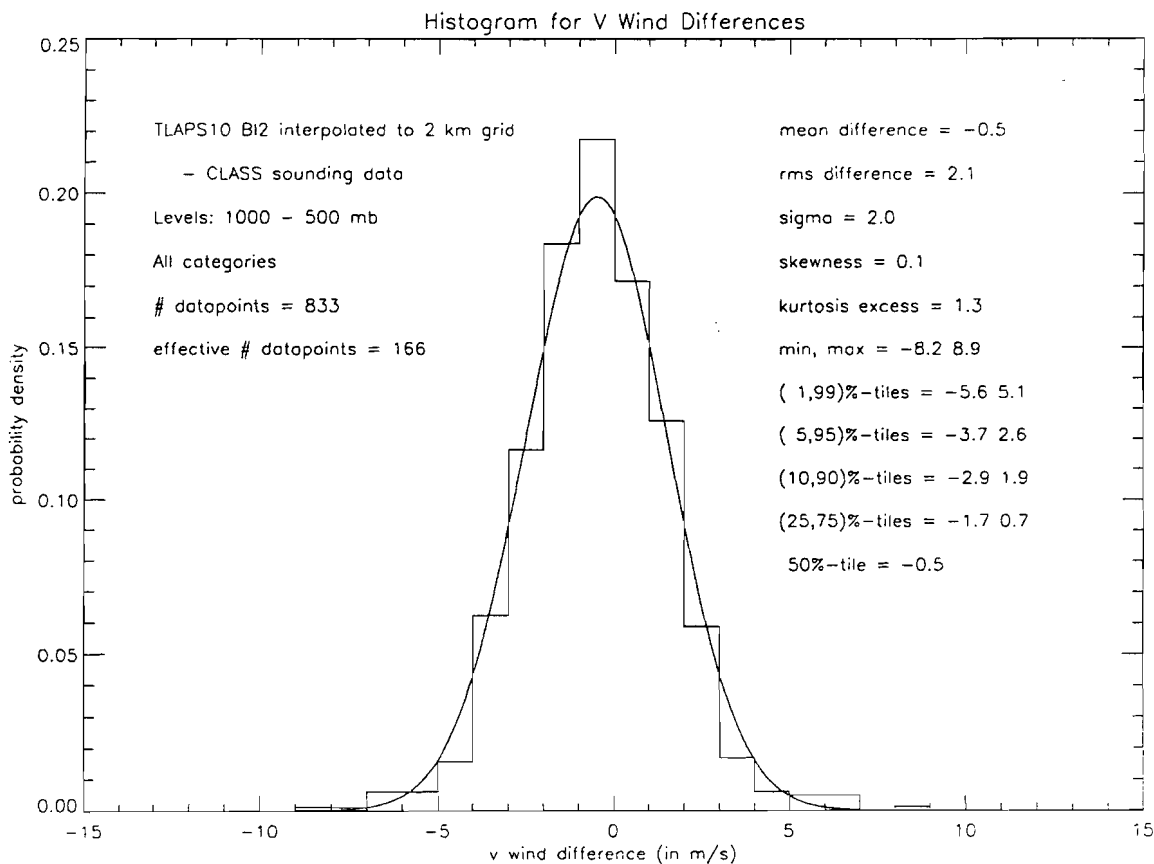
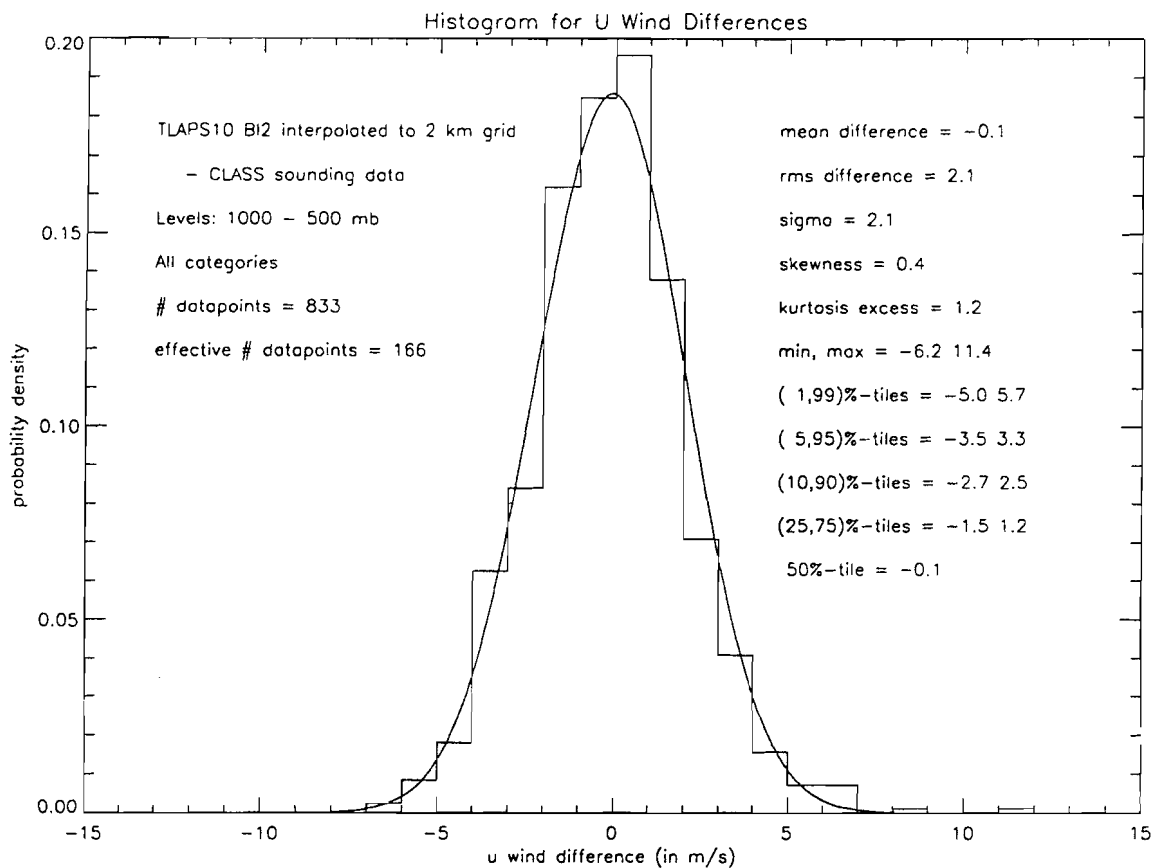


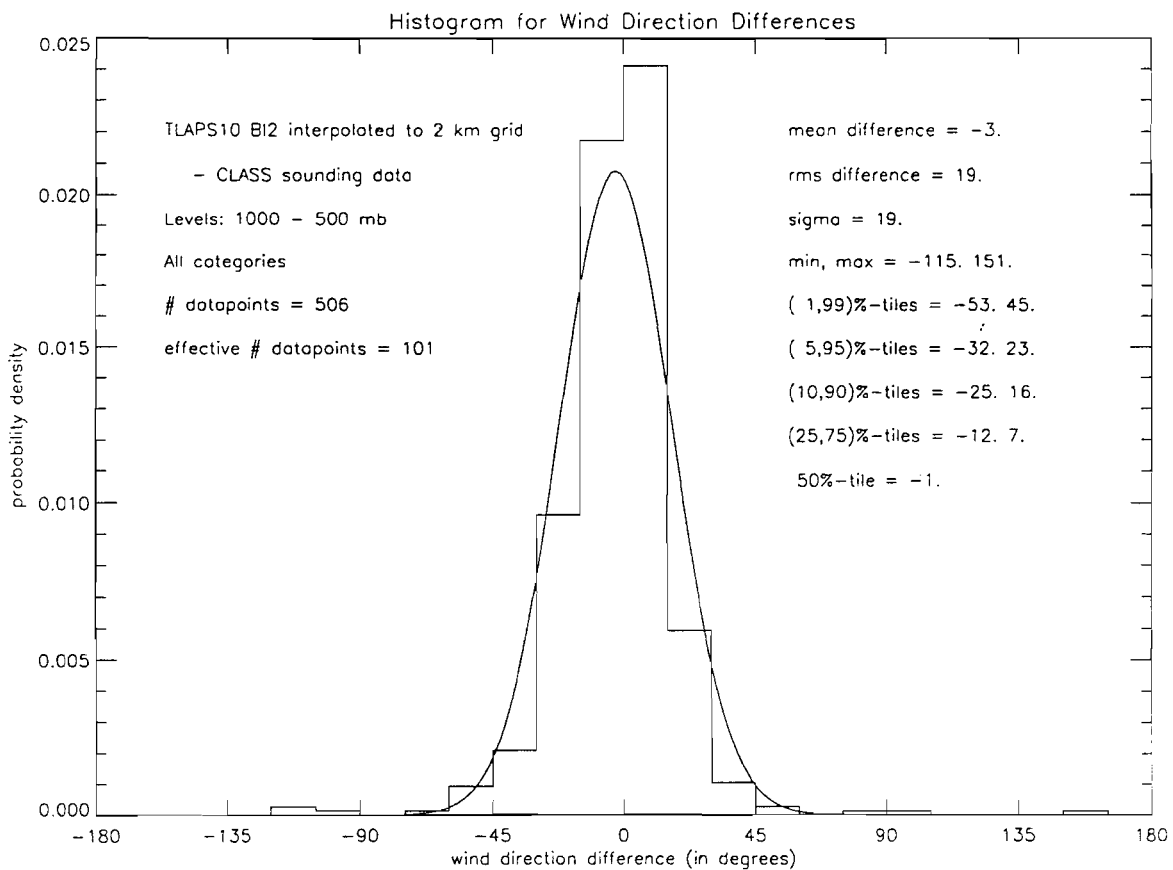
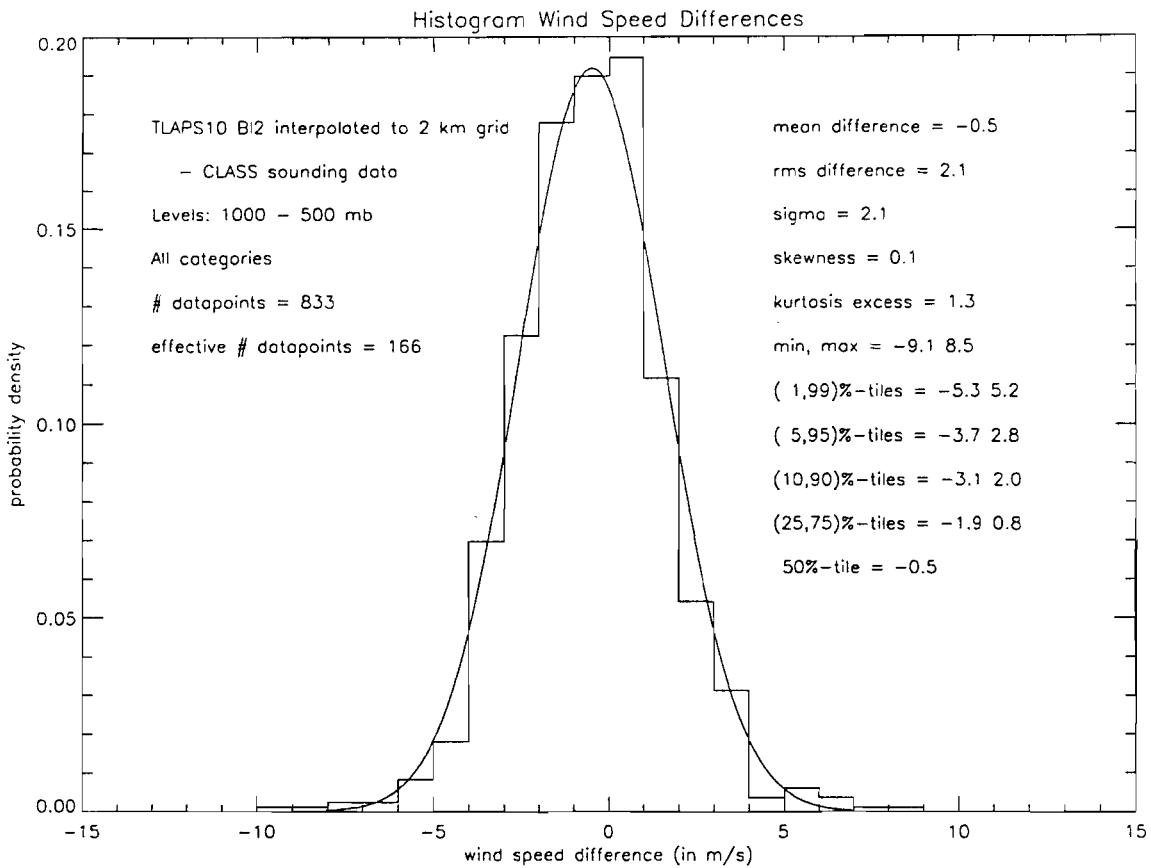
Histogram for Wind Direction Differences

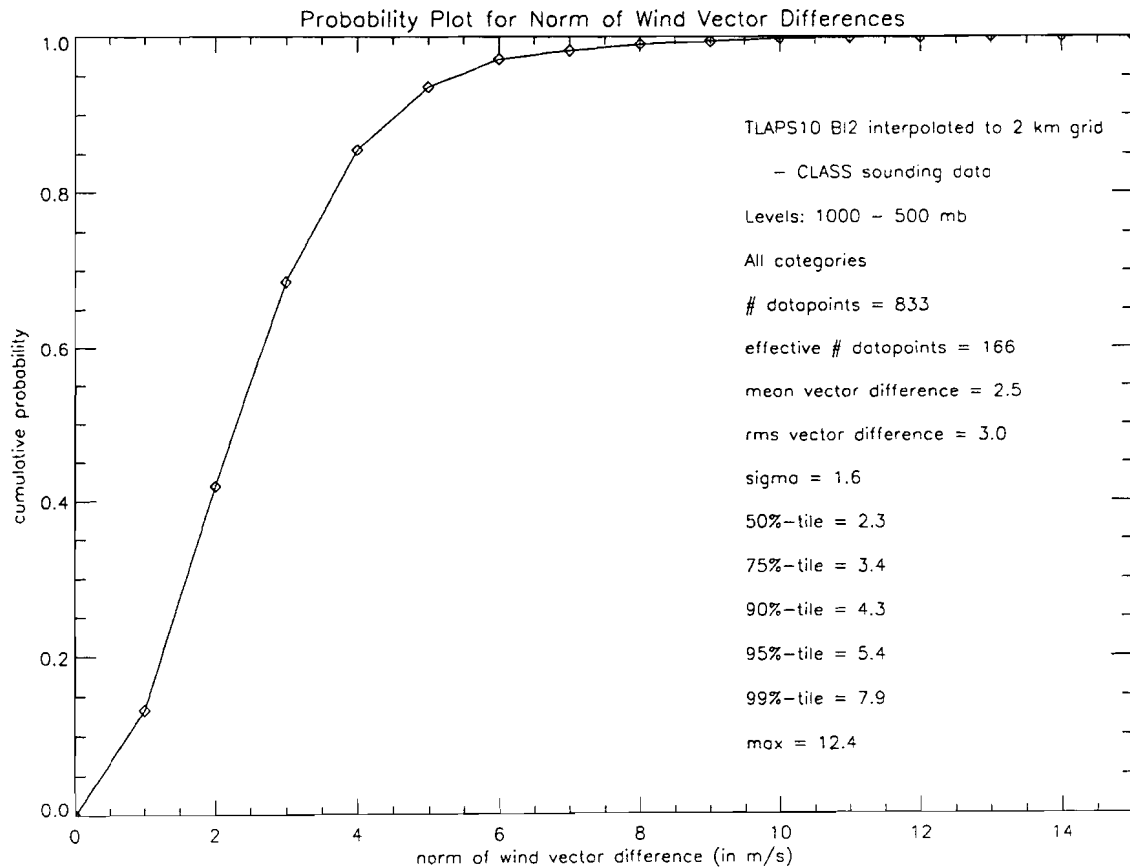
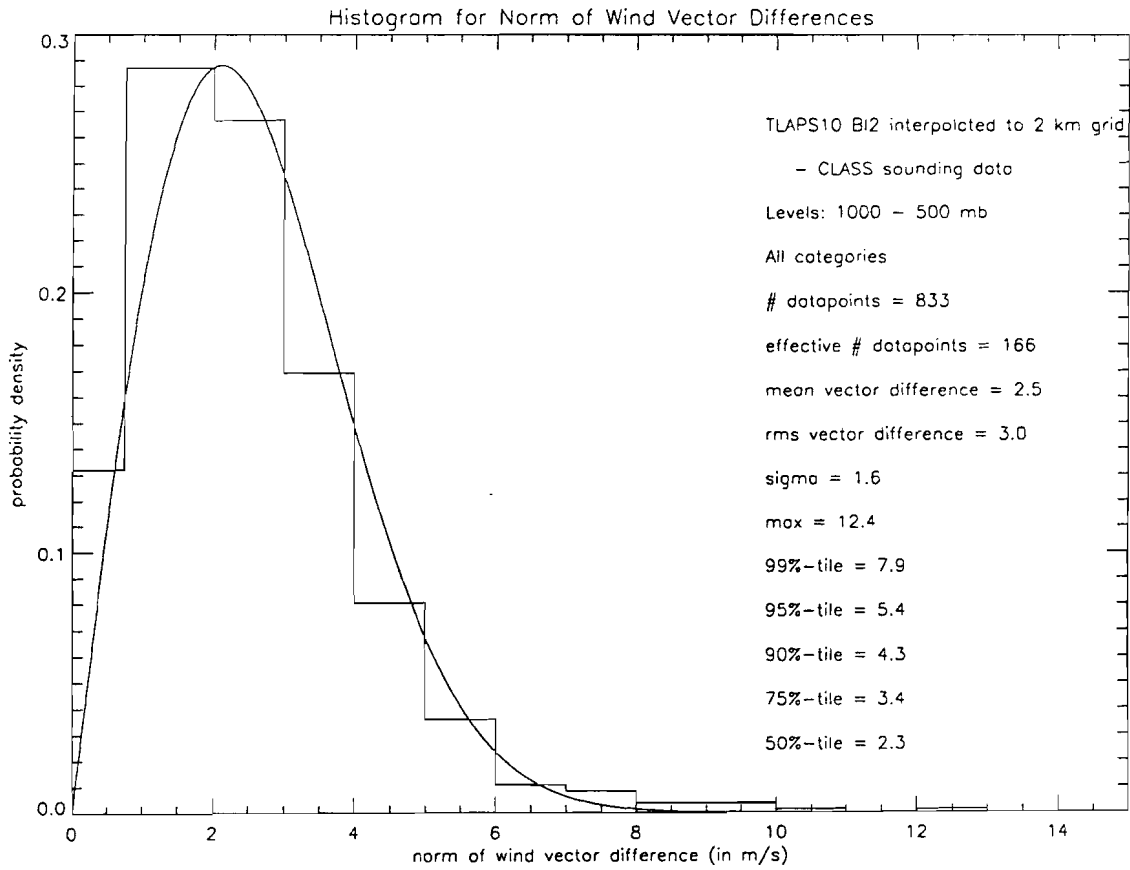




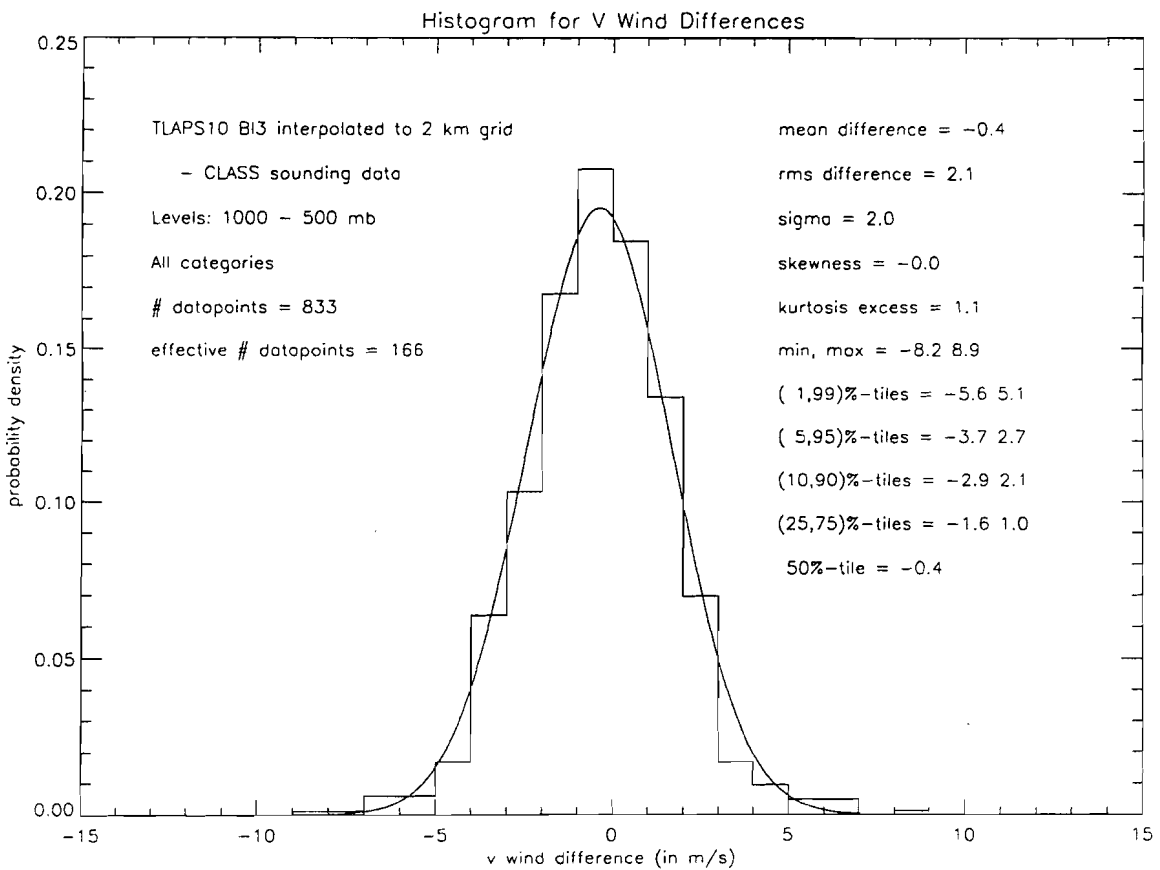
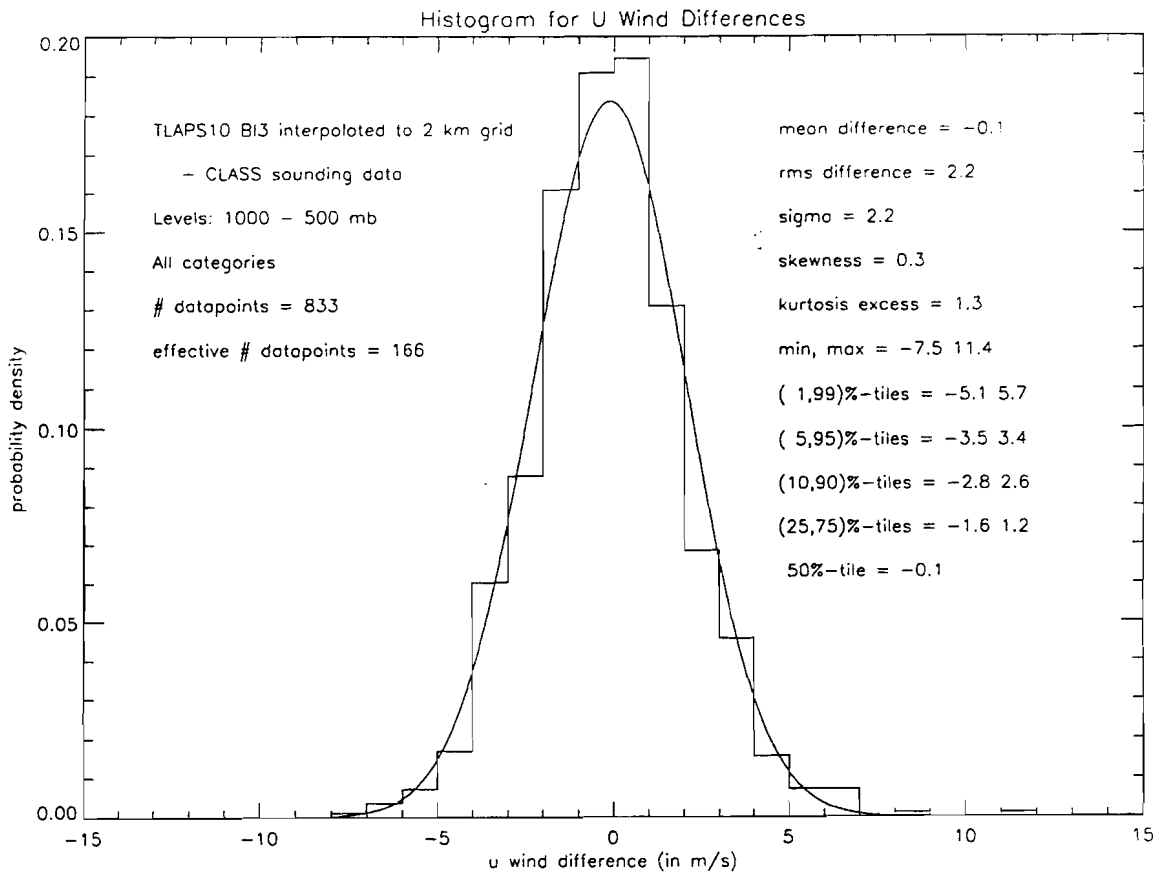
SECTION C-8



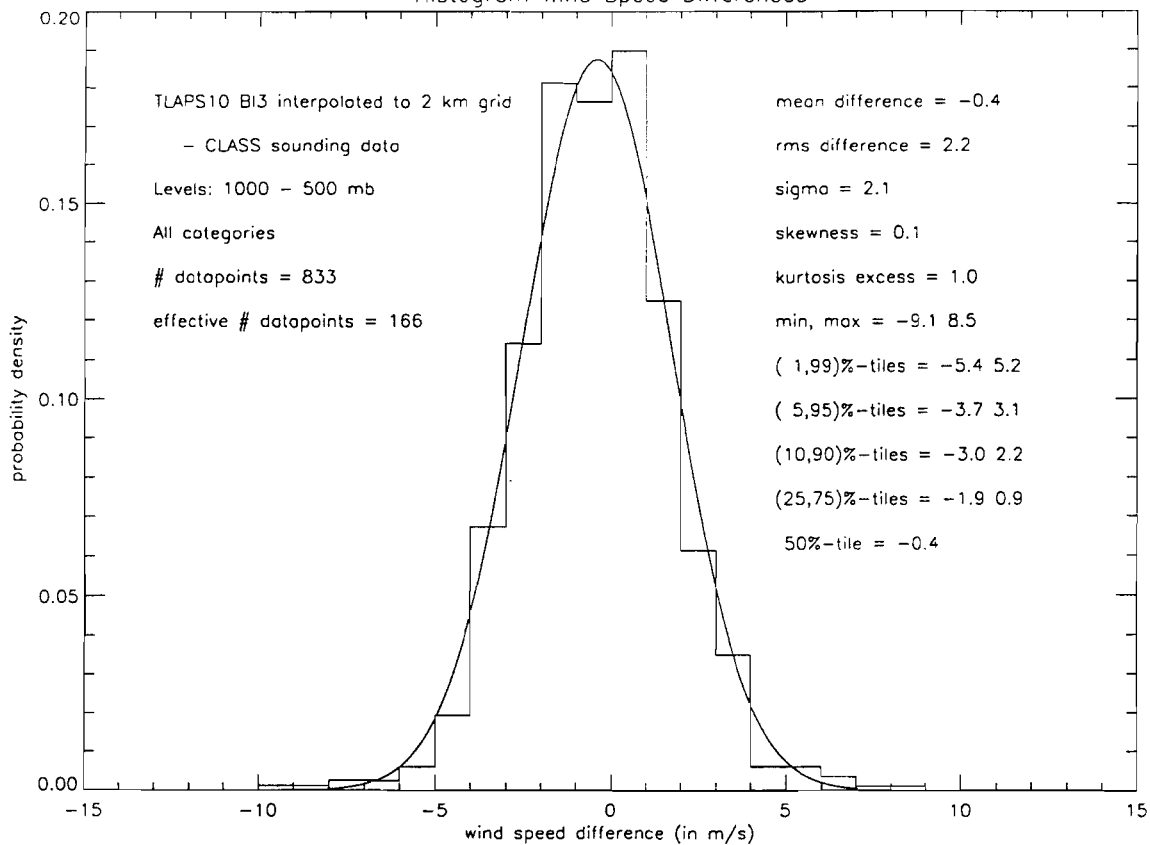




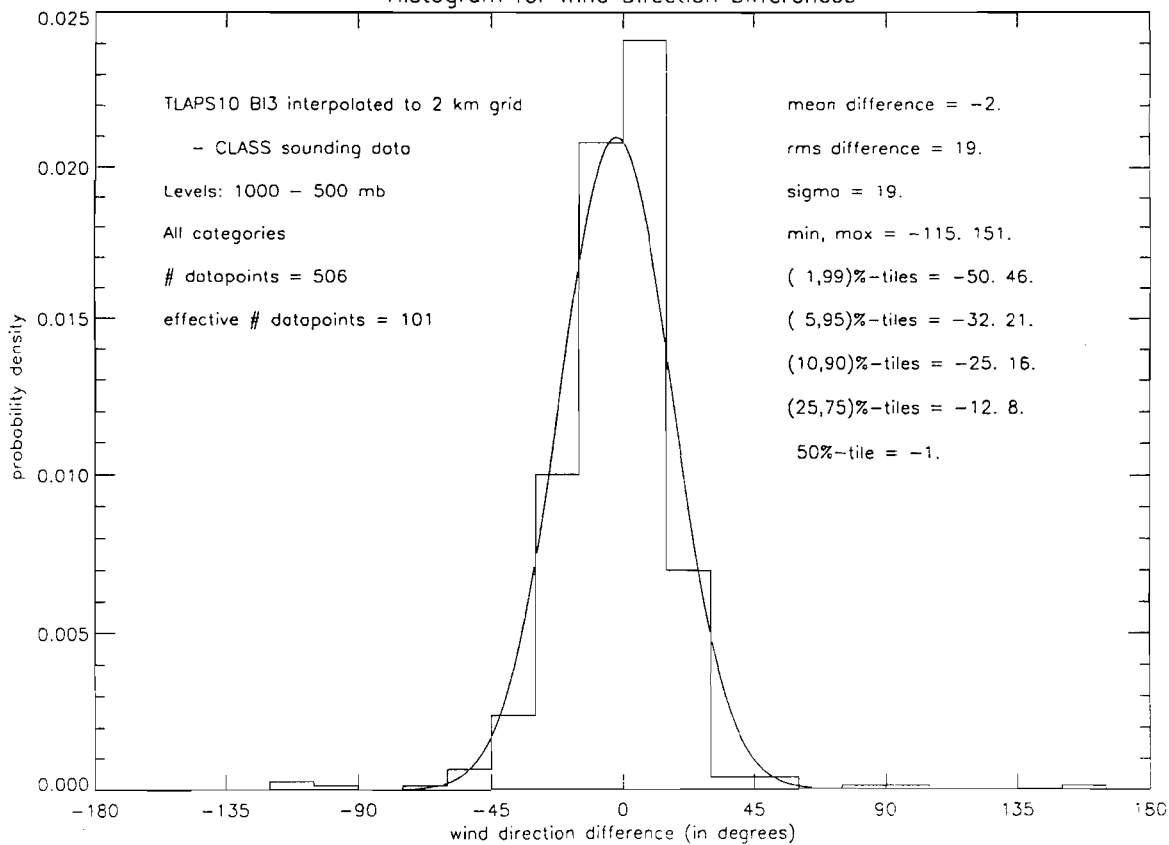
SECTION C-9

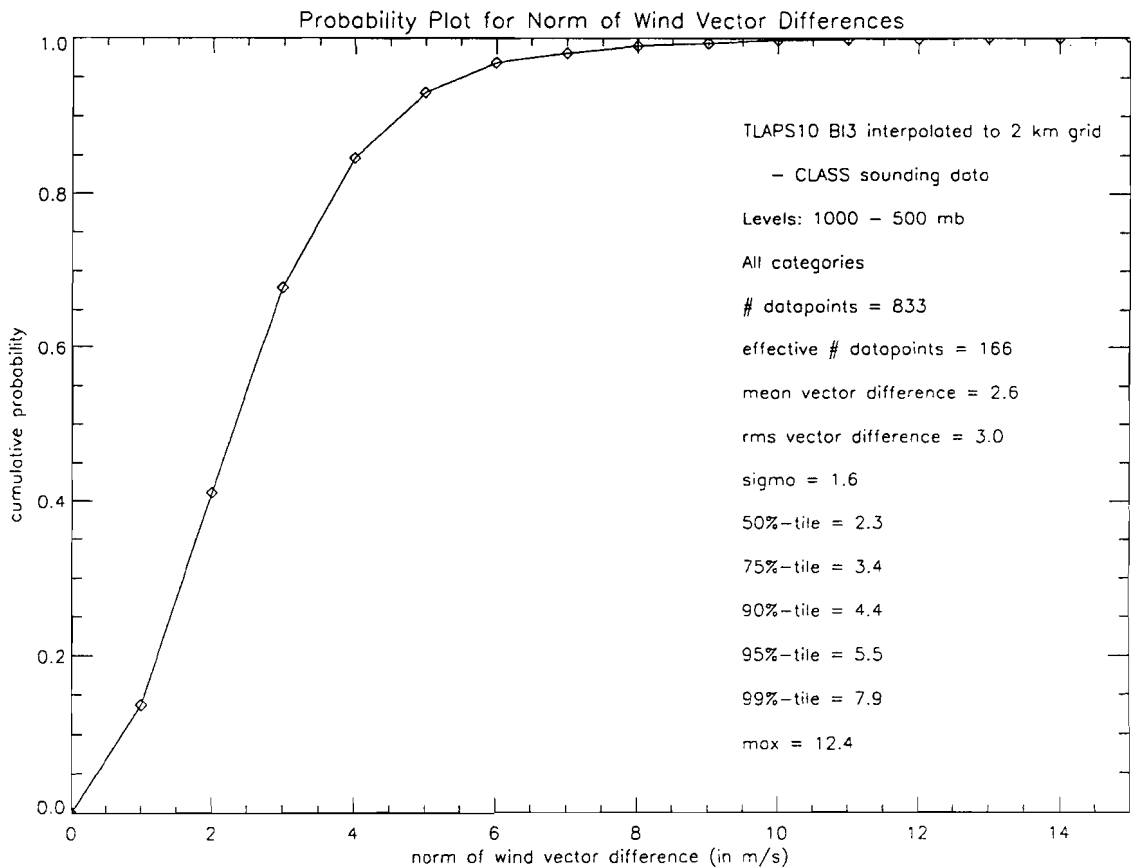
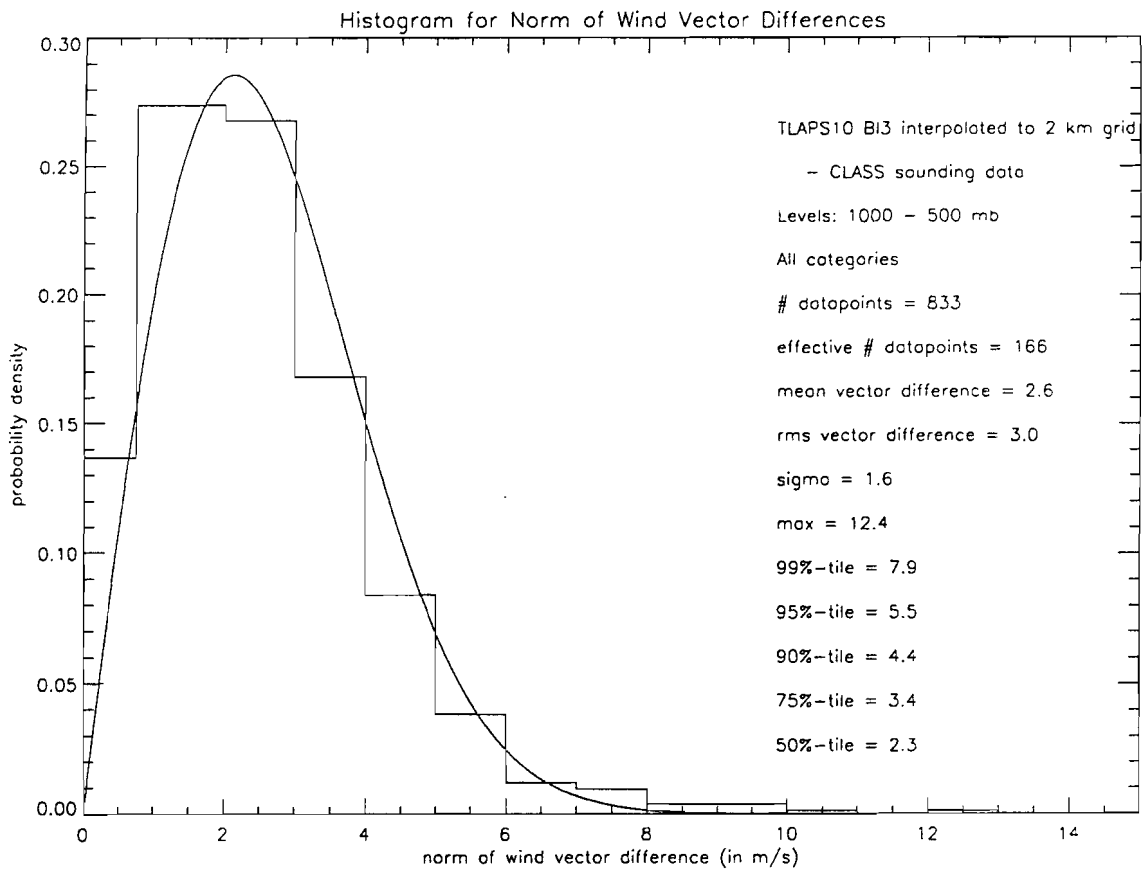


Histogram Wind Speed Differences

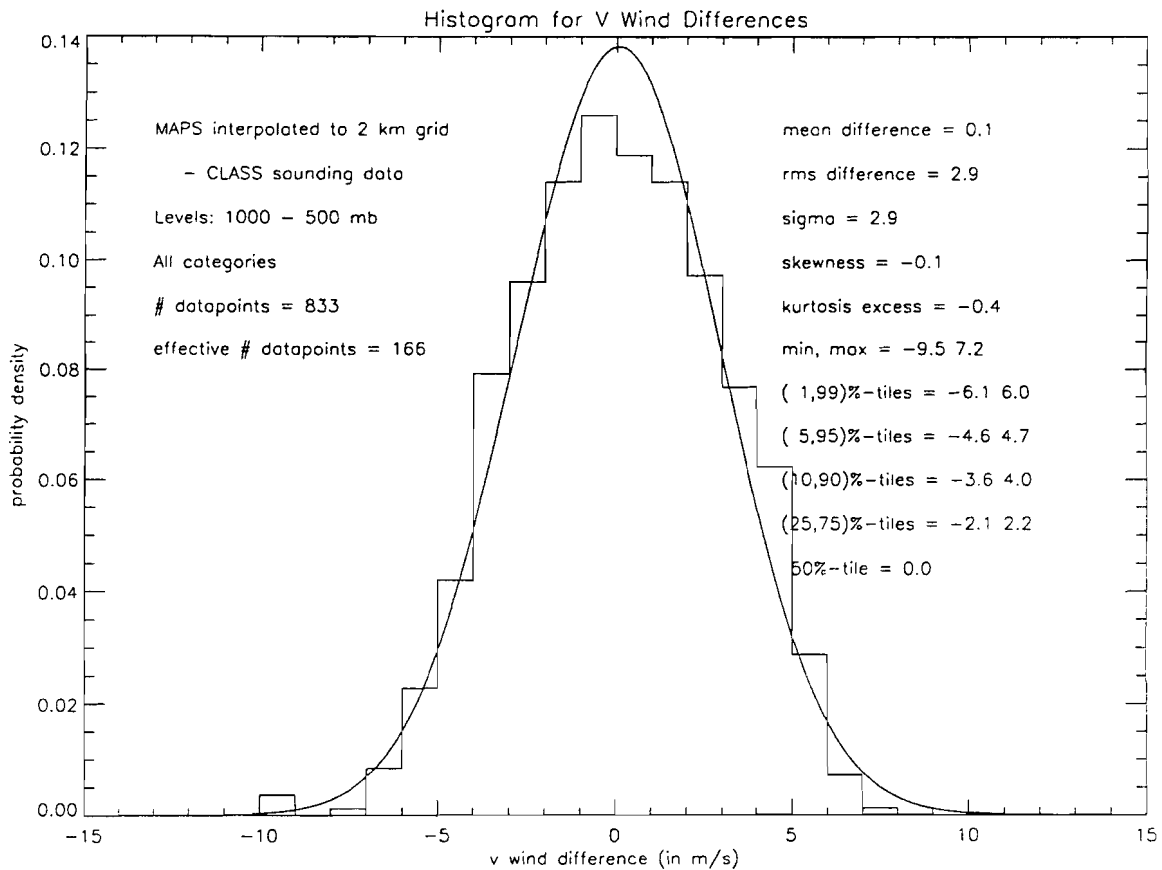
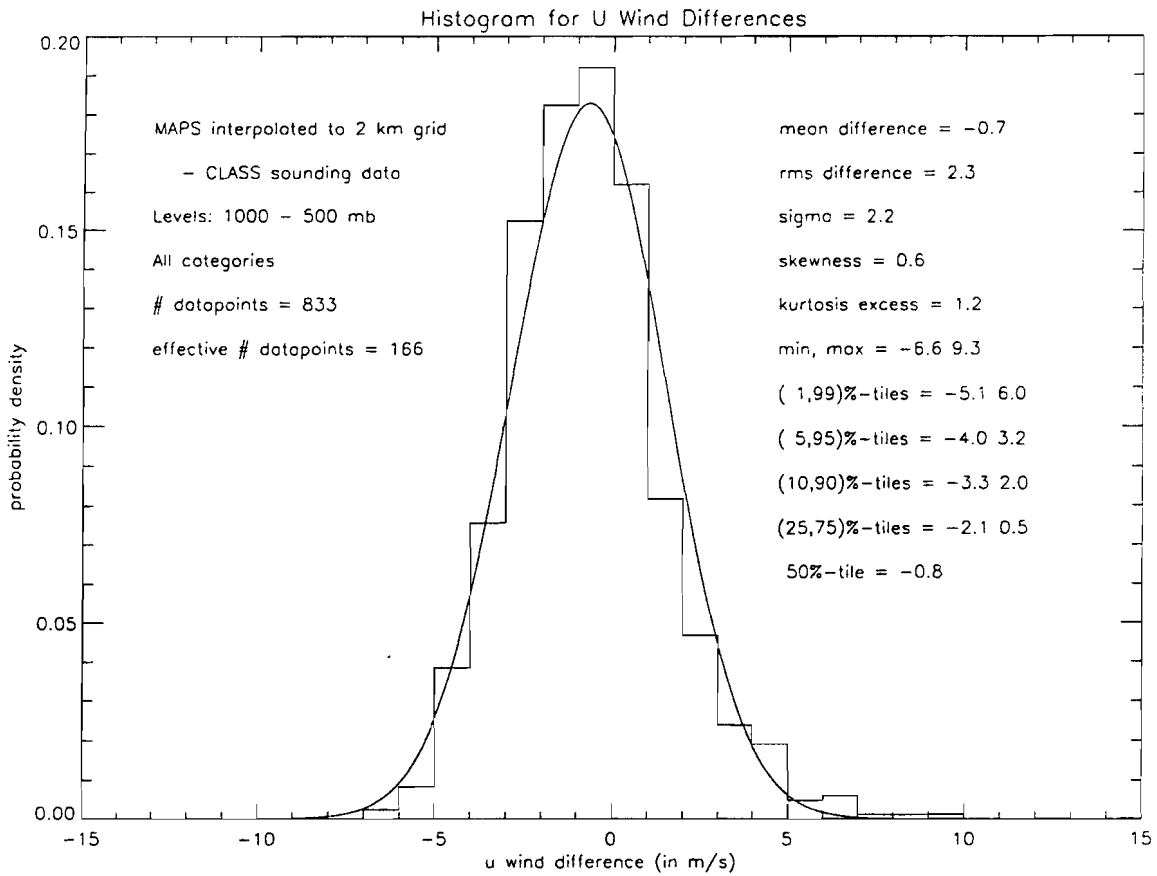


Histogram for Wind Direction Differences

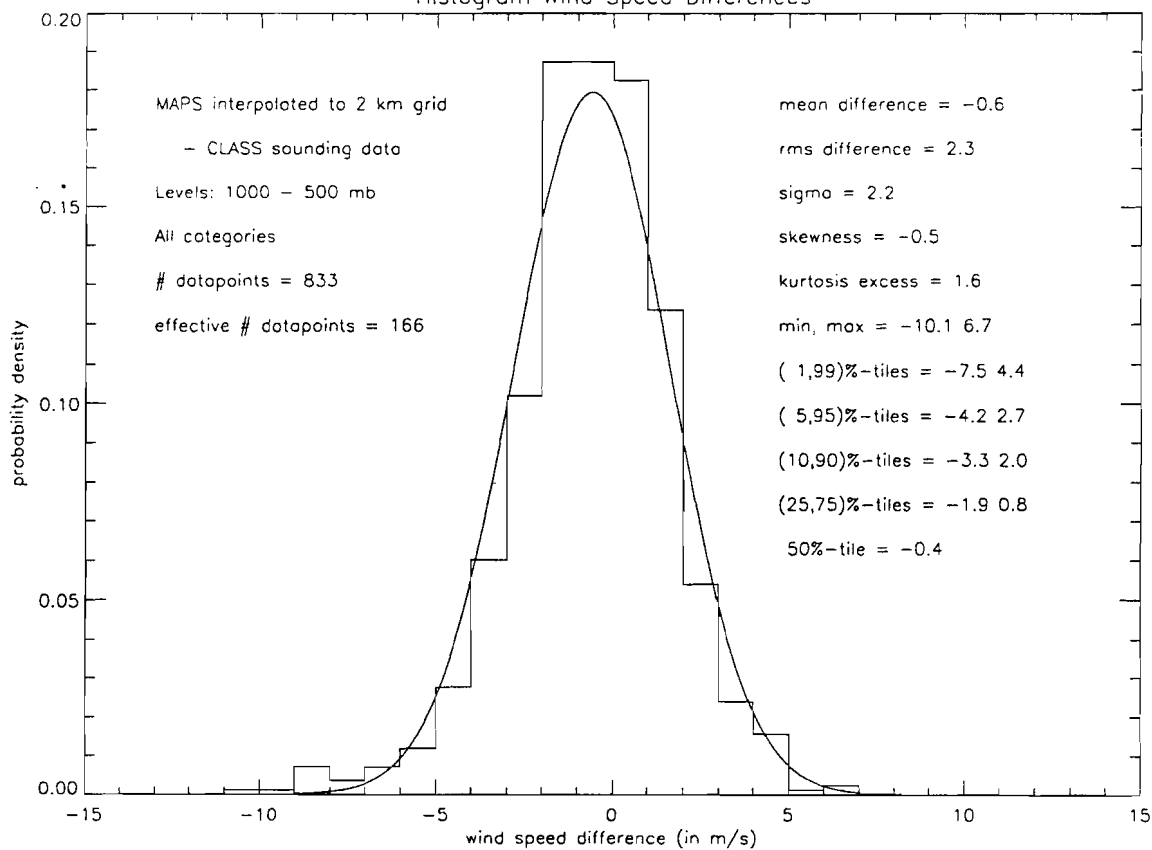




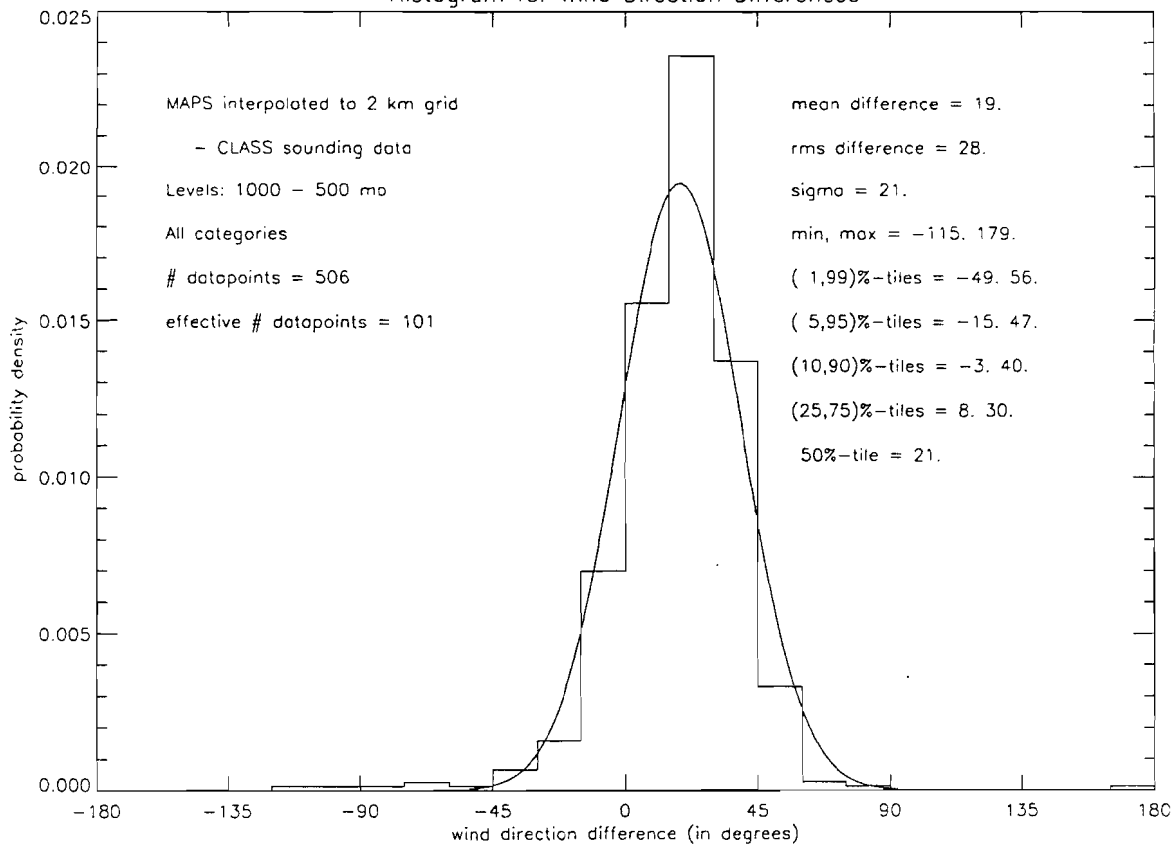
SECTION C-10

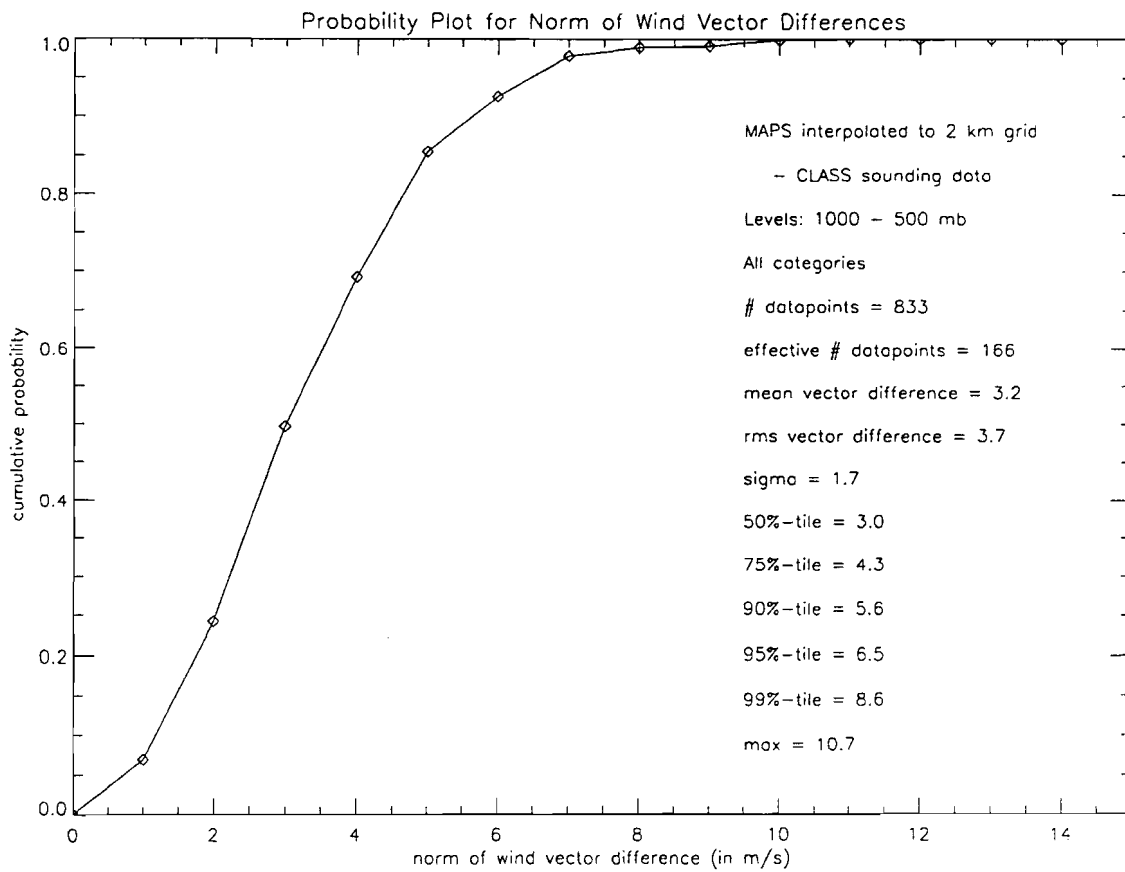
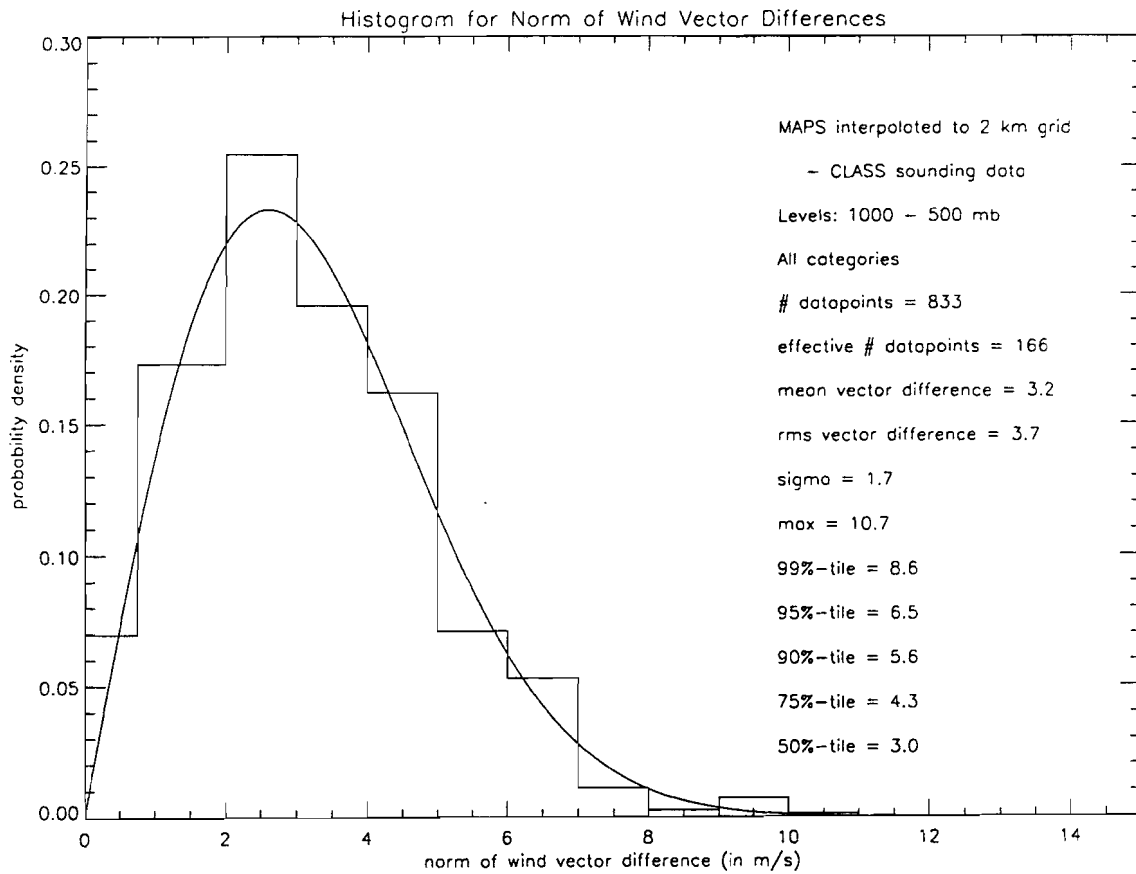


Histogram Wind Speed Differences

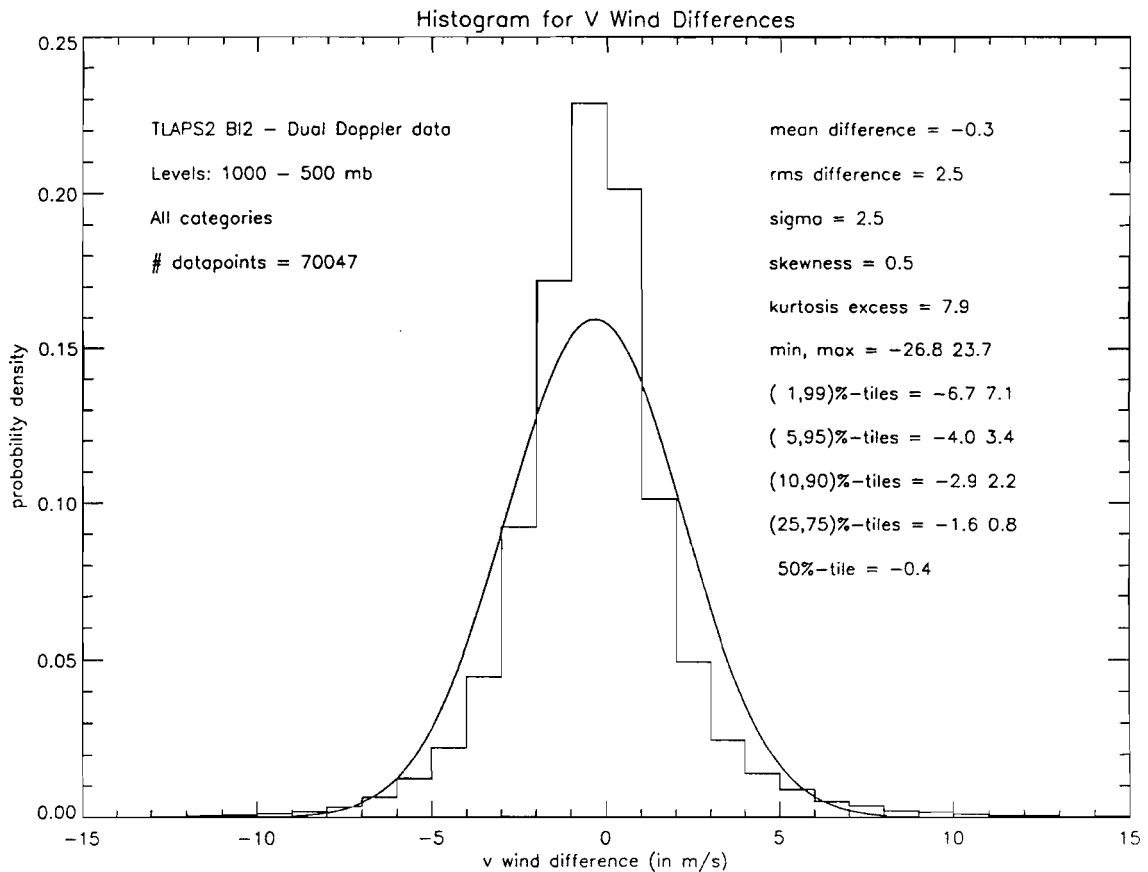
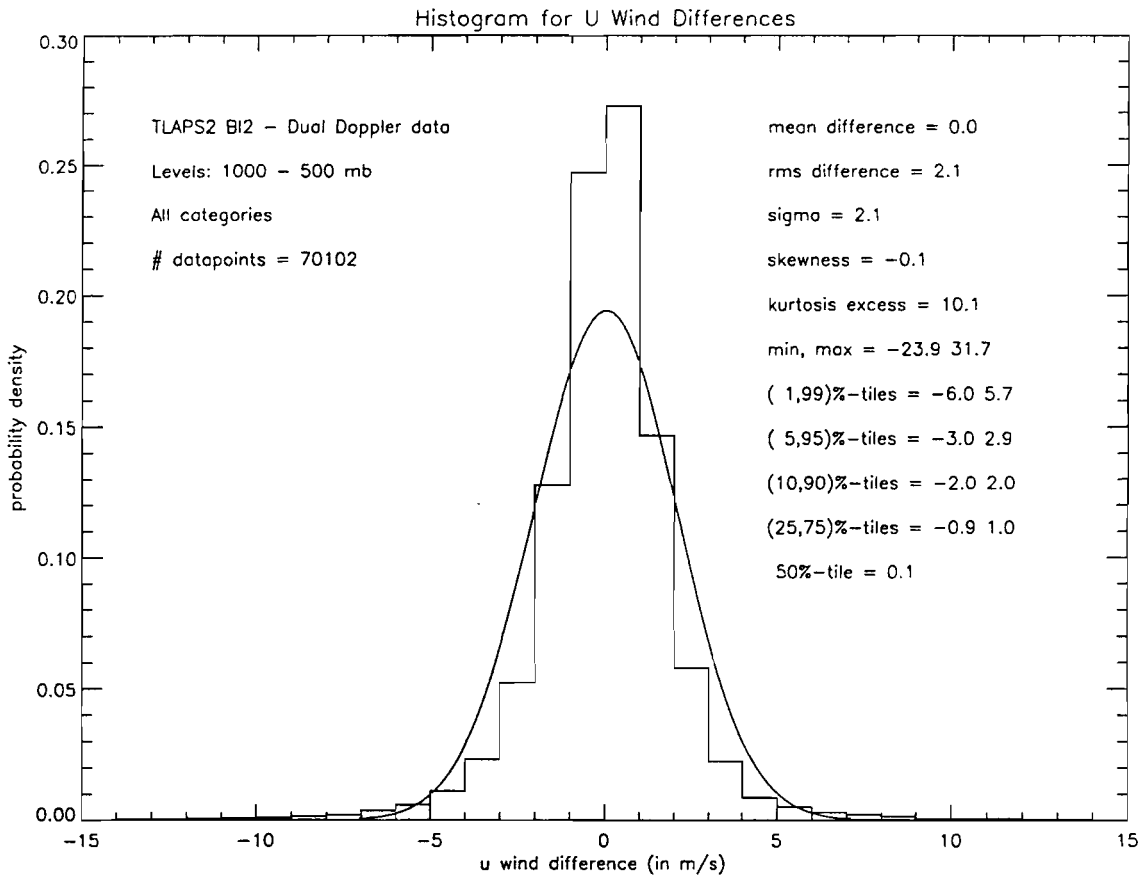


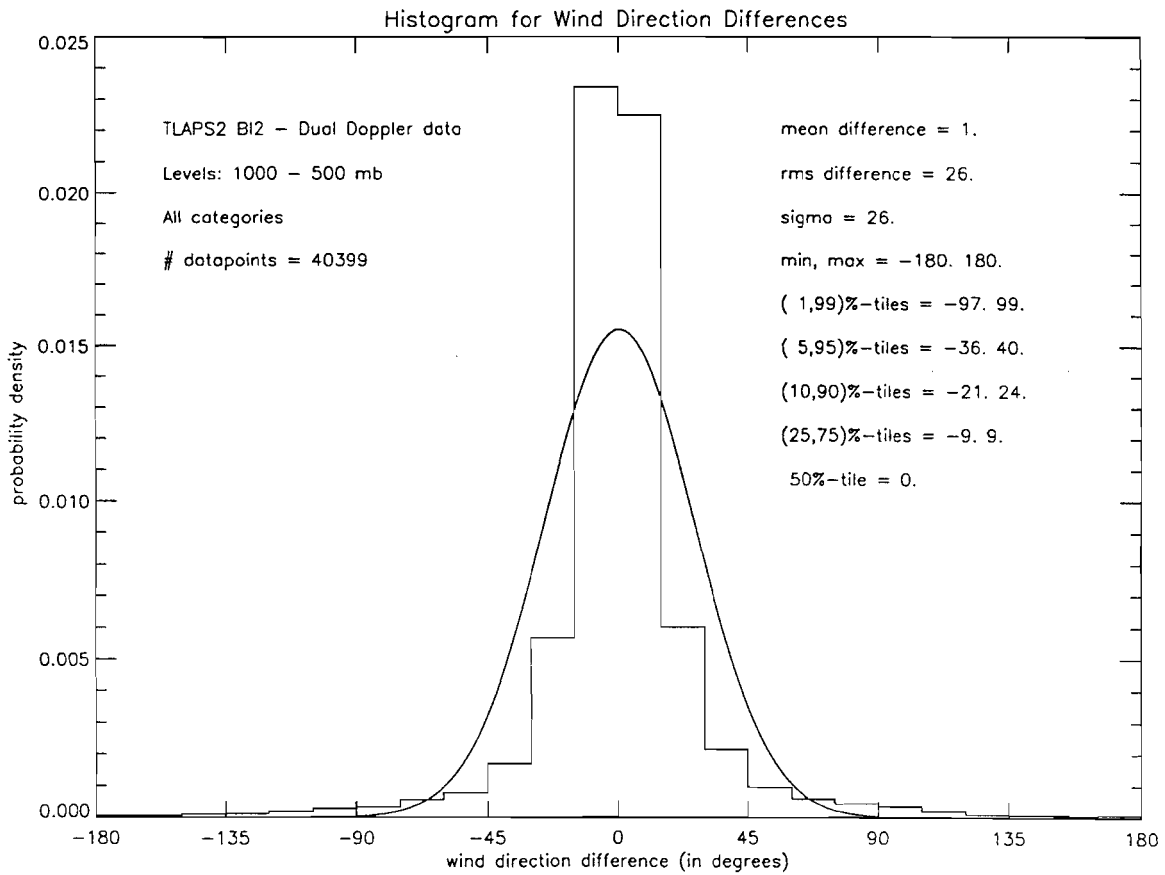
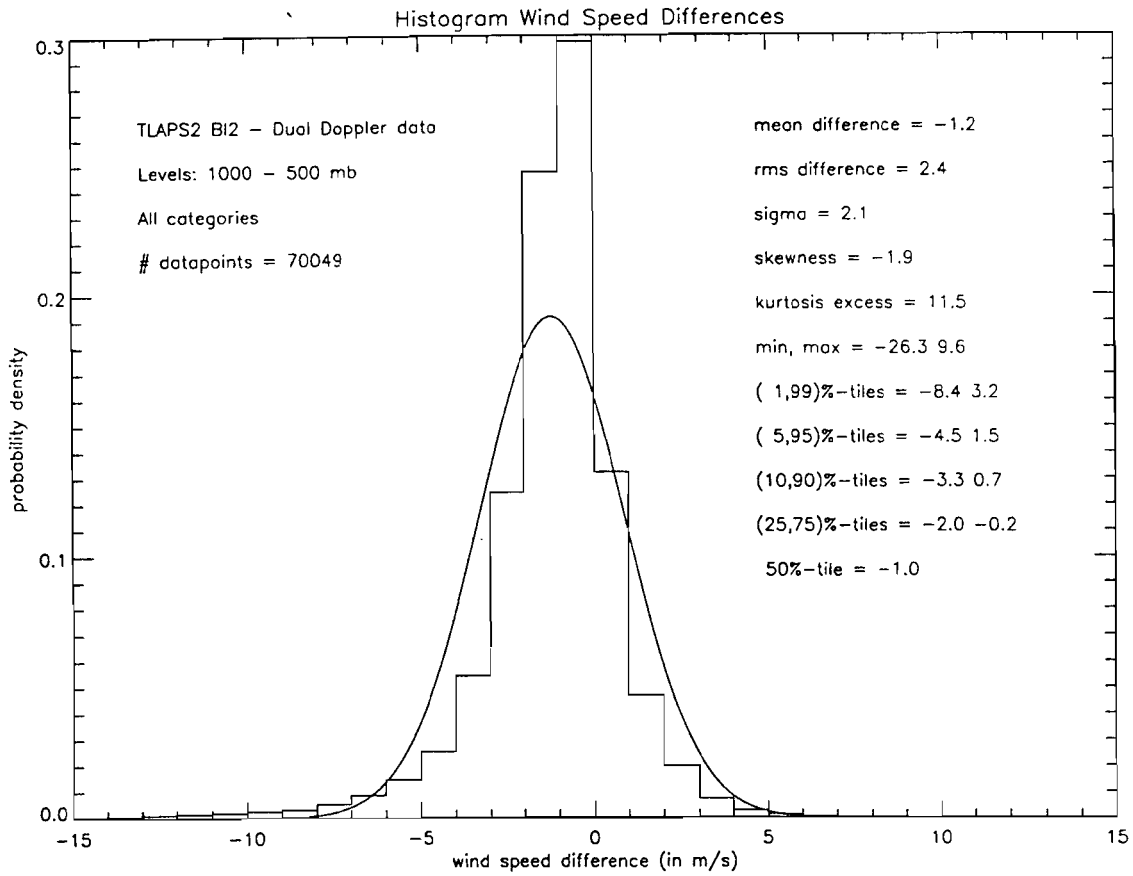
Histogram for Wind Direction Differences

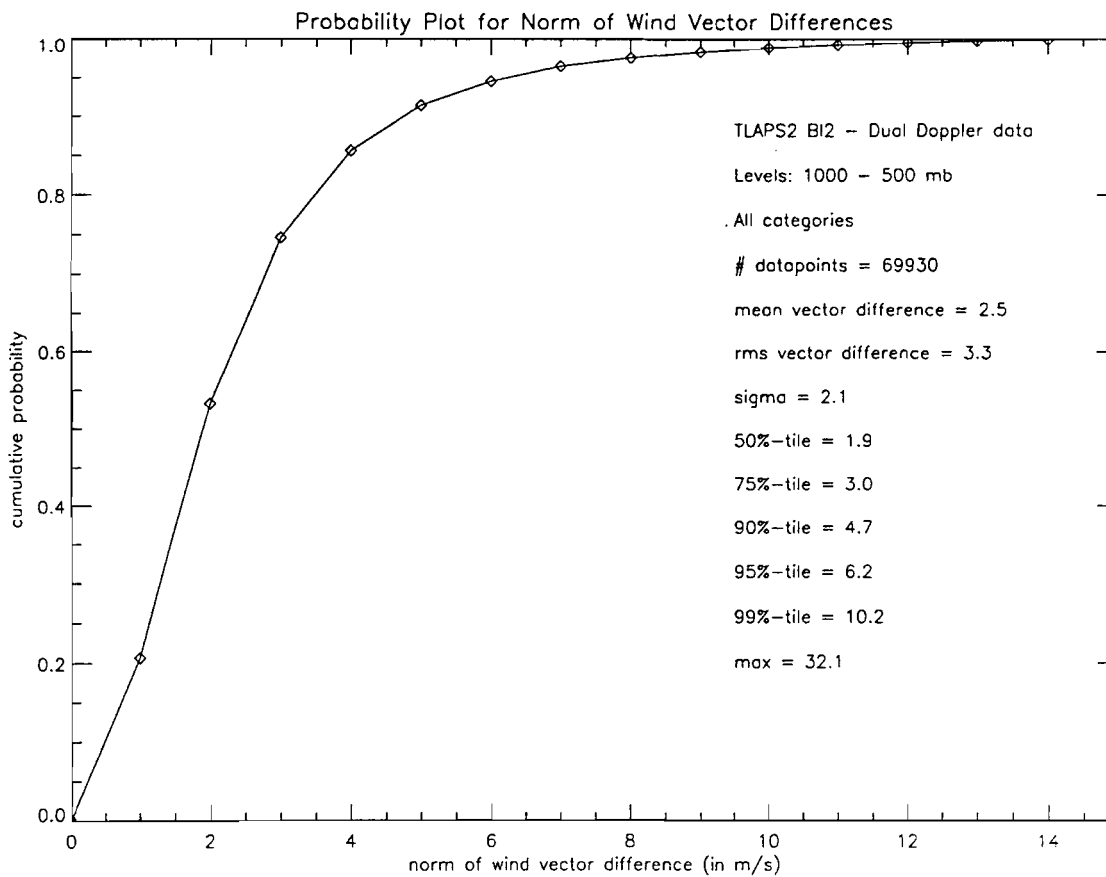
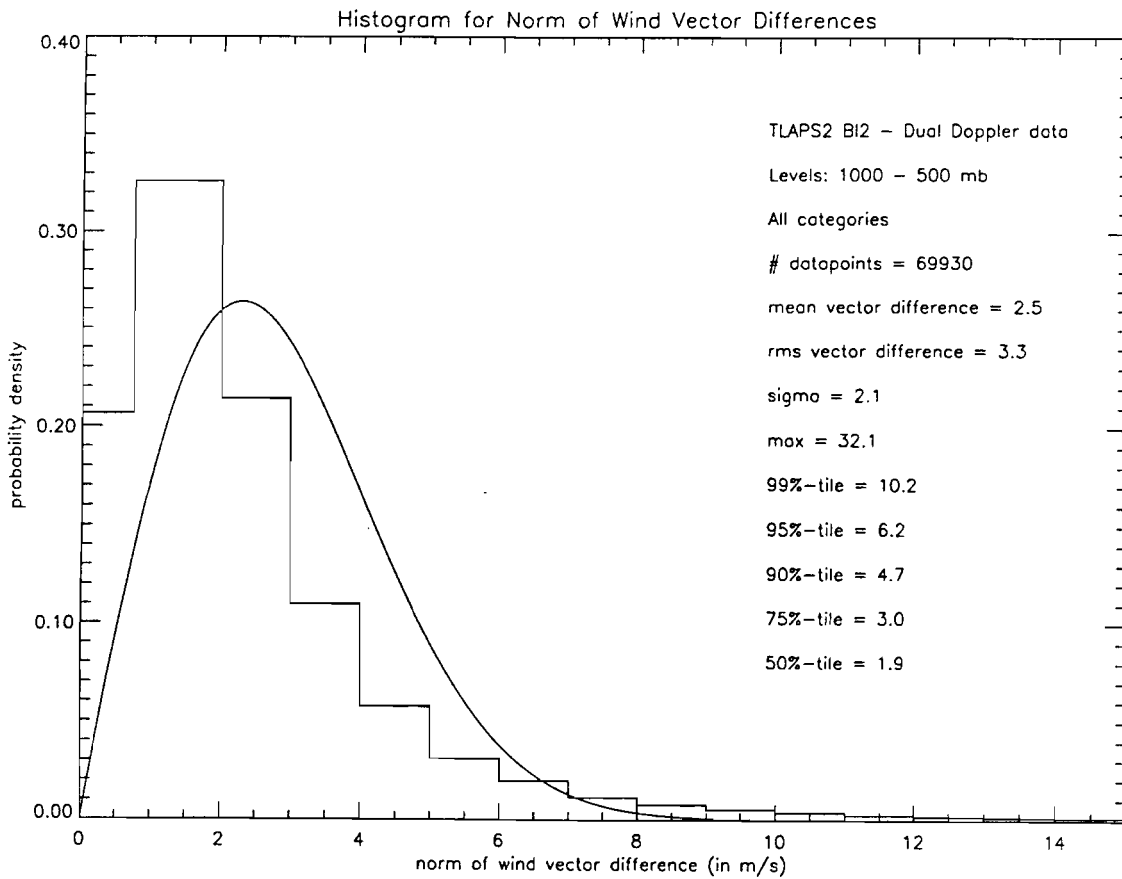




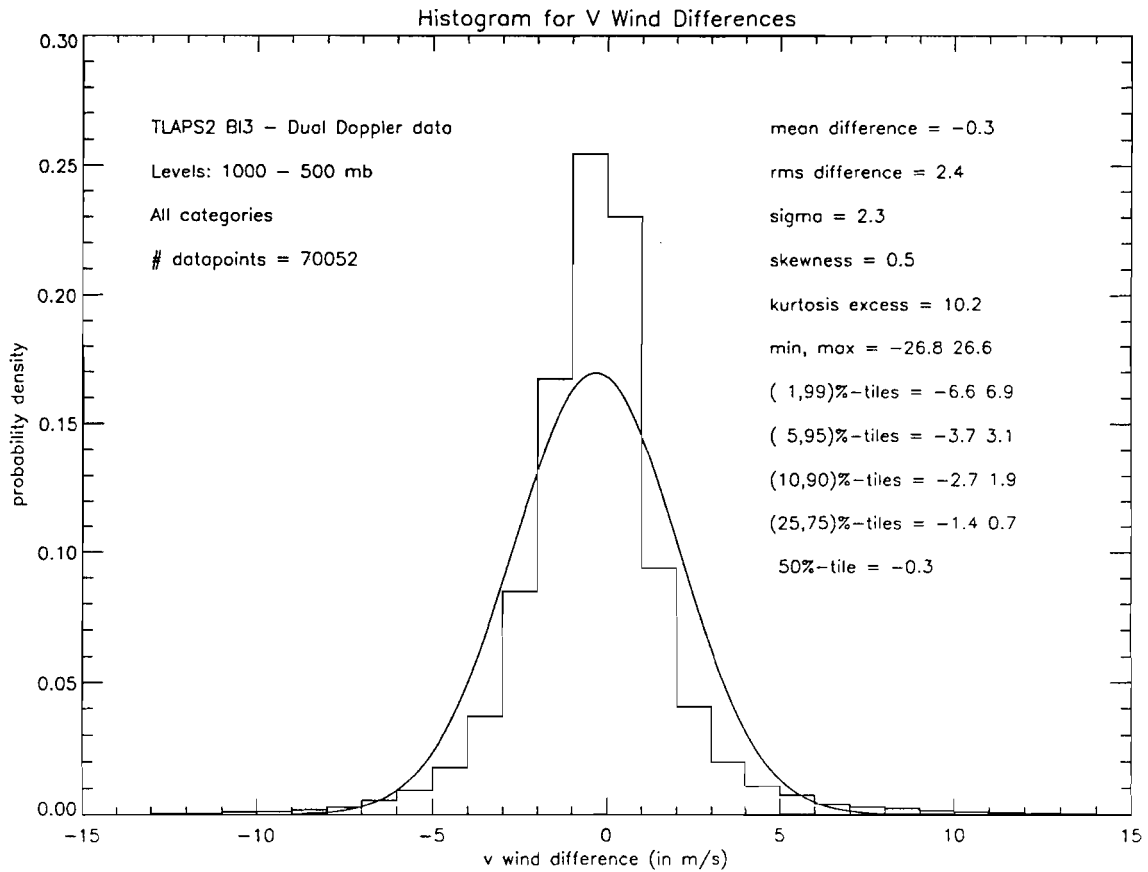
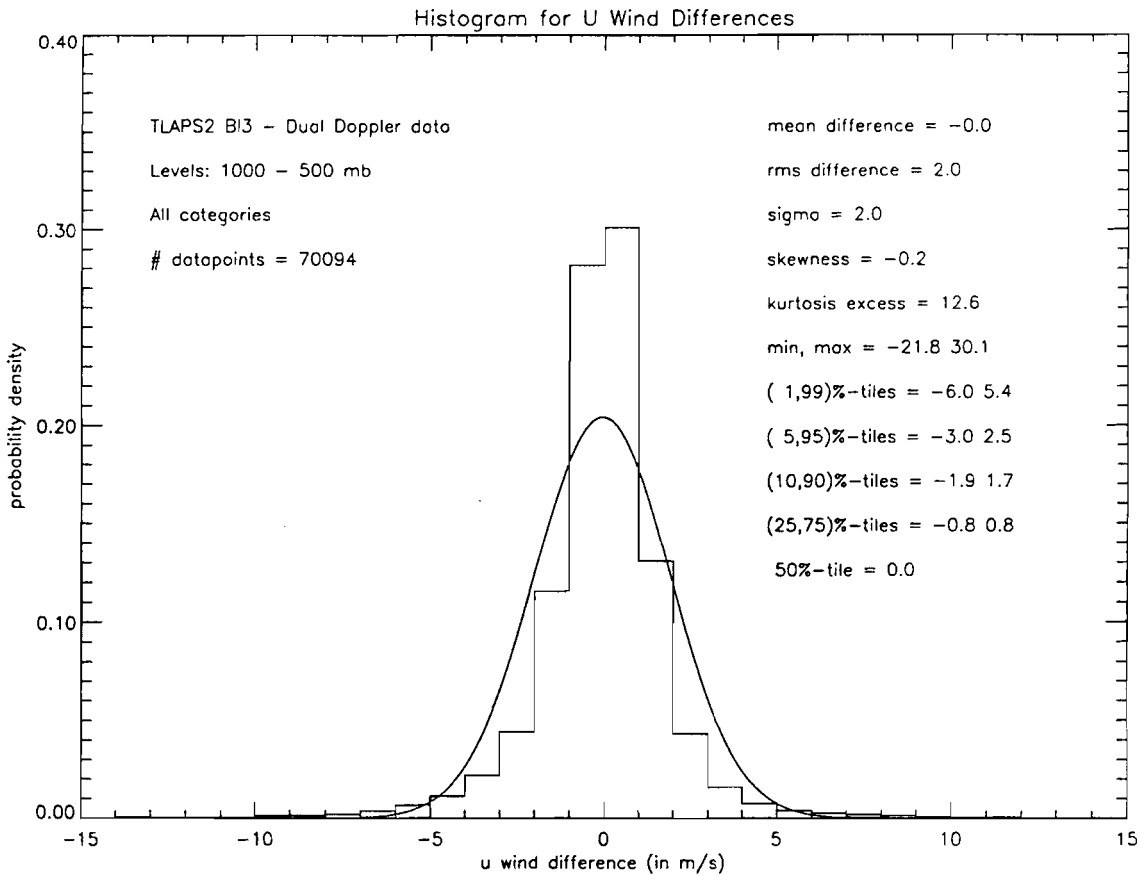
SECTION C-11

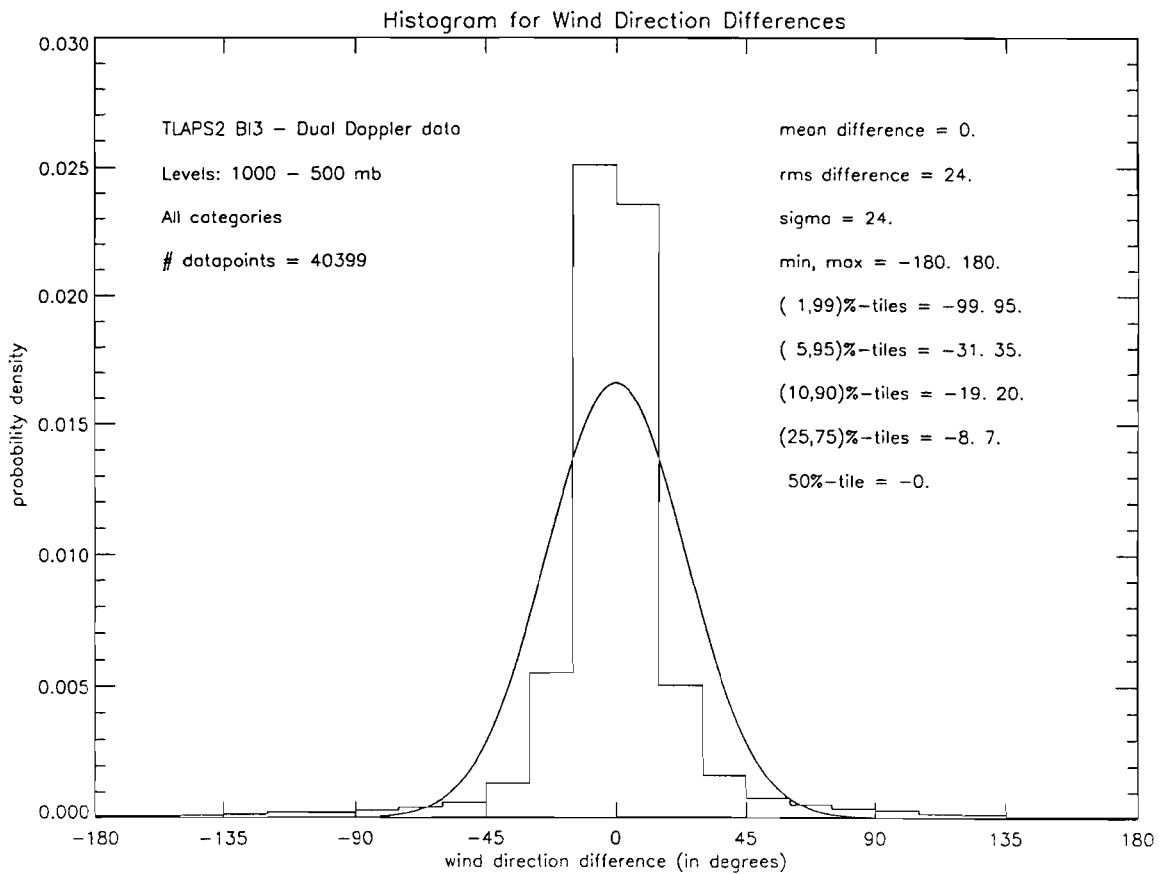
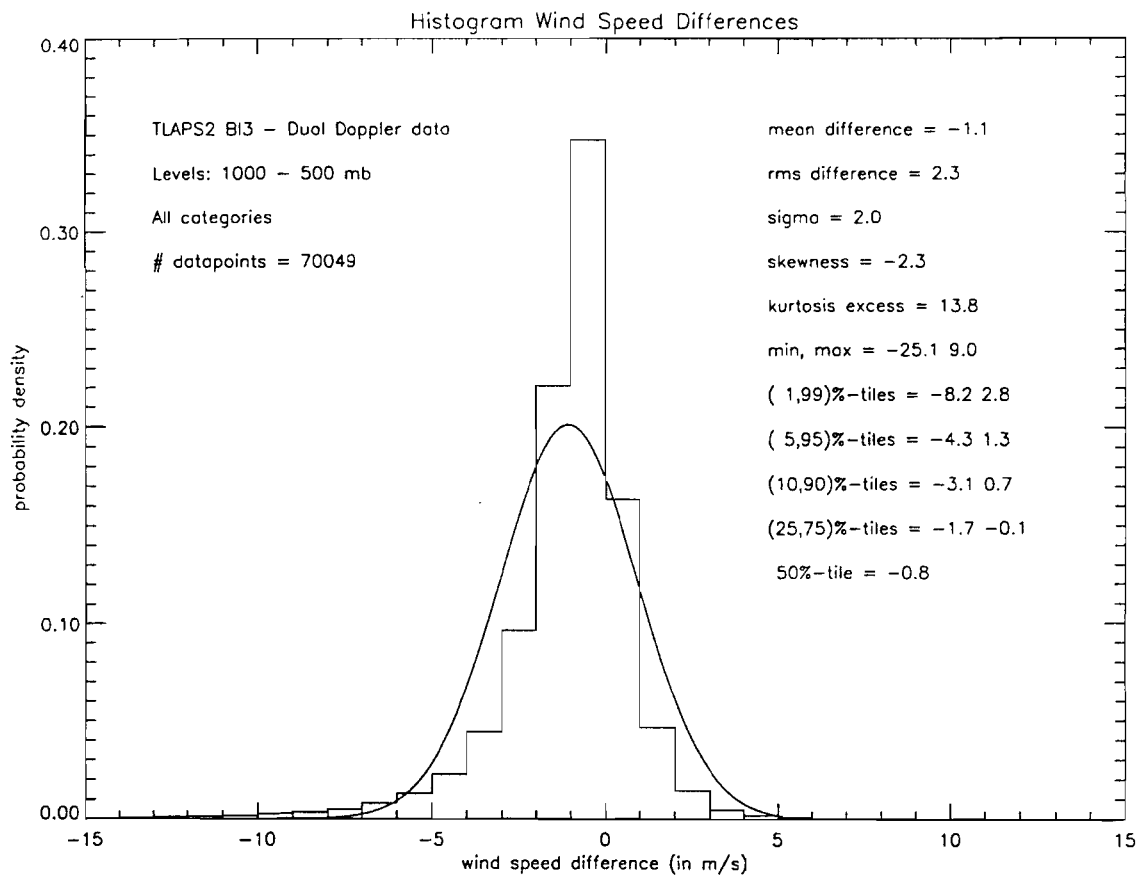


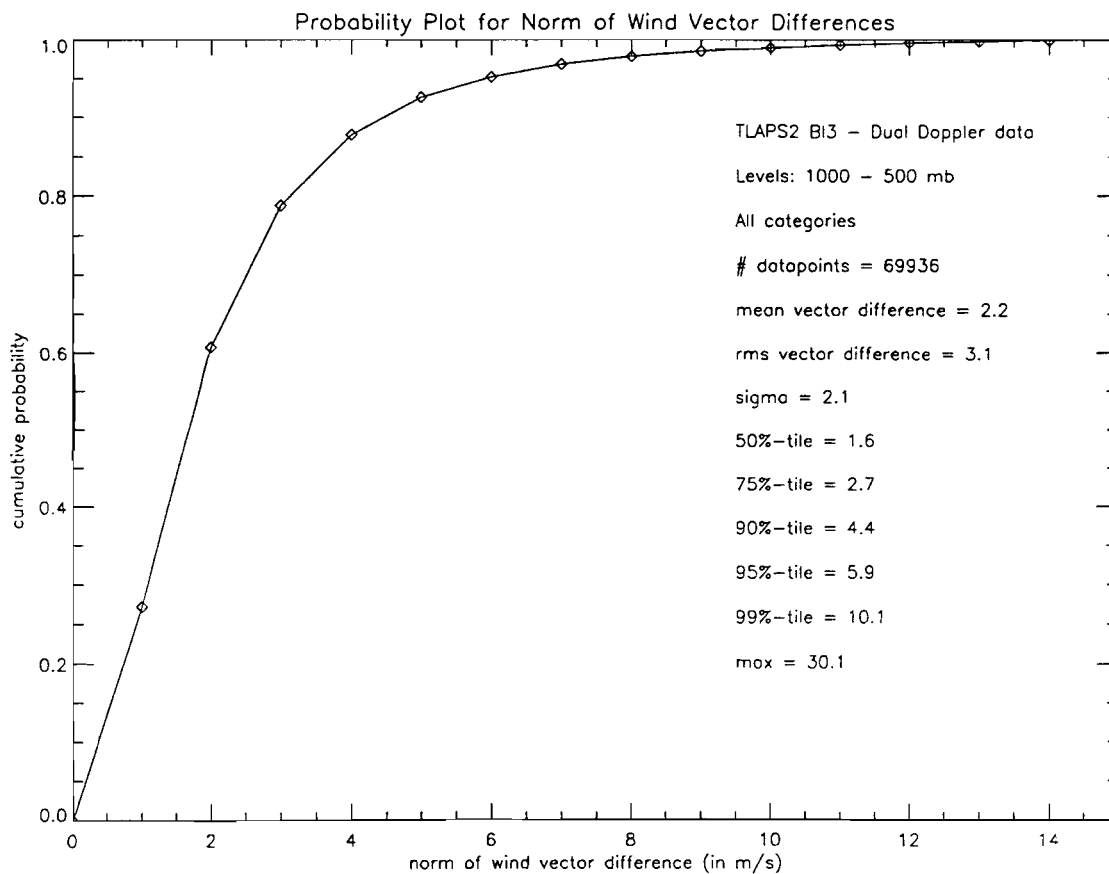
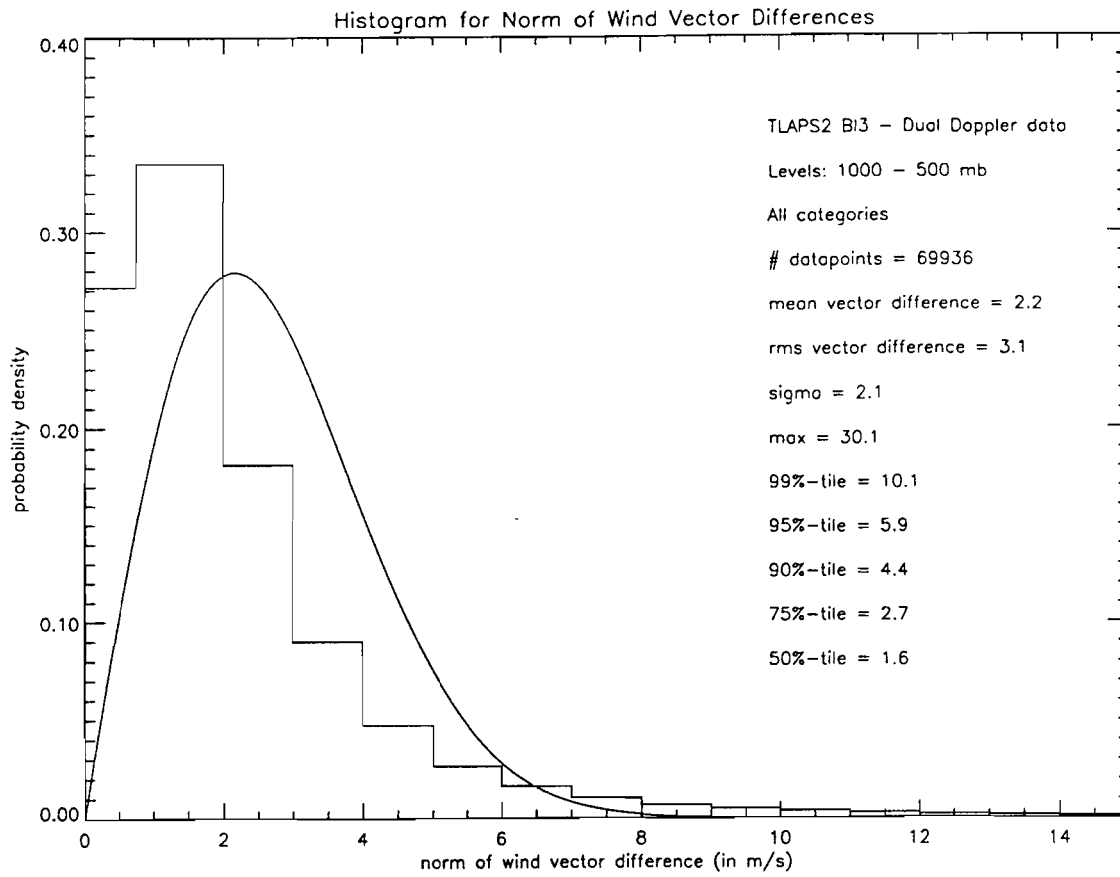




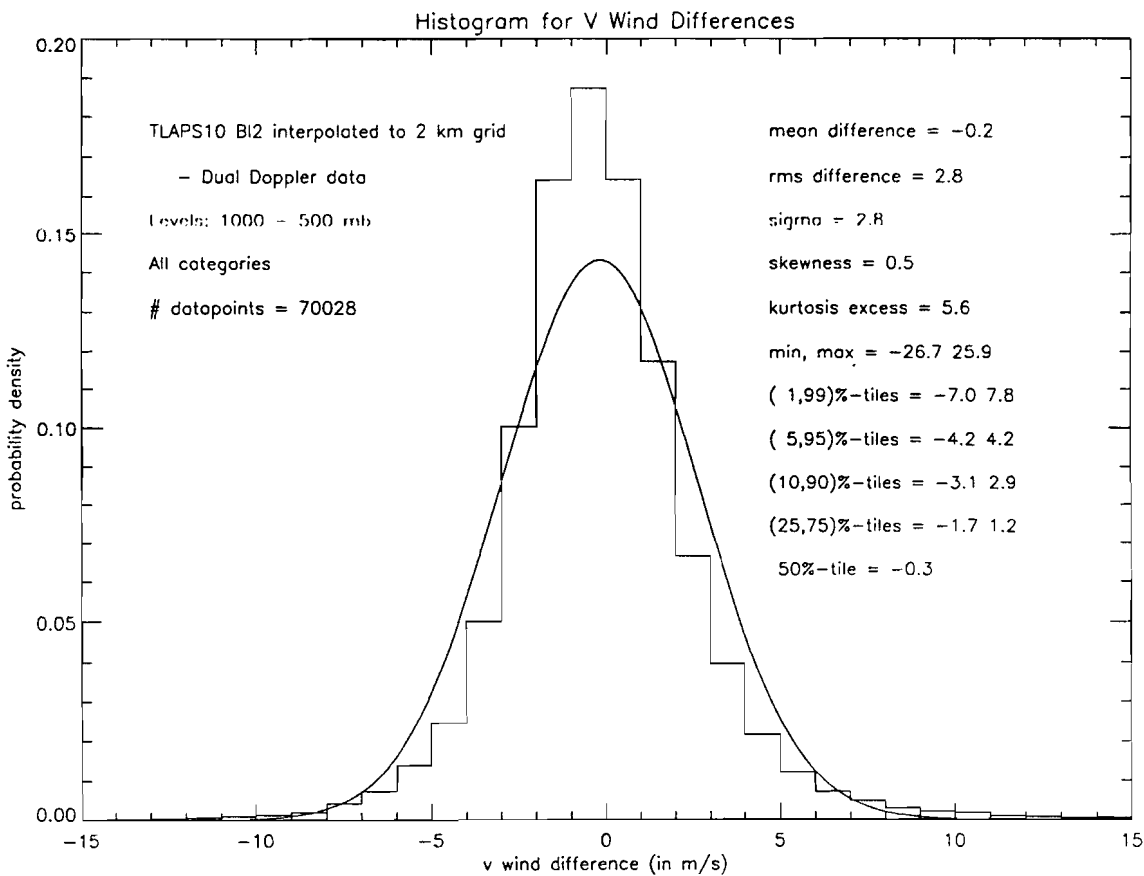
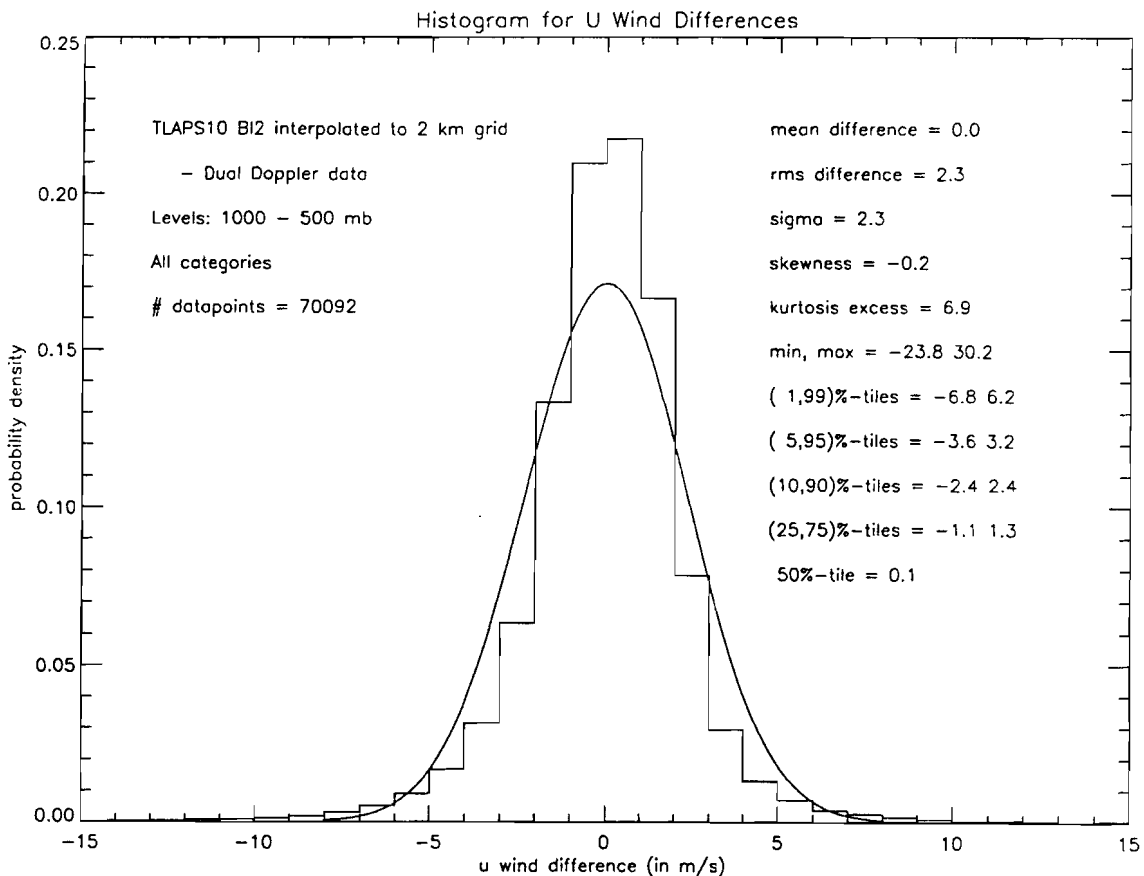
SECTION C-12

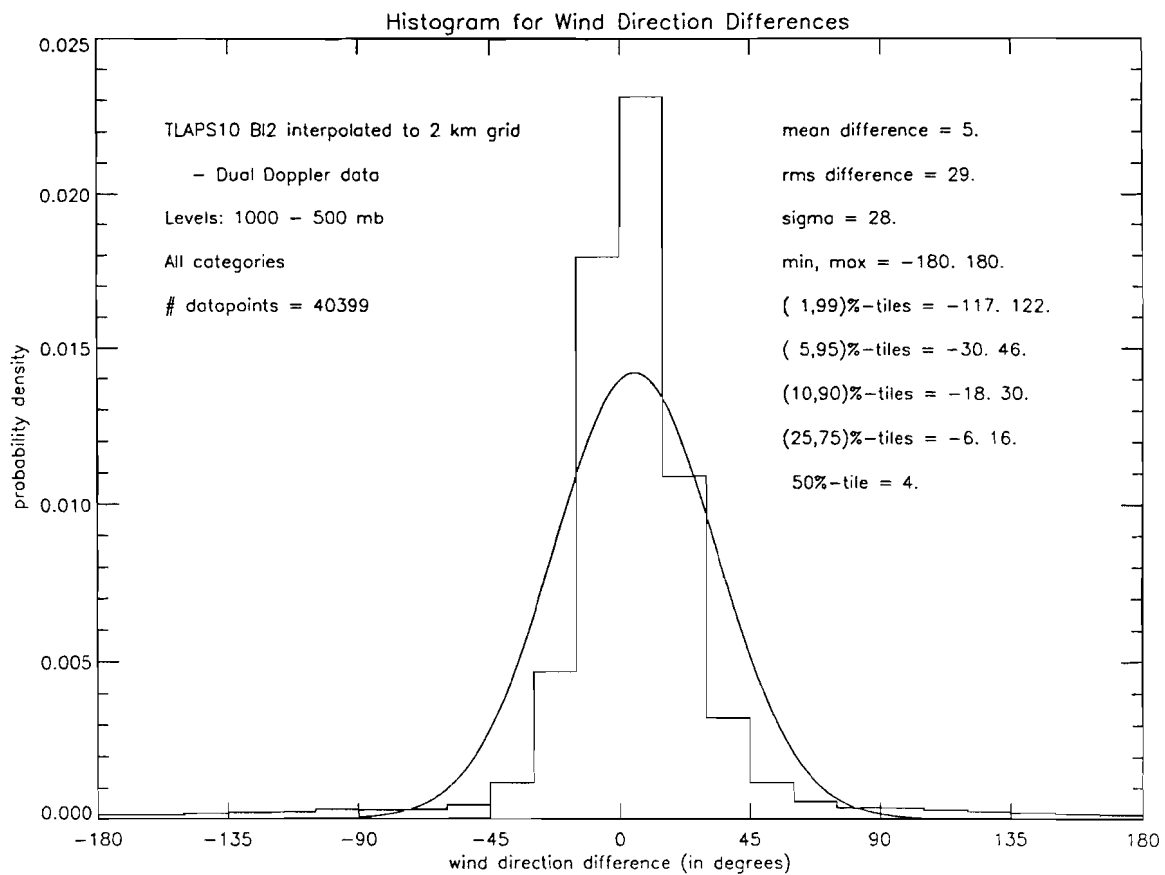
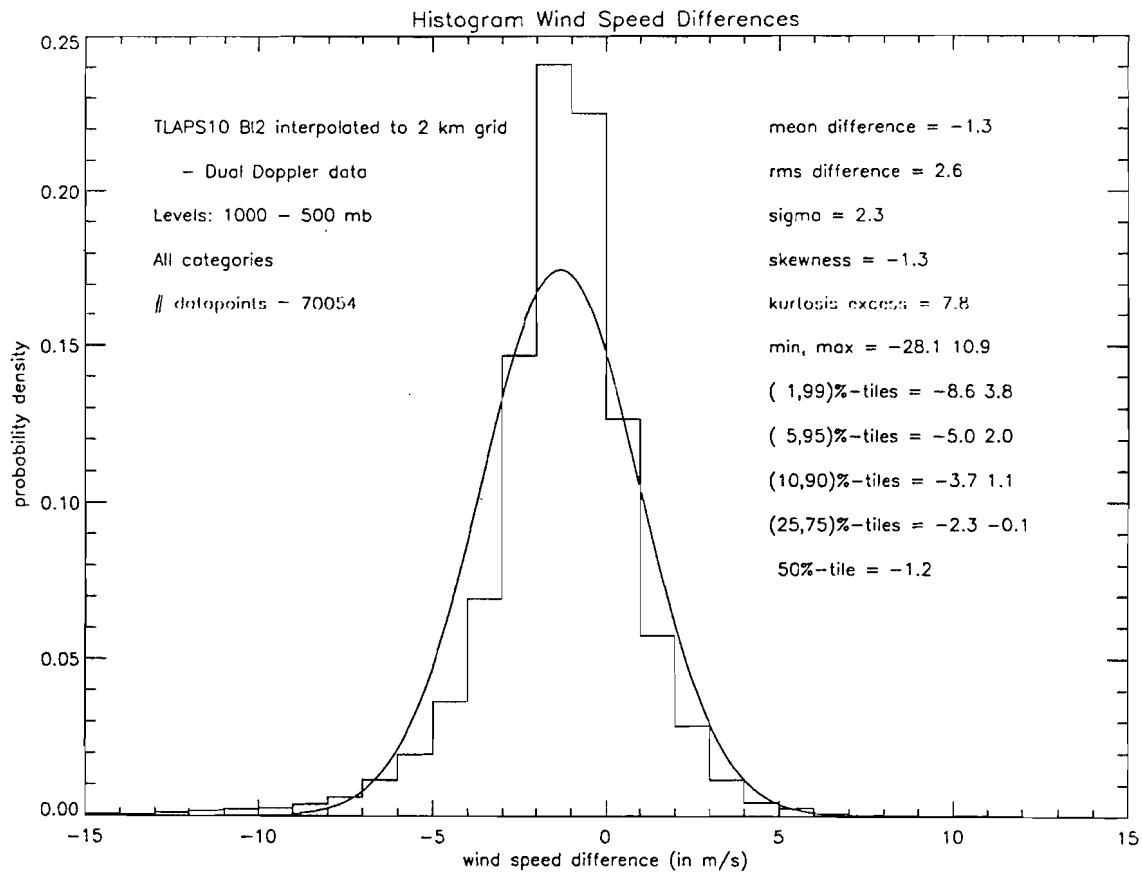




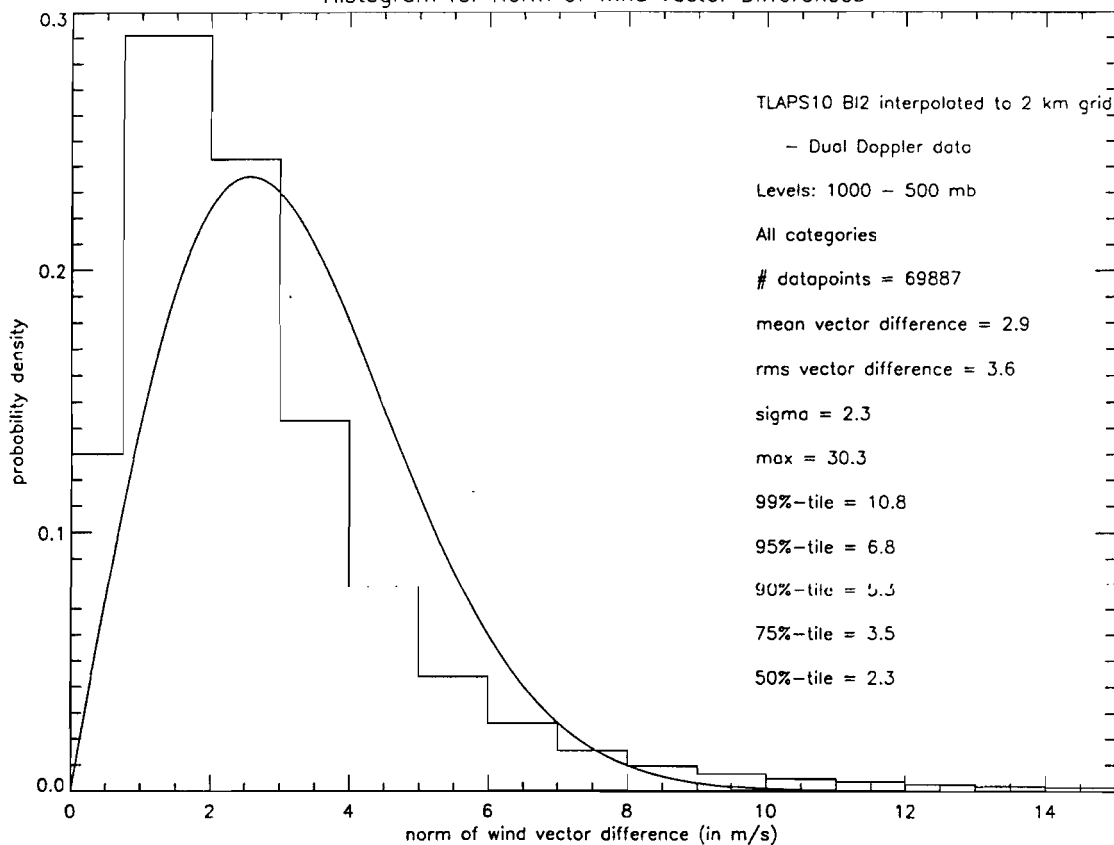


SECTION C-13

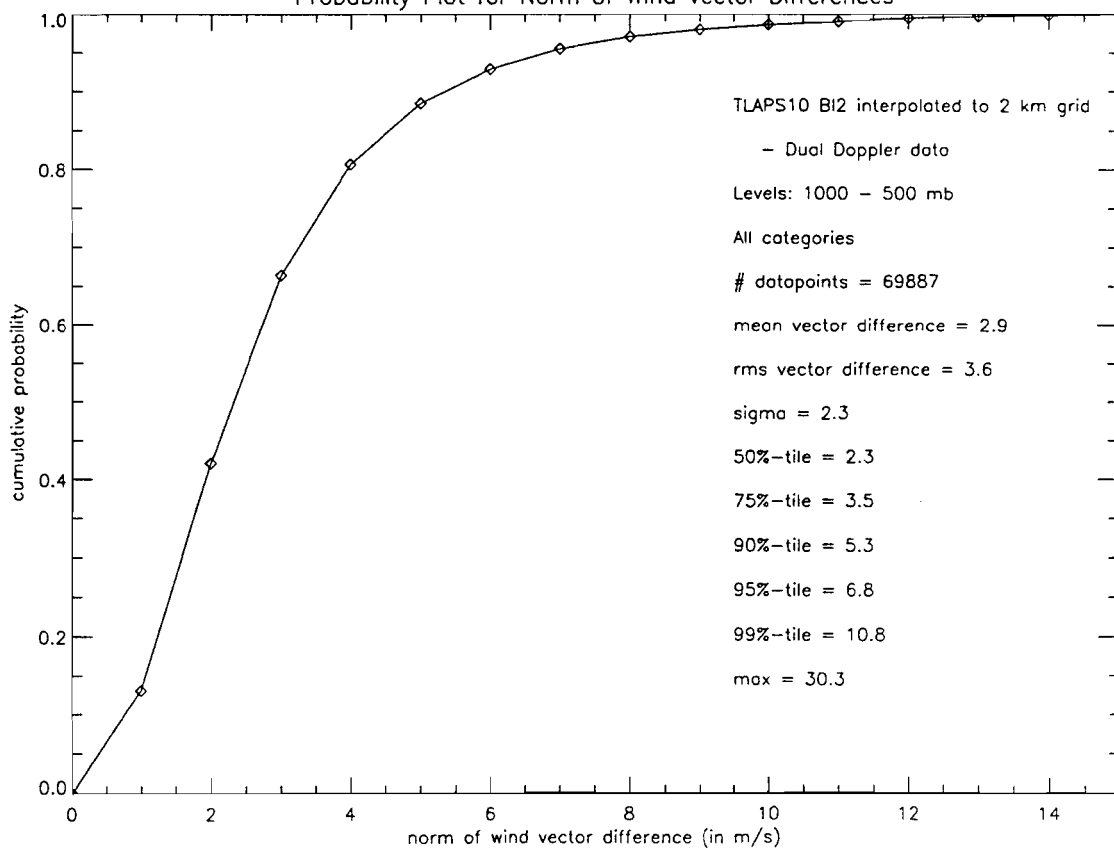




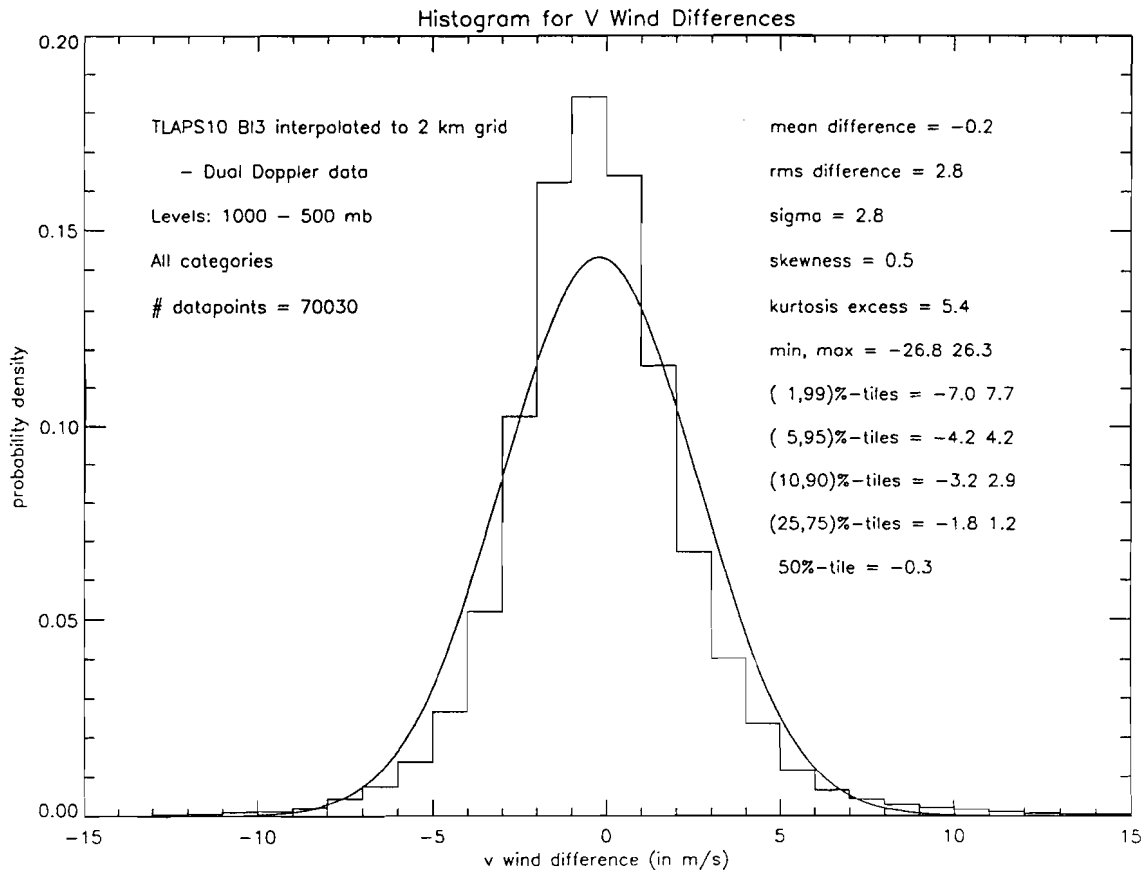
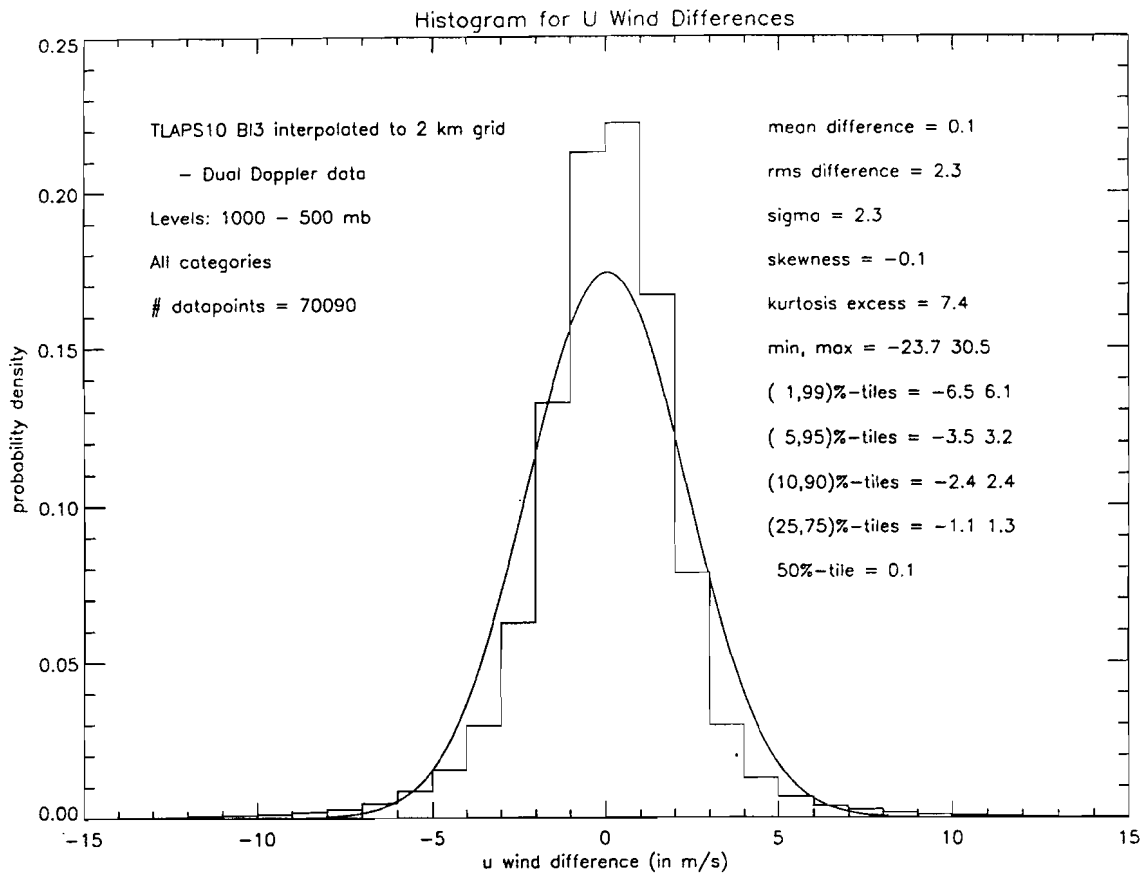
Histogram for Norm of Wind Vector Differences

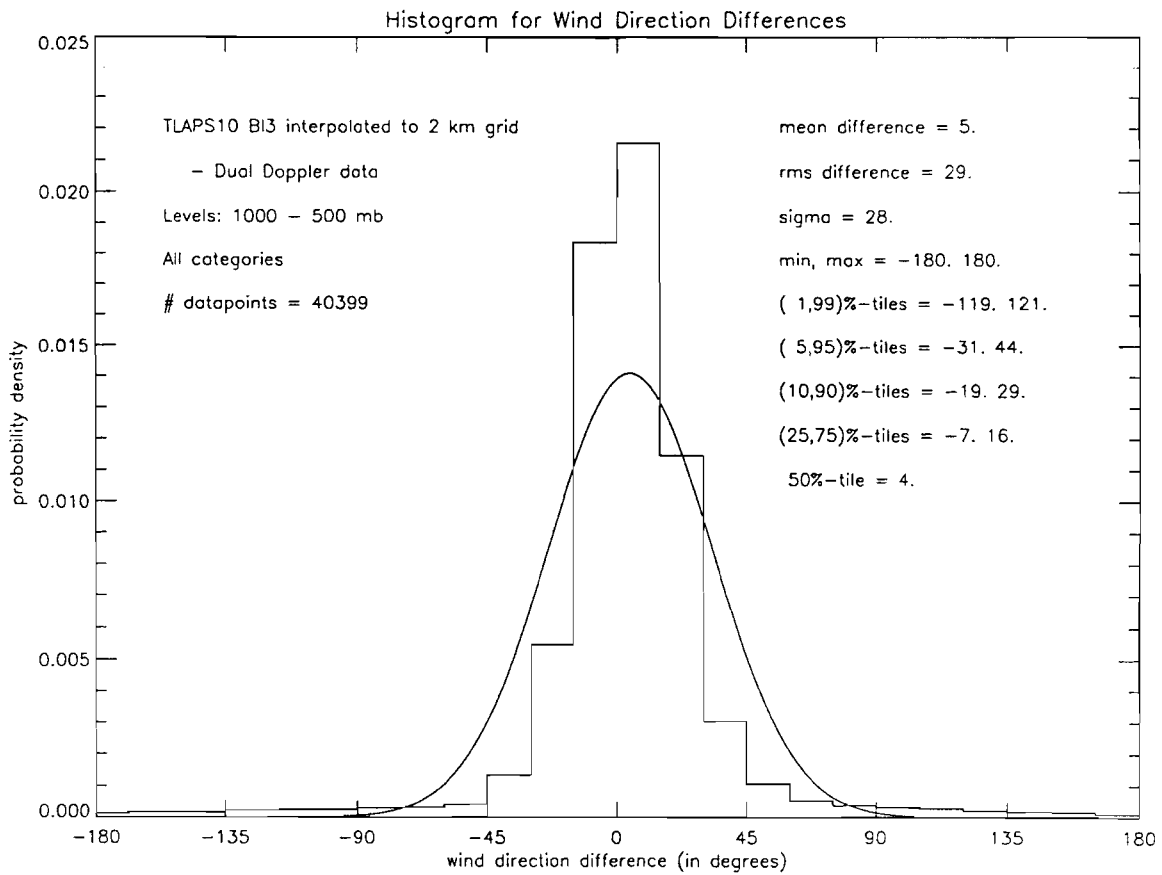
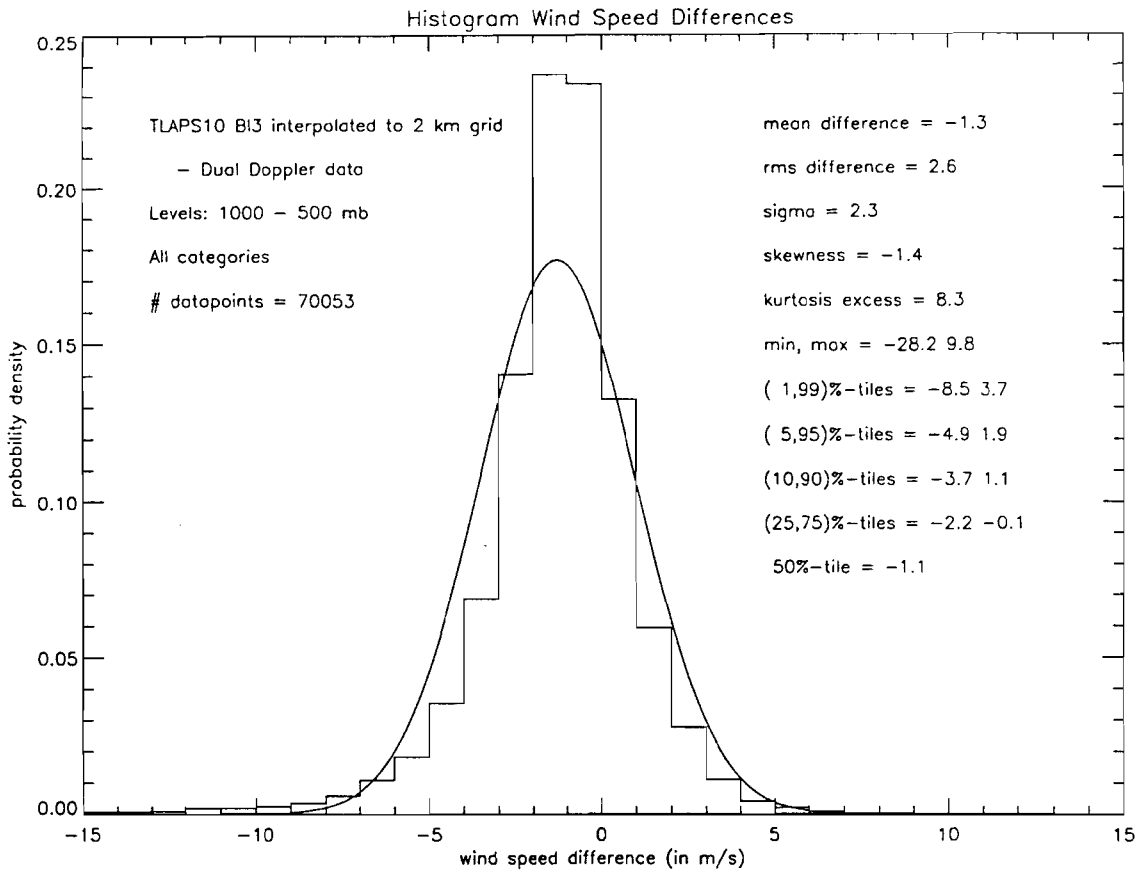


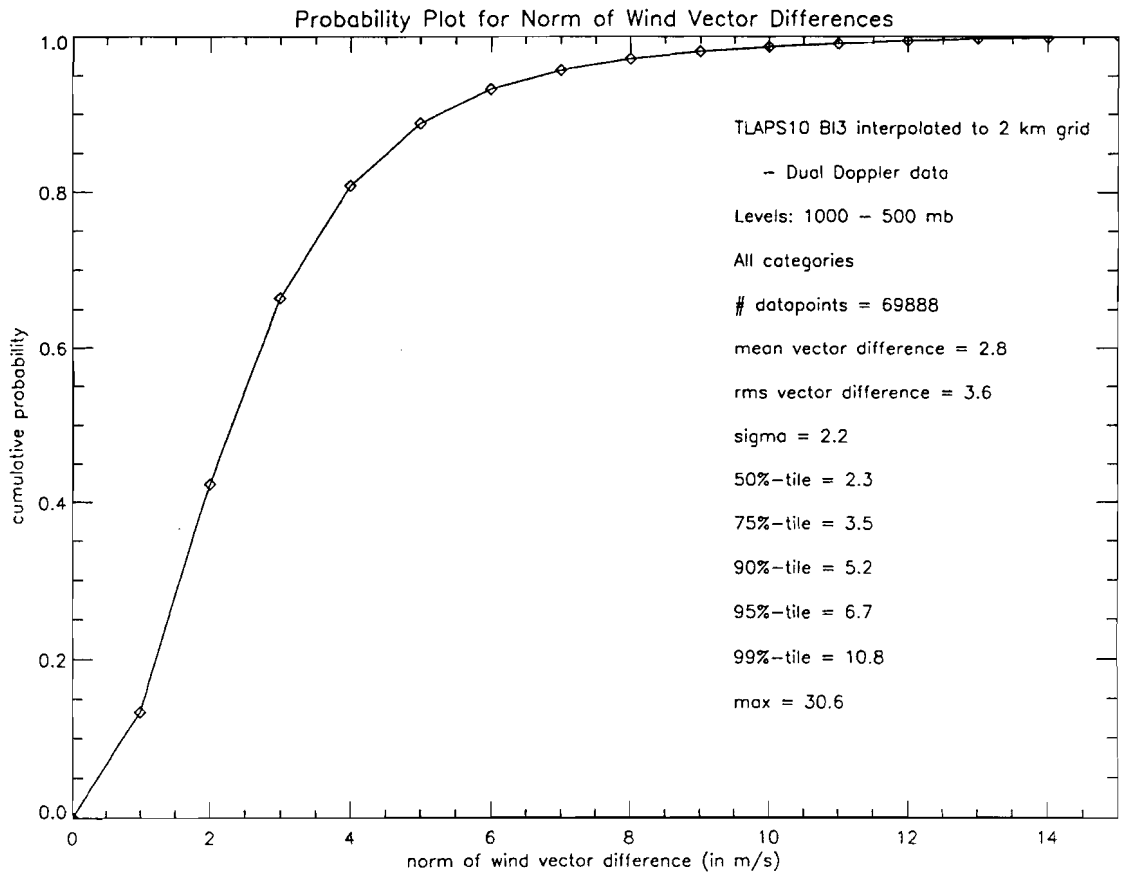
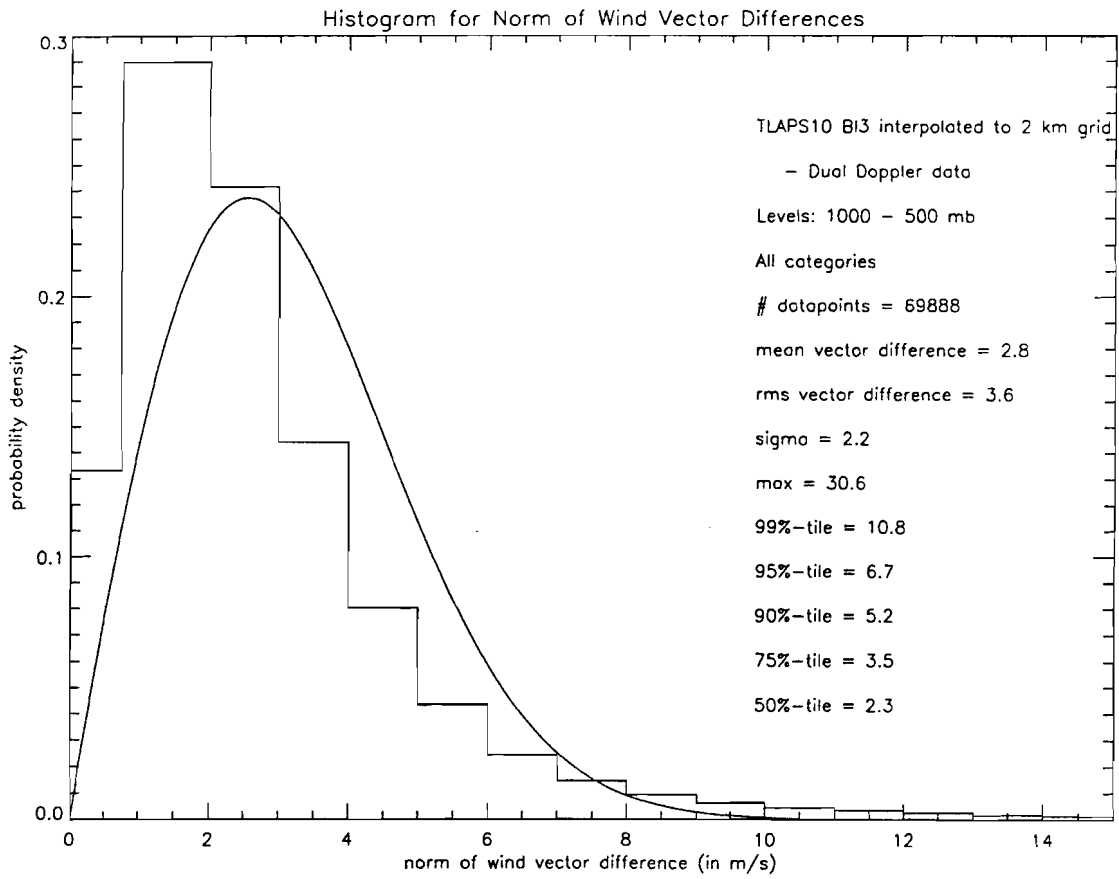
Probability Plot for Norm of Wind Vector Differences



SECTION C-14







SECTION C-15

